~20

Structure and Thermodynamics of Diol Inclusion Compounds

A Thesis submitted to the
UNIVERSITY OF CAPE TOWN
in fulfilment of the requirements for the degree of
MASTER OF SCIENCE

by

Wolf-Dieter Schubert
B.Sc. (Hons) Cape Town

Department of Chemistry
University of Cape Town
Rondebosch
7700
South Africa

April 1991

ACKNOWLEDGEMENTS

I would like to thank:

Professor L. R. Nassimbeni for his inspired yet patient supervision, for his guidance and interest,

Professor M. R. Caira for expert advice freely given,

Dr. M. Niven for the data collections and assistance in solving the crystal structures,

Dr. D. Bond for help in systhesis of the host compound and cooperation regarding NITRANN,

My collegues in the Long Room for their friendship and interest; especially Susan Bourne for her help in proof reading.

ABSTRACT

This work is predominantly concerned with the structural analysis of the coordinatoclathrates formed by the host compound trans-9,10-dihydroxy-9,10-diphenyl-9,10-dihydroanthracene (1) with compounds containing neutral nitrogen atoms (Lewis bases).

The structures of inclusion compounds with two nitriles (acetonitrile and 3-hydroxypropionitrile), with pyridine and with three substituted pyridines (3-methylpyridine, 2,4-dimethylpyridine and 2,6-dimethylpyridine) have been solved by single crystal X-ray diffraction methods. The crystal packing modes and hydrogen bonding schemes have been elucidated, while the guest cavities have been investigated.

The thermal stability of the complexes was analysed by thermogravimetric analyses and differential scanning calorimetry. These techniques were employed in determining the guest content, in investigating the thermal properties of the compounds and in establishing the activation energies for the desorption processes. Desorption studies, utilising X-ray powder diffraction, were used to investigate the structures resulting from the desorption of guest from the complexes.

The selectivity of the host for either of the isomers 2,4- and 2,6-dimethylpyridine was investigated.

ABBREVIATIONS USED IN THE TEXT

b.p	Boiling point
CFOM	Combined figure of merit
DSC	Differential scanning calorimetry
G	Guest
H	Host
H:G	Host to guest ratio
m.p.	melting point
s.o.f	site occupancy factor
TG	Thermogravimetric Analysis
XRD	X-ray powder diffraction

CODE NAMES OF INCLUSION COMPOUNDS OF (1)

Code Name	Guest	(Common Name)
NITRANN	Acetonitrile	
PROP	3-Hydroxypropionitrile	
PYD	Pyridine	
3PIC	3-Methylpyridine	(3-Picoline)
24LU	2,4-Dimethylpyridine	(2,4-Lutidine)
26LU	2,6-Dimethylpyridine	(2,6-Lutidine)

TABLE OF CONTENTS

FIGURES:

TABLES

CHAPTER 1.

INTRODUCTION

1. INTRODUCTION

1.1. INCLUSION COMPOUNDS: AN HISTORICAL OVERVIEW

Inclusion Compounds are not an human invention. Many, like zeolites or hydrate inclusion compounds have been present in nature for millions of years in the form of minerals and various different forms of ice. Most, as was the case with Werner clathrates, Hofmann type inclusion compounds and crown ethers, were discovered by chance.

The honour for discovering the first inclusion compound goes to H. Davies[1] who prepared the chlorine gas hydrate in 1811. But because M. Faraday[2] was the first to prepare and characterise this gas hydrate in 1823, this date is usually taken to represent the beginning of inclusion chemistry[3].

Other inclusion compounds discovered in the same century include the graphite intercalates in 1841 (C. Schafhäutl)[4], the β-quinol H_2S clathrate in 1849 (F. Wohler)[5], the cyclodextrin inclusion compounds in 1891 (A. Villiers)[6] and the cyanide ammonia inclusion compound of benzene - or Hofmann's complex- in 1897 (K. A. Hofmann and F. Küspert)[7].

Thus, though a number of inclusion compounds had been discovered during the nineteenth century and more followed during the first half of the twentieth, their significance was not recognised. In some cases their discoverers realised that, though a new compound with unique properties was obtained, no chemical reaction as such had occurred between the components. Instead they described one component of their compounds as being 'some how locked in' [8] by the other(s) without being able to clarify the interaction between the constituents. Instead, they evaded the issue by making use of the as yet undefined dot (•) to indicate the formula of their compounds. The first Hofmann type compound, for example, was denoted by $Ni(CN)_2 \cdot NH_3 \cdot C_6H_6$ - though Hofmann later added an explanation that "strict spatial requirements conditioned the uptake of benzene by the 'lückenhafte Komplex $Ni(CN)_2NH_3$'". [9]

This inability to describe the nature of the interaction between molecules was more than partly due to the fact that experimental techniques for structural investigations had not yet been developed. Only with the discovery of X-rays and of the reciprocal relationship between crystal lattice dimensions and diffraction patterns, was the way cleared for the development of crystallographic techniques. Thus, for the first time

information on atoms, and the interactions between atoms and molecules, could be obtained directly.

By 1945 crystallographic techniques had advanced sufficiently for H. M. Powell and D. E. Palin [10,11] to establish the structure of the complex discovered 86 years previously [12], known until then as "an addition complex of quinol (hydroquinone) and sulphur dioxide". The complex was recognised to demonstrate an unusual packing of the quinol molecules. In fact, the hydroquinone molecules, as depicted in figure 1.1 below, link up to give two infinite, interlocking frameworks. Each of the frameworks is held together by approximately planar hexagons of hydrogen bonded oxygen atoms. The two hydroquinone frameworks are shifted half a unit cell (in the direction perpendicular to the hydroxylic hexagons) in relation to each other, thereby giving rise to cavities between the successive oxygen rings. These cavities, sufficiently large to accommodate small molecules (sulphur dioxide in this case), are laterally bounded by the aromatic rings of hydroquinone molecules, which prevent the guest molecules from escaping. The empty hydroquinone structure was named 'β-quinol', in place of the complex clathrate of methanol and hydroquinone, $3C_6H_4(OH)_2 \cdot CH_3OH$, that had previously been referred to as β-quinol [13,14].

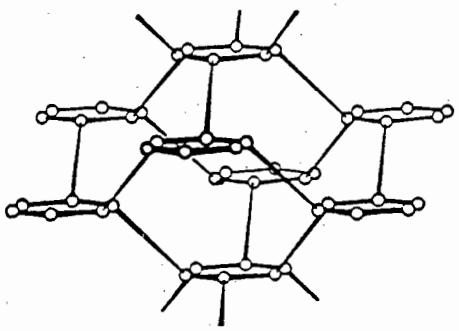

Figure 1.1 The β-hydroquinone structure as discovered by H. M. Powell (only one of the interlocking frameworks is shown). The hydroquinone aromatic rings are indicated by thick lines for clarity.

Powell was the first to realise that molecules in a crystal do not necessarily pack as tightly as their shapes would permit, corresponding to a potential energy minimum. He concluded that a cage structure could be formed by one type of molecule including a second component in the process, even though very little attraction existed between the enclosing and enclosed species. Such special reasons were found to be given only if forces stronger than van der Waals forces, such as hydrogen bonds, existed between the molecules.

To describe these new aggregate compounds Powell introduced the term 'clathrate'[15,16,17] (from the Latin *clathratus*: enclosed or protected by the crossbars of a grating) thereby initiating the study of inclusion compounds.

Other researchers quickly realised that the novel type of association between molecules proposed by Powell could be used to describe many other previously unexplained phenomena.

In the following years the study of inclusion compounds expanded rapidly. New groups of compounds were discovered and added to those already being investigated. A number of reviews on the subject, that have appeared in the last few years, are listed in the reference section[3,18,19,20].

A range of inclusion compounds based on inorganic and organometallic host lattices have been studied over the years. Some prominent examples include:

The **gas hydrates** or **clathrate hydrates**[1,2,21], the first inclusion compounds to be discovered were only identified as true clathrates[15] in 1951/2, after the crystal structures of the two types of gas hydrate had been solved[22,23,24]. They are characterised by a regular arrangement of water molecules arising from the tetrahedrally coordinated oxygen atoms of the water molecules (each oxygen atom donates two and accepts two hydrogen bonds). This leads to the formation of three-dimensional four-connected nets, based on various polyhedra, the pentagonal dodecahedron (see figure 1.2) being the most common. The structural stability of the host lattice is dependent upon the polyhedral cavities being occupied by one or more types of gas molecule (the guest).

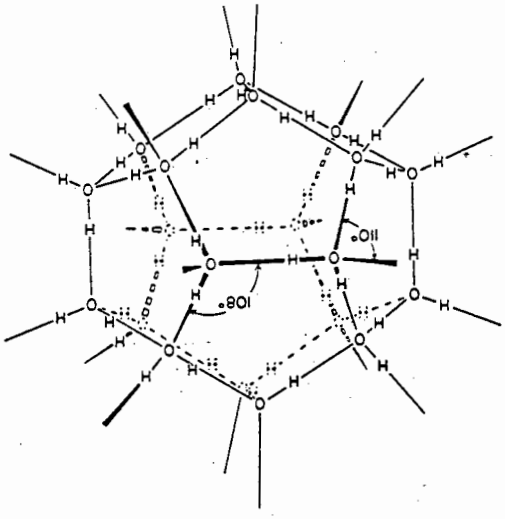

Figure 1.2 The pentagonal dodecahedron formed by water molecules in gas hydrates.

Approximately eighty compounds are known to form clathrate hydrates, with the guest ranging in size from argon to dioxane and containing at maximum a single strong (or a number of moderately strong) hydrogen-bonding functional group(s). Thus, while acetone[25], ethanol[26,27], most ethers[28] and cyclic imines[29] form clathrate hydrates, polyhydric alcohols and carbohydrates do not.

Though **Zeolites**[30], a large family of aluminosilicates, have been studied by mineralogists for more than 200 years[31], their chemical properties were first studied in 1850[32]. Structurally zeolites are characterised by their intricate networks of cavities and channels and by their structural stability. These properties have combined to make zeolites industrially attractive. Their applications include shape-selective catalysis, molecular sieving, uses as storage media for certain types of nuclear waste, for producing high vacuums and for intensive drying of gases and liquids.

Both groups of compounds referred to as **Hofmann type**[33] inclusion compounds and **Werner clathrates**[34] are characterised by their combination of an aromatic guest and a metal coordination complex as the host.

Hofmann's benzene compound, $Ni(NH_3)_2Ni(CN)_4 \cdot 2C_6H_6$, was discovered in 1897[7]. However, only when its structure was solved by Powell in 1949[35,36], was it recognized that it consisted of infinite layers of alternate square planar four and octahedral six coordinate nickel(II) ions connected by bridging CN-ligands, with benzene trapped between the layers by the ammine ligands. Variations of this compound were achieved by replacing the six coordinated Ni(II) by M (where M = Mn, Fe, Co or Cu), the four coordinated Ni(II) by M' (where M' = M or a platinum group metal) and the guest by other small organic molecules.

Werner clathrates were discovered by Schaeffer and his co-workers in 1957[37]. The host component coordination compounds have the general formula MX_2A_4 (where M denotes a divalent cation: Fe, Co, Ni, Cu, Zn, Cd, Mn, Hg or Cr; X is an anionic ligand: NCS^-, NCO^-, CN^-, NO_3^-, NO_2^-, Cl^-, Br^-, I^-; A represents an electrically neutral substituted ligand.)

As is the case in Hofmann type inclusion compounds, no coordination is possible between the host complex and the guest molecule in the inclusion compounds formed by Werner coordination complexes. Thus both groups of inclusion compounds are true clathrates since the guest is retained solely by steric barriers created by the host lattice.

1.2 ORGANIC INCLUSION COMPOUNDS

In the last two decades a new trend in inclusion chemistry has been discernible. This trend involves the attempt by chemists to imitate the highly specific molecular recognition observed in biological systems. Thus for example enzymes and carriers bind their substrates selectively and in doing so enhance their conversion, or transport them through membranes.

Essentially two routes have been employed in achieving this aim. These can best be described by the terms *supramolecular* and *multi-supramolecular* research[38]. The first of these terms describes host-guest compounds in which the guest is enclosed within a cavity formed by the host compound, while a multi-supramolecular species refers to a system in which the guest is included in the crystal matrix. Neither of these systems relies on covalent or ionic interactions for stability. Instead the aggregates are stabilised exclusively by van der Waals interactions and hydrogen bonds.

Enormous progress has been made in the field of supramolecular systems. This was acknowledged by the 1987 Nobel prize for chemistry being awarded to three chemists for their pioneering work in the field: To C. J. Pedersen[39], for his discovery of macrocyclic polyethers (crown ethers)[40,41], to D. J. Cram[42] for his work on designing suitable host compounds (spherands, cryptands, corands and podands)[43] and to J.-M. Lehn [44] for his work in synthesising the first macrobicyclic ligands (cryptands)[45,46].

The first crown ether (2), which was discovered in 1967 is depicted in figure 1.3. The common feature of crown ethers is that they are ring structures composed of oxygen atoms which are linked by ethano-bridges. Because of the inward facing oxygens (Lewis bases) these rings have the unique property of being able to bind metal and other small, positive ions.

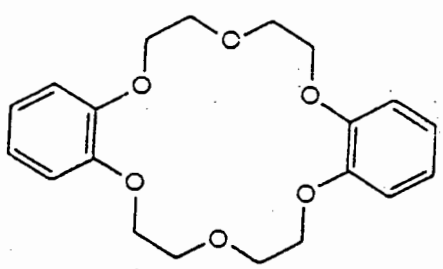

Figure 1.3 The first crown ether, Dibenzo[18]crown-6 (2), synthesised in 1967.

An overwhelming number of derivatives of the original crown ether have been synthesised over the years by varying the ring size, the nature and number of the donor sites, the molecular flexibility, by adding bridges and by opening the ring. While open-chain compounds are referred to as podands, monocyclic molecules are called coronands and oligocyclic representatives are named cryptands. Only coronands exclusively containing ether oxygens are still referred to as crown ethers. (For a list of recent reviews on crown ethers see reference 47.)

Apart from crown ethers and their three dimensional macrobicyclic ligand derivatives (cryptands, spherands etc.), cyclodextrins and cyclophanes are also important host compounds in the study of molecular recognition. Cyclodextrins are permanent cyclic oligosaccharides formed by the junction of six (α), seven (β) or eight (γ) D(+)-glucopyranose molecules. They are torus-shaped, with a height of not less than 8 Å, and display a confined cavity or a channel at their centre, depending on the arrangement of the successive sugar units. (see figure 1.4) They are soluble in water but, because of their large hydrophobic cavity or channel they include (though rather unspecifically) a large range of non-polar guest molecules.

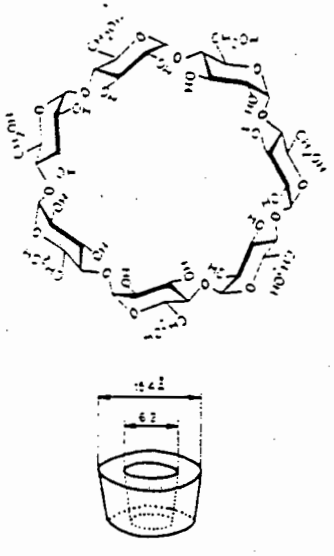

Figure 1.4 The truncated-cone shape of β-cyclodextrin.

Numerous macrocyclic rings containing one benzene ring had been synthesised during the first half of the twentieth century[48,49]. Synthesis of the first ring containing two benzene rings was achieved in 1949[50] (3), though more systematic work on a range of such compounds had been under way for some time[51] (4),(5). Varying the size of the rings by changing the number of aromatic units as well as the size and nature of the

bridging groups, led to the birth of the cyclophanes[52], molecules characterised by intramolecular, but functionally neutral cavities[53]. Their ability to include a large variety of non-polar molecules with varying degrees of specificity has ensured that they are amongst the most studied host compounds today[54,55].

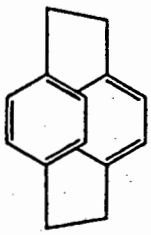

[2.2]paracyclophane

(3)

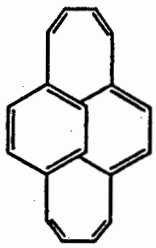

(4)

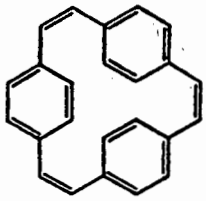

(5)

Until fairly recently not nearly as much success had been achieved in the study of multi-supramolecular (lattice-type inclusion) systems, as has been outlined above for the supramolecular (molecular inclusion) systems. This applied in particular to clathrate hosts (ie. host without functional groups), whose irregular, yet rigid shape generally resulted in so-called solvates being formed. Solvates are those inclusion compounds which enclathrate solvent molecules solely to fill intermolecular voids in the host lattice and thereby achieve thermodynamic stability. Because this often leads to poor matching between host and guest[56] the guest molecules are positionally disordered within their cavities.

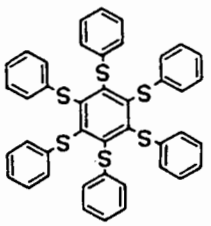

(6)

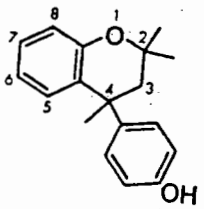

(7)

In the early seventies McNicol designed the first new clathrate host family, the so-called hexahosts[57] (6). He had noticed that both the famous β-hydroquinone structures and the inclusion compounds of Dianin's compound (7) were based on an hexagonal ring of hydrogen bonded hydroxyl groups. He imitated this arrangement by synthesising hexa-substituted benzene derivatives. The distance between the α-atoms (carbon or others) of the substituents, which are coplanar with the benzene ring, is approximately equal to the distance between the oxygen atoms in the hexagonal hydroxyl rings.

Recently a number of empirical rules that govern the formation of clathrates have been proposed[58,59,60,61]. This has led to the design of host molecules with shapes conducive to

improved packing in the presence of suitable guests. So far these rules have been applied successfully in designing tetraaryl-substituted allene hosts [62] (**8**), various, chemically diverse 'scissor-shaped' (**9**) and 'wheel-and-axle' hosts [63] (**10**) and to Spirotriphosphazenes [64] (**11**).

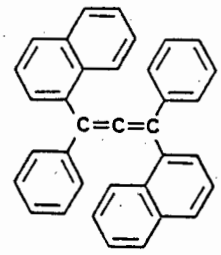

(**8**)

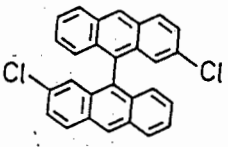

(**9**)

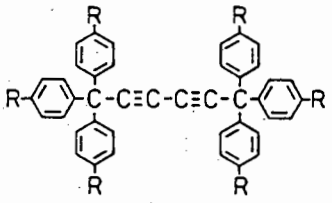

(**10**)

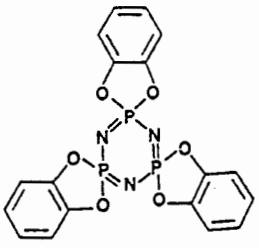

(**11**)

However, chemoselective inclusion of a guest, be it polar or not, by clathration alone is difficult to achieve. Consequently researchers in the field started exploring the concept of coordinatoclathration instead [65]. This, in broad terms, involves linking a host, with a functional group (COOH, OH, NH_2, etc.) and a suitable (often polar) guest by means of hydrogen bonds. The resulting inclusion compounds are referred to as coordinatoclathrates. Though Dianin's compound and hydroquinone both have hydroxyl groups, these are generally not involved in bonding to the guest molecules. Instead, the inclusion of ethanol by 1,1'-binaphthyl-2,2'-dicarboxylic acid [66] gave impetus to this development.

Theoretical considerations[58] indicated that the features required for an efficient coordinatoclathrand (the host) are that it have a bulky hydrocarbon skeleton (ideally a number of phenyl rings), that it be structurally rigid and that it have a functional group (or sensor group) which can hydrogen bond to the guest.

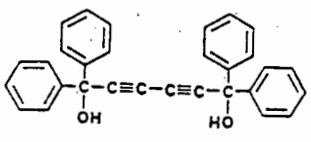

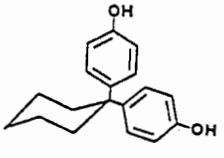

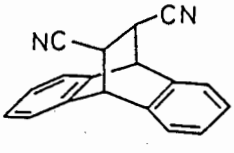

Figure 1.5 Some examples of coordinatoclathrands

By applying these criteria an overwhelming number of host compounds, especially diol hosts, have been synthesised over the past few years [59,67,68,69] (see figure 1.5 for a few examples). These have generally been shown to include a large series of guest species with matching functional groups, through coordination by hydrogen bonds [70,71,72], and/or of nonpolar guests by clathration [73]. However, despite the fact that each host compound

includes such a varied group of guests, it generally displays a marked selectivity for one chemical species above others, when two or more solvents are present during crystallisation[74]. As a consequence enclathration of solvents has been employed in the isolation and optical resolution of materials[75] especially where this is difficult to achieve by other methods.

1.2. THE HOST COMPOUND

Any elementary textbook on Organic Chemistry will explain that anthracene, a tricyclic aromatic is essentially a planar molecule. This is due to the sp^2-hybridised carbon atoms of its three fused hexagonal rings.

By contrast the shape of a closely related molecule, 9,10-dihydroxyanthracene and its derivatives is not nearly as well defined. In fact the conformation of the 1,4-cyclohexadiene ring, forming the centre of the 9,10-dihydroxyanthracene molecule has for a long time been the source of much controversy [76,77]. Surprisingly this debate could only be laid to rest fairly recently [78].

Essentially three categories of molecules need to be considered in this context: The 1,4-dihydrobenzenes, the 1,4-dihydronaphthalenes and the 9,10-dihydroanthracenes.

Initially it was assumed that the two parent compounds 1,4-dihydrobenzene and 1,4-dihydronaphthalene could best be described as existing in a boat-shaped and highly puckered conformation [79] respectively.

A planar structure for 1,4-dihydrobenzene was first proposed in 1949 [80]. This was later supported by results obtained by various techniques including Raman and Infrared analyses [81], electron diffraction [82] as well as *ab initio* calculations [83]. But this conclusion was contradicted by a conflicting electron diffraction report [84] as well as semi-empirical calculations [85] and NMR studies on substituted 1,4-cyclohexadienes [86].

Only advances in NMR techniques could finally settle the question [87,88] showing conclusively that 1,4-dihydrobenzene is a planar molecule.

As mentioned, the 1,4-dihydronaphthalene molecule was initially assigned a boat-shaped conformation [89]. On closer inspection this interpretation was replaced by the view that the molecule was planar [87]. More accurate measurements finally reversed this trend by revealing that the molecule was not in fact planar but slightly puckered [90].

In contrast to 1,4-dihydrobenzene and 1,4-dihydronaphthalene, whose conformations were difficult to resolve, early X-ray diffraction studies of the conformation of 9,10-dihydroanthracene performed in 1954 [91] (and repeated more recently [92]) clearly showed it to be a folded molecule. The central ring was found to correspond to a boat-shaped or C_{2v} conformation, while the dihedral angle between the two benzene rings was

reported to be 144,7°. Recent calculations have demonstrated that this conformation corresponds to a shallow potential minimum in both the gaseous and solid states [93].

Complexation of a guest such as 1,3,5-trinitrobenzene can however lead to a flattening of the molecule as was observed in the 9,10-dihydroanthracene:bis(1,3,5-trinitrobenzene) complex [92].

As may be expected, the introduction of any substituents in the 9 and 10 positions of the 9,10-dihydroanthracene moiety are accommodated by a deformation of the molecular conformation.

In an effort to reconcile the conformational preference of the central ring to the degree of substitution and the nature of the substituents, a large number of crystal structures of mono- and disubstituted 9,10-dihydroanthracenes has been reported over the past 30 years [94,95,96].

The first example of a planar 9,10-dihydroanthracene structure was that of 9,10-dihydro-1,2,5,6-dibenzanthracene reported in 1958 [97]. However, closer scrutiny of this structure [98] revealed this to be an incomplete interpretation. In fact, the two 'naphthalene' groups situated on either side of the central 1,4-cyclohexadiene ring, though planar and parallel to each other were not coplanar. In other words, the central ring was slightly inclined in relation to the 'naphthalene' moieties with the result that the planes described by them were parallel but separated by a perpendicular distance of 0,18 Å.

Recent research [99] has indicated that *trans*-9,10-dialkyl-9,10-dihydroanthracenes further substituted in the 9,10 or *meso*-positions are constrained by *meso-peri* interactions into planar conformations. Thus a large number of compounds following this criterion should in theory be achievable by synthesis.

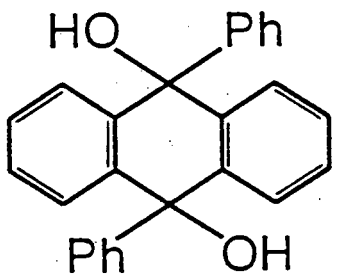

(1)

Even though its phenyl substituents are not aliphatic, the compound *trans*-9,10-dihydroxy-9,10-diphenyl-9,10-dihydroanthracene (1) is similar enough to the group of

compounds described above for it to conform to the structure predicted for these compounds. And, indeed, its central 1,4-cyclohexadiene ring has been found to adopt a planar or near planar conformation in the solid state [100] or in crystalline adducts [101,102].

However, as part of the work presented here, it will be tested to what degree this conformation can be said to be the norm for the complexes of this molecule. As in the case of the parent compound 9,10-dihydroanthracene, where the complexation of a guest by the host leads to a dramatic change in host conformation, the conformation of the host compound of this thesis can be expected to be affected by the inclusion of a guest.

The host compound *trans*-9,10-dihydroxy-9,10-diphenyl-9,10-dihydroanthracene was first synthesised by Haller and Guyot in 1907 [103]. At the time, a percentage yield of 10% was reportedly obtained, while the melting point of the new compound was given as 242°C.

During their analysis of "The Structure of the Benzene Nucleus" in 1926, C. Ingold and P. Marshall [104] modified this process with the object of improving the yield. They reported a yield of 34% while they observed the melting point of this compound to be 252-4°C.

Only in 1983 as part of their efforts to extract ethanol and other alcohols from aqueous solutions did a research group at the Japanese University of Ehime under the leadership of F. Toda [105,106] discover the ability of this compound to form inclusion complexes with a wide variety of solvents.

The search for host compounds with useful inclusion properties has long been concentrated on diol molecules. Generally, molecules with hydroxyl groups in an anti arrangement are considered to be a prerequisite for efficient guest inclusion [107]. However, it is just as important that the host be rigid and have a molecular geometry that is not conducive to efficient packing which results in voids being formed that can be filled by suitable guests.

Furthermore, hosts designed for the extraction of organic solvents, such as alcohols from aqueous solutions, should contain a large proportion of aromatic rings since this would result in these compounds being highly hydrophobic and lead to efficient solvent separation.

(1) was found to comply with all the stipulated criteria. Of especial relevance is the relative inaccessibility of the hydroxyl groups and the rigidity of the structure which permits a large variety of small organic solvent molecules to be included.

1.3. CLASSIFICATION OF INCLUSION COMPOUNDS

Ever since D. E. Palin and H. M. Powell determined the structure of the β-hydroquinone complex[10,11], and Powell coined the term clathrate [15,16,17], thereby initiating the study of inclusion phenomena, a large variety of such molecular complexes have been discovered. With time the name 'clathrate' lost its original meaning and came, instead, to be used as generic term to denote any inclusion compound whatsoever [108]. In attempting to describe the structures of the novel, but hugely diverse complexes, researchers invented new words which, though often descriptive - not to say exotic - were usually only poorly defined.

While these inventions proved to make the study of inclusion compounds linguistically intriguing, they did not help in making the subject accessible to other researchers. Whereas one term would be used by different researchers to describe vastly different structures, similar structural properties were often denoted by various unrelated terms. A few of the names in general use will suffice to prove the point: addition compound, associate, cage compound, cascade complex, clathrate complex, coronand [109], clathrate hydrate, gas hydrate, hydrocarbon clathrate, interlamellar sorbent, lock and key complex, loose addition complex, Möbius Strip molecules [110], molecular complex associate, octopus molecules [111], podand, supermolecular complex, speleate, tweezer molecules....[112]

As a consequence of this plethora of terms E. Weber and H.-P. Josel proposed a new system of nomenclature applicable to all inclusion compounds [58,61,113]. It was devised to classify and name all host-guest-type compounds on the basis of the host to guest interactions and topographical considerations. Because the system does not classify host guest complexes on a strictly chemical basis it is remarkably flexible. Thus it not only covers all host to guest interactions discovered to date but simultaneously makes provision for any types that will be discovered in the future.

Initially any host-guest compound is classified on the basis of a) the type of host-guest interaction and b) the topology of the host-guest interaction. Figure 1.6 is particularly useful in demonstrating the relationship between the alternative categories.

a) The host-guest interactions are best illustrated by the following two extremes : The guest may be bound to the host by coordination as exists between a metal and its ligands. Such host-guest aggregates are termed *complexes*. In this context metal ion

complexes of crown ethers can be mentioned as an example. Alternatively no interactions (other than weak van der Waals forces) bind the guest to the host. Thus the guest is retained within the host lattice by purely steric barriers. These aggregates are called *clathrates* (or *cavitates*).

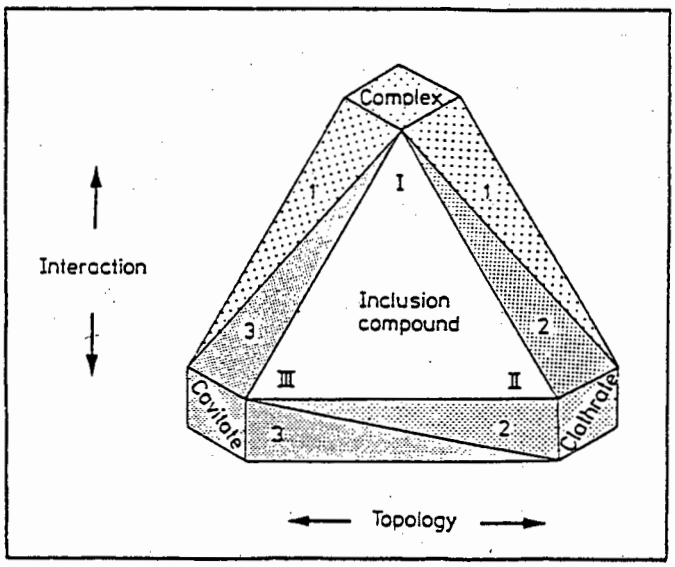

Figure 1.6 Classification of host-guest-type compounds, (1) coordinative interaction, (2) lattice barrier interaction, (3) mono-molecular shielding interaction, (I) coordination-type inclusion compound (inclusion complex), (II) lattice-type (multi-molecular) inclusion compound, (III) cavitate-type (mono-molecular) inclusion compound. (taken from reference 58.)

Host-guest aggregates which do not fall into either of these categories may be described as *coordinatoclathrates* if they display a dominant clathrate character with a certain degree of coordination (eg. hydrogen bonds) between host and guest. The inclusion compounds generally formed by hydroxy hosts constitute an example of this group. Alternatively *clathratocomplexes* are host-guest aggregates in which the guest molecules are predominantly bound to the host by weak coordinative forces. Crown ether complexes with uncharged guests can be mentioned in this connection.

b) Topologically one distinguishes between *cavitates* and *clathrates*. The first term denotes intra-molecular aggregates in which the guest occupies a cavity inside the host, while the second describes extra-molecular inclusion compounds in which the guest occupies voids in the host lattice.

Further topological features of inclusion compounds, where significant, are incorporated into the names in the form of prefixes. Thus sandwich-type aggregates consisting of alternate host and guest layers are denoted by the prefix *intercalato*. Similarly the prefixes *tubulato*, *aediculato* and *cryptato* describe cavities that are channel-shaped, pocket-shaped or completely closed off respectively, while *coronato* and *podato* define ring-shaped or open-chain hosts.

The incorporation of a three part code to denote the number of hosts, guests and chemical constituents respectively rounds off the system: the total number of chemical constituents of the aggregate is indicated by a 'b' (binary) or 't' (ternary) in front of the name, while the number of host molecules (eg. monomolecular = 1m) and guest molecules (eg. binuclear = 1n) follow.

Thus, for example, of the inclusion compounds presented in this study **NITRANN**, **PYD** and **3PIC** are identified as binary monomolecular binuclear (tubulato)coordinatoclathrates (b, 1m, 1n-tubulato-coordinatoclathrates).

CHAPTER 2.

AIM AND SCOPE

2. AIM AND SCOPE

This project has been undertaken in order to characterise the inclusion compounds formed between the host (1) and a variety of guest molecules, all of which contain nitrogen as a potential acceptor for the formation of O-H···N hydrogen bonds.

A more general study of the geometry of these hydrogen bonds has been carried out .

The thermal stability of these inclusion compounds has been investigated and the results rationalised as far as possible in terms of their structure.

Competition experiments between two closely related guests have been carried out in order to test the selectivity of the host compound.

CHAPTER 3.

EXPERIMENTAL PROCEDURES AND INSTRUMENTATION

3. EXPERIMENTAL PROCEDURES AND INSTRUMENTATION

3.1. PREPARATIVE PROCEDURES

3.1.1. Host Synthesis

The host compound *trans*-9,10-dihydroxy-9,10-diphenyl-9,10-dihydroanthracene was synthesised according to an improved version [114] of the method of Ingold and Marshall (1926) [104] which itself was a modification of the earlier process of Haller and Guyot (1904) [103]:

Preparation of the Grignard reagent: A solution of 10,4 ml (98,8 mol) bromobenzene in 30 ml dry diethylether was prepared. An initial volume of 5 ml of this was added to a heated and stirred mixture of 2,4 g (98,7 mmol) of magnesium (previously washed in diethylether) in 10 ml of absolute diethylether. When it was apparent that the reaction had commenced, the remainder of the solution was added dropwise to the reaction mixture over a time span of half an hour.

After heating under reflux for a further hour the Grignard reagent (now brown) was itself added dropwise to a stirred and heated mixture of 4 g (19,2 mmol) of anthraquinone, (recrystallised from glacial acetic acid) in 100 ml dry ether. The reaction (initially luminescent green) was permitted to continue for 15 to 20 hours under reflux conditions.

Acidification to a pH of 2 with 2 M hydrochloric acid and cooling on ice resulted in a grey-green precipitate. This was initially dissolved in 300 ml of acetone. On being cooled in ice, crystals of the acetone inclusion compound formed within a few minutes. The resulting material (after desorption of the acetone from the unstable acetone complex) was repeatedly recrystallised from benzene, until a pure white crystalline powder with a melting point of 262°C was obtained. The composition of this compound was verified by microanalysis and was deemed to be acceptable only when its percentage composition (%C and %H) differed by no more than 0,4% from the theoretical values of:

$C_{26}H_{20}O_2$: C 85,9 % H 5,2 % O 9,9 % (%O by difference)

A yield of just under 40% was generally obtained.

3.1.2. Crystal Growth

Crystals were obtained by slow evaporation of dilute solutions of host (**1**) in the solvent that was to be included. Generally, a proportion of 20 mg of host to 2,5 ml of solvent was found to be optimal.

The host powder was added to boiling solvent in a sample tube. The boiling solution was then filtered with the help of a syringe and a 0,45 μm MILLEX-HV filter unit to prevent possible dust particles from providing an excessively large number of nucleation sites. The solution was allowed to cool to room temperature. Slow evaporation of the solvent resulted in the formation of suitable crystals over periods varying from a few days in the case of **3PIC** (3-methylpyridine) to as much as three weeks for **24LU** (2,4-dimethylpyridine) and **PROP** (3-hydroxypropionitrile).

For experiments where superior crystal quality was not of prime importance (for example in the case of X-ray powder diffraction patterns, Chapter 7), more concentrated solutions resulted in time required for crystal formation being appreciably reduced.

3.2. GENERAL ANALYSIS AND CHARACTERISATION

3.2.1. Density Measurement

Density measurements were obtained using the flotation method. Crystals were suspended in mixtures of saturated aqueous potassium iodide solution and distilled water and the density of the mixture was then determined using a Paar DMA 35 Digital Densitymeter. Where crystals had visibly decayed due to loss of guest during the course of the experiment, they were replaced by fresh crystals before densities were determined.

Measurements were repeated at least once. If this resulted in significantly different values (> 0,03 $g.cm^{-3}$) being obtained or if the experimental values deviated appreciably from the calculated values further measurements were made.

3.2.2. Melting Point Determination and Optical Observation

For optical observations of crystals a Nikon Stereoscopic Microscope SMZ-10 was used. Polarisation filters meant that the quality of crystals could be verified by checking their ability to extinguish plane polarized light.

Observations - for example the melting point determination of the host compound and the thermal decomposition of the crystals - requiring crystals to be heated were made by using the microscope in conjunction with a Linkam Hot Stage TH600 coupled to a Linkam CO 600 Controller. A Nikon FX-35 camera operated via a Nikon Microflex AFX-II Photomicrographic Attachment made for simple photographic capture of any important observations.

3.2.3. Microanalysis

The percentage composition (C, H and N) of crystals were determined using a Heraeus Universal combustion analyser (Model CHN-Rapid). The samples, which were unstable, were prepared as follows: after removing the crystals from their mother liquor they were placed on filter paper. A few drops of diethylether were dropped onto the crystals to remove excess solvent and to dry them. Thereafter they were rapidly analysed. The usual technique of drying crystals by subjecting them to vacuum could

not be employed as this would have led to guest desorption and inaccurate results would have been obtained.

3.2.4. ^{1}H NMR

^{1}H NMR was only applied to test the purity of the host. Because of the overlap of the aromatic signals of the host and a number of the guests this method was not employed to determine the host to guest ratio.

The samples were dissolved in $CDCl_3$ and their spectra recorded on a Varian 200 multinuclear spectrometer. The reference compound used was sodium 2-dimethyl-2-silapentane (DSS).

3.2.5. Mass Spectrometry

The system used for the determination of mass spectrographs consisted of a VG Micromass 16F mass spectrometer run in cooperation with a VG System 2000 PDP-8/a microprocessor. Measurements were obtained at an operating potential of 70 eV and an emission control level of 185 μA.

Small samples of uncrushed material were dried before being placed in the opening port of the spectrometer.

This technique was only employed in the case of the complex **PYD** to test the assumption that desorption of the guest is not accompanied by a reaction between the host and guest compounds. This assumption proved to be justified as only the m/e peak of pyridine was observed at temperatures ranging from 80 to 150°C.

3.3. THERMODYNAMIC STABILITY AND SELECTIVITY

3.3.1. THERMAL ANALYSIS

Thermogravimetric analysis (TG) and Differential Scanning Calorimetry (DSC) were performed on a Perkin-Elmer PC 7-Series Thermal Analysis System. This consisted of a PE TGA7 Thermogravimetric Analyser, a PE DSC7 Dynamic Differential Calorimeter, a PE TAC 7/PC Thermal Analysis Instrument Controller, controlled by means of an Epsom PC AX2 personal computer which in turn was equipped with a Hewlett-Packard Color Pro plotter.

Calibration procedures as recommended by the manufacturers were employed.

TGA 7 Analyser : - Temperature calibration is achieved by measuring the magnetic transitions of two standards, Nickel and Perkalloy.
- A 100-mg Class M calibration standard weight was used for performing weight calibrations.
- Furnace calibration is accomplished with the help of a special software programme.

DSC 7 calorimeter : - Observed melting points and enthalpies of melting of Indium and Zinc are compared to accurately known theoretical values in order to achieve calibration.

Samples were prepared as follows: In the case of TG, a crystalline sample of between 2 and 5 mg was removed from the mother liquor, then dried and crushed between two layers of filter paper. The crushed sample was transferred to a standard pre-weighed platinum pan which was then suspended from the "hang down" wire of the TGA 7 microbalance by means of its custom-made platinum wire stirrup.

Once the mass of the sample had been determined, the temperature programme was started without delay in order to minimise the loss of guest due to desorption. The mass lost from the sample due to evolution of guest was automatically measured to an accuracy of 0,1 μg and electronically recorded.

Throughout the scan the sample chamber was purged with high-purity, dry nitrogen (H_2O < 10,0 vpm) which was passed over the sample at a rate of 35 ml.min^{-1}, while the same gas at 70 ml.min^{-1} was used as the balance purge gas.

For DSC the crystalline sample of between 2 and 5 mg was prepared as above. Once placed in a pre-weighed 30 or 50 μl aluminium pan, its mass was determined by

difference on a six-place Sartorius Micro Balance 1802. The aluminium crucible covered with an aluminium cover was then sealed by cold welding in a Perkin Elmer Universal Sealing Press. As before this procedure was performed as fast as possible to prevent deterioration of the sample. Typically, for both TG and DSC experiments no more than 1 minute elapsed between removing the sample from its mother liquor and starting the run.

The energy evolved or absorbed by the sample is determined and compensated for by the system and the power required to maintain the sample pan temperature at that of the reference pan is recorded. A baseline previously determined by running an empty sample pan against the reference pan is automatically subtracted to yield a scan of the variable thermal behaviour of the sample.

3.3.3. X-Ray Powder Diffractometry

a) Preparation of the sample for X-ray powder diffraction involved grinding the sample to a fine powder in a mortar and pestle. It was found that the build up of static electricity frequently encountered during grinding could be overcome by preparing the sample in the presence of a small amount of solvent without affecting the X-ray intensity scans. In fact, the results were found to improve through this treatment as unwanted guest desorption prior to the sample being placed in the sample chamber could be prevented.

b) The Instrumentation: The crystal powders were pressed firmly into Perspex holders to prevent crystal alignment due to preferred orientation effects. These were placed inside the sample chamber of a Philips X-ray Powder Diffraction Assembly. This consisted of a Philips vertical goniometer PW1050/80 mounted on a Philips PW1130/90 X-ray generator operating at 30 mA and 40 kV and controlled by a Philips PW 1394 motor control unit in conjunction with a Philips PW1390 channel control unit. This system, being coupled to a Bondwell personal computer, ensures direct, electronic storage of intensity data.

The reflected X-ray intensity of all samples was scanned over a 2θ-angle range of 10° to 30°(2θ). Scanning proceeded in steps of 0,1°(2θ) with a time constant of 1 s. Divergence and receiving slits both with apertures of 1° were chosen as being most suited to a sample of width 2 cm because this made for optimal data capture for the scanning range used. No antiscatter slit was used.

3.3.4. Gas Chromatography

Three different Gas Chromatographs were employed with varying degrees of success. Only details concerning the instrumental setup will be given in this section while precise instrumental settings will be given in Section 6.2.

1)	Chromatograph	Philips Pye Unicam PU4500 Chromatograph equipped with a PM8251 Single Pen Recorder
	Column	1,5 m x 4 mm glass column packed with 10% squalane on 80-100 mesh Gas-Chrome P (Applied Science Laboratories, Inc). Isothermal 180°C[115]
	Carrier Gas and Flow	Nitrogen at 30 $ml.min^{-1}$
	Detector	Flame Ionization Detector (200°C)
	Injector	On column standard Injector (200°C)
2)	Chromatograph	Carlo Erba Strumentazione Fractovap 4200 series FTV/4200-41 Chromatograph equipped with a Spectra-Physics sp4290 Integrator
	Column	2,0 m x 4 mm glass column packed OV225
	Carrier Gas and Flow	Helium at 45 $ml.min^{-1}$
	Detector	Flame Ionization Detector (250°C)
	Injector	On column standard Injector (250°C)
3)	Chromatograph	Carlo Erba Strumentazione Vega Series 2 model 6000 Chromatograph in conjunction with an Intelligent Control Unit ICU 600 equipped with a Spectra-Physics sp4290 Integrator
	Column	20 m x 1 mm WCOT glass capillary column coated with OV225
	Carrier Gas and Flow	Helium at 1,5 $ml.min^{-1}$
	Detector	Flame Ionization Detector FID 40 (250°C)
	Injector	Capillary Cold On Column Injector OC

3.4. SINGLE CRYSTAL X-RAY DIFFRACTION

3.4.1. Crystal Preparation

In each case a suitably sized crystal, chosen for its ability to extinguish plane polarized light uniformly, was lodged inside a 0,3 mm Lindemann tube which was then sealed by exposing it to a naked flame. In addition to the crystal, a small amount of mother liquor was introduced into the capillary before it was sealed in order to prevent or limit the loss of guest solvent before the capture of information could be completed.

3.4.2. X-Ray Photography and Space Group Determination

X-ray oscillation and Weissenberg photographs were used to determine the space group and preliminary cell parameters. Space groups were inferred from systematic absences in Weissenberg photographs. The photographs were captured on X-ray film in a camera of radius 28,65 mm mounted on a Stoe goniometer. For this purpose nickel-filtered copper radiation (CuK_α, λ = 1,5418 Å) generated by a Philips PW 1120/00 generator operating at 20 mA and 40 kV was used.

3.4.3. Data Collection

Data sets were collected through the use of an Enraf-Nonius CAD-4 diffractometer with graphite-monochromated MoKα radiation (λ = 0,7107 Å) which was generated by a Philips PW1730 generator operating at 20 mA and 50 kV.

Accurate lattice constants were determined by least-squares analysis of 24 reflections in the approximate range of $16° \leq \theta \leq 17°$. In all cases the data were collected in the ω-2θ scan mode with a final acceptance limit of 20σ at 20°min^{-1} and a maximum recording time of 40 s. The intensities of three reference reflections were monitored throughout the data collections after every 3600 s as a measure of crystal stability while centering was checked every 100 reflections.

The intensities were corrected by the application of a Lorentz-polarisation factor and while empirical absorption corrections were not applied, as the ratio μR, where μ and R, respectively, are the linear absorption coefficient and the mean radius of the crystal, was found to be less than 0,1 in all structures and the absorption correction factors for σ

in the range ($0° \leq \theta \leq 45°$) was found to essentially be invariant [116]. Tables 5.1.1, 5.2.1, 5.3.1, 5.4.1, 5.5.1 and 5.6.1 list further crystal data and experimental details.

3.4.4. Computation

All structures were solved by direct methods using the SHELXS-86 [117] and refined by full-matrix least-squares using the SHELX-76 [118] program system.

Complex neutral atom scattering factors were taken from Cromer and Mann [119] for non-hydrogen atoms, from Stewart, Davidson and Simpson [120] for hydrogen and dispersion corrections from Cromer and Liebermann [121].

Molecular parameters including bond lengths, bond angles, torsion angles, least-square planes and the dihedral angle spanned by these planes were calculated by PARST [122] while all drawings were obtained using the plotting program PLUTO [123].

CHAPTER 4.

PRELIMINARY CHARACTERISATION

4. PRELIMINARY CHARACTERISATION

4.1. INTRODUCTION

In an effort to accumulate as much information as possible regarding the inclusion properties of the host compound **(1)** with nitrogen-containing solvent compounds, crystals were prepared with a range of aromatic pyridine derivatives as well as short, branched and unbranched nitriles.

Compounds for further study would be chosen from these on the basis of the following criteria:

- Is the solvent included by the host compound?
- Have these complexes previously been studied?
- Are the crystals formed of sufficient quality to warrant further investigation?

Thus only inclusion complexes forming suitable crystals and that had not been subjected to investigation were to be scrutinized.

The solvents tested included the following:

Nitriles:

- Acetonitrile
- Methoxyacetonitrile
- Propionitrile
- 2-Chloropropionitrile
- 3-Chloropropionitrile
- 3-Ethoxypropionitrile
- 3-Hydroxypropionitrile
- Lactonitrile
- Butyronitrile
- 4-Chlorobutyronitrile
- Isobutyronitrile

Pyridine derivatives:

- Pyridine
- 2-Methylpyridine
- 3-Methylpyridine
- 4-Methylpyridine
- 2,4-Dimethylpyridine
- 2,6-Dimethylpyridine
- 3,4-Dimethylpyridine
- 3,5-Dimethylpyridine

4.2. IDENTIFICATION OF INCLUSION

4.2.1. Visible Desorption of Guest

A simple yet instructive method of detecting inclusion compounds, especially those in which the guest is a volatile solvent, is to watch the crystals under a microscope for various lengths of time at constant or increasing temperature. Initially most crystals of good quality, whether they include guest molecules or not, are colourless, translucent, sharp-edged prisms which extinguish plane polarised light. With time and/or increasing temperature crystals with included solvent will start to deteriorate, the exact events depending on the individual crystal. Pure host crystals, however, remain translucent until the crystal breaks up into a mosaic of small crystals due to internal stresses, only to melt sharply at 262-264°C.

For example the surface of crystals of **26LU** start to turn opaque at 80°C. That they maintain their internal structure is manifested by the fact that the crystals retain their translucence under plane polarised light. On further heating, this diminishes and disappears entirely by 130°C. However, the macroscopic shape of the crystal is retained up to approximately 260°C when it collapses into a pile of microcrystals which then rapidly dissolve at 262°C.

By contrast figure 4.1. depicts the isothermal decomposition of **NITRANN**. The process takes a few minutes at most, the time being dependent upon the size of the crystals.

Group A: Solvents found not to be included by **1** and thus eliminated on the basis of the first selection criterion included:
Methoxyacetonitrile, propionitrile, 2-chloropropionitrile, 3-chloropropionitrile, 3-ethoxypropionitrile, lactonitrile, butyronitrile, 4-chlorobutyronitrile, isobutyronitrile

Group B: Solvents resulting in crystals of insufficiently good quality for potential deterioration to be monitored by visual methods:
3,4-dimethylpyridine, 3,5-dimethylpyridine

Group C: Solvents found to be included by **1** :
Acetonitrile, 3-hydroxypropionitrile, pyridine, 2-methylpyridine, 3-methylpyridine, 4-methylpyridine, 2,4-dimethylpyridine, 2,6-dimethylpyridine. (Of these the complexes of 2- and 4-methylpyridine had already been subjected to intensive investigation[124] and were consequently dropped from the list. All others were retained for further analysis.)

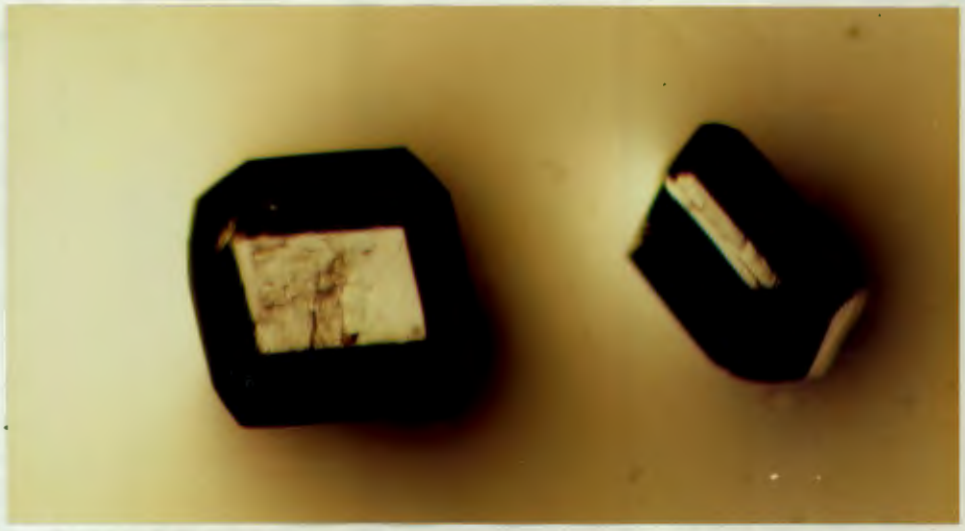

a) Crystals covered by mother liquor (t = 0min.)

b) The crystals have been drawn together by the evaporating solvent (t = 2min.)

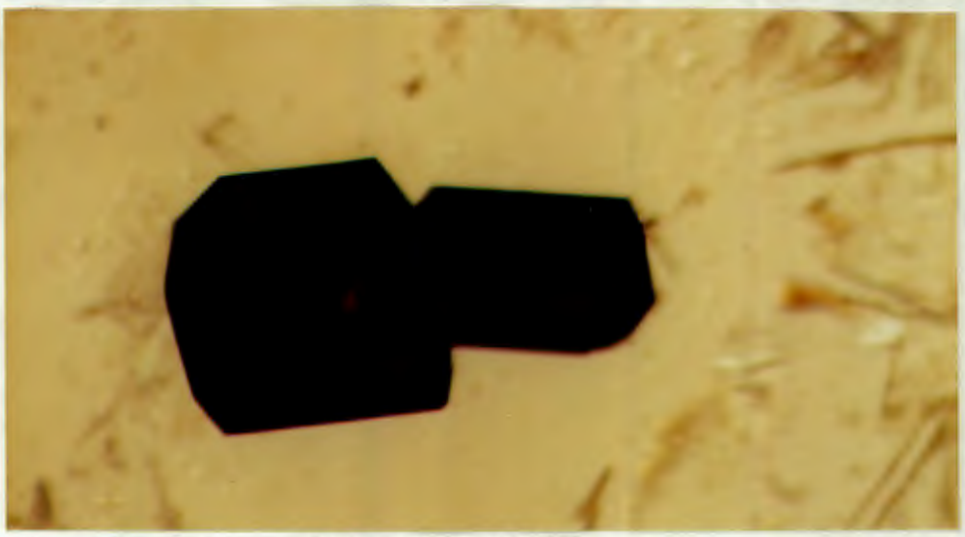

c) The surface has turned opaque (t = 4min)

Figure 4.1. The isothermal decomposition of **NITRANN**.

4.2.2. Microanalysis

Though guest inclusion had been unambiguously established in the crystals of Group C (4.2.1) by visual observation, exact Host to Guest (H:G) ratios had yet to be determined. The first method employed to determine this, was to submit samples of the crystals for microanalysis.

For all complexes the calculated percentages listed were determined for host to guest ratios of 1:2 except in the case of **24LU** where a host to guest ratio of 1:1 was used.

Table 4.4.2. : Percentage Composition by Microanalysis (%O by difference)

	H:G	%C	%H	%N	%O
NITRANN					
(calculated)	1:2	80,7	5,8	6,2	7,3
(observed)		75,4	5,15	3,3	16,15
PROP					
(calculated)	1:2	75,9	5,9	5,5	12,7
(observed)		74,3	6,2	6,2	15,6
PYD					
(calculated)	1:2	82,8	5,8	5,4	6,0
(observed)		82,3	5,5	5,3	6,9
3PIC					
(calculated)	1:2	82,9	6,2	5,1	5,8
(observed)		82,4	6,0	4,9	6,7
24LU					
(calculated)	1:1	84,1	6,2	3,0	6,7
(observed)		83,6	6,0	3,0	7,4
26LU					
(calculated)	1:2	83,0	6,6	4,8	5,6
(observed)		82,1	6,3	5,0	6,6

As is clear from this table the CHN-composition of most complexes agrees well with that calculated from idealised host to guest ratios. The obvious exception is **NITRANN** for which the observed and calculated do not agree. Though this could be explained as arising from a non-stoichiometric host to guest ratio a more satisfying answer to this deviation is that because of the high volatility of acetonitrile at room temperature a partial desorption of the guest occurs before the percentage composition can be determined. The guest loss is exacerbated by the long delay that is required between the initial weighing of the sample and the final combustion. In the other complexes

where the guests are not as volatile the complexes are not as prone to guest desorption and percentage compositions much closer to the theoretical values were obtained.

4.2.3. Density Measurements

Host to guest ratios of the complexes were calculated from their experimentally determined densities using the following equation:

$$Z_H M_H + Z_G M_G = D_m V N_A$$

where : Z_H / Z_G - the number of host / guest molecules per unit cell
M_H / M_G - the molecular masses of host / guest molecules
D_m - the experimentally determined density of the crystal
V - the unit cell volume determined crystallographically (cf. Chapter 6)
N_A - Avogadro's number ($6{,}0220.10^{23}$ mol^{-1})

Assuming for crystallographic reasons that Z_H is integral this allows the determination of the H:G ratios. The densities, unit cell volumes as well as the H:G ratios (rounded to the first decimal place) are listed below in Table 4.3.2. Densities calculated from idealised H:G ratios are also given.

Table 4.3.2 Measured and Calculated Densities

Compound	V / Å^3	D_m / g.cm^{-3}	H:G	D_c / g.cm^{-3}
NITRANN	1237,11	1,176	1:1,8	1,199
PROP	1326,63	1,278	1:2,1	1,189
PYD	1396,32	1,239	1:2,0	1,243
3PIC	2984,33	1,226	1:2,0	1,225
24LU	1228,41	1,259	1:1,0	1,275
26LU	824,39	1,175	1:2,0	1,166

As can be seen from these values all experimentally determined densities result in host to guest ratios which are very close to either 1:1 or 1:2. These values are in agreement with those obtained from TG (cf. 4.2.6) and could thus be taken to represent the true values

4.3. CONCLUSION

From the range of solvents that had formed part of the initial investigation into the inclusion properties of the host (1), only a handful could be used for further study. On the basis of the criteria mentioned in the introduction to this chapter, six were chosen. The investigation of the structural as well thermal properties of these aggregates form the main body of this project. They are:

Solvent	Code Name of Complex
Acetonitrile	**NITRANN**
3-Hydroxypropionitrile	**PROP**
Pyridine	**PYD**
3-Methylpyridine	**3PIC**
2,4-Dimethylpyridine	**24LU**
2,6-Dimethylpyridine	**26LU**

CHAPTER 5.

STRUCTURE SOLUTION

5. STRUCTURE SOLUTION

5.1. INTRODUCTION

In this chapter the structure solutions for the six inclusion complexes comprising this thesis will be discussed.

5.1.1. The Numbering Scheme and a Note on Tables

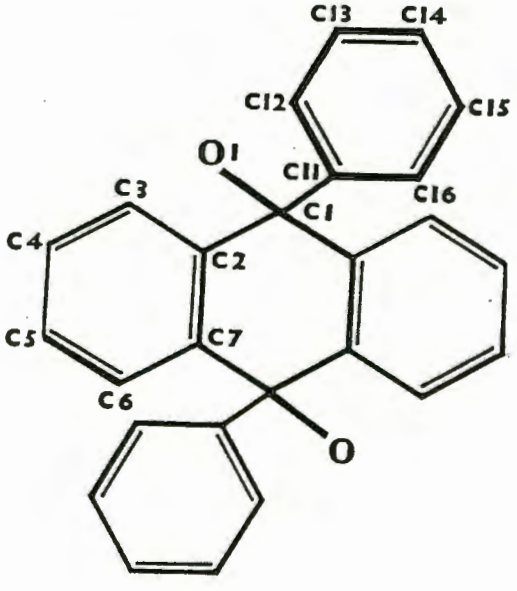

Figure 5.1.1 The numbering scheme for the host molecule

The atomic numbering scheme used for the host (1) is indicated in figure 5.1. Due to its inherent symmetry the host molecule invariably occupies a centre of inversion in crystals. Consequently only one half of each crystallographically distinct host molecule is contained in the asymmetric unit, thus greatly simplifying the required numbering scheme. The numbering scheme employed in the case of guest molecules is included in the relevant sections. For all structures the guest nitrogen is invariantly referred to as N(21) while the adjoining carbon is coded for as C(22) etc.

In the structures **PYD, 3PIC** and **24LU** which each contain two crystallographically distinct host molecules, the numbering scheme indicated in figure 5.1 is amended for the second molecule by the addition of the letter B to each atom number thus C(1) becomes C(1B) etc. The same applies to the numbering of the second guest molecule in **PYD** and **3PIC.**

At the end of each section tables containing the following indispensable information have been included. A consistent table numbering system - as exemplified by **NITRANN** below - was chosen for faster cross referencing :

Table 5.2.1. : Crystal Data

Table 5.2.2. : Data Collection Parameters

Table 5.2.3. : Final Refinement Data

Table 5.2.4. : An Analysis of Variance

Table 5.2.5. : Fractional Atomic Coordinates and Thermal Parameters

Table 5.2.6. : Hydrogen Bonding Data

In addition the following compilation tables listing the appropriate data for all compounds have been included at the end of this chapter to permit comparison of equivalent parameters of the six structures:

Table 5.1 : Bond lengths

Table 5.2 : Bond angles

Table 5.3 : Torsion angles

Appendix 3 contains six separate microfilm plates. Each of these lists the data for one of the six structures including (apart from atomic coordinates, bond lengths etc.) the least-squares planes as well as observed and calculated structure factors.

The term U_{eq} in the tables 5.2.5, 5.3.5 etc. is an equivalent isotropic thermal parameter, defined as

$$U_{eq} = (1/3) \sum_i \sum_j U_{ij} a_i^* a_j^* a_i \cdot a_j$$

The expressions for the various R factors, where not defined in the text may be found in Appendix 1.

5.1.2. Experimental and Computation

All six inclusion complexes were observed to be unstable when exposed to air due to the loss of their guest by desorption. Consequently, all crystals had to be sealed in Lindemann tubes together with a small amount of mother liquor. For all structures the intensity data were collected at 293 K on an Enraf-Nonius CAD-4 diffractometer using graphite-monochromated MoKα radiation, λ_{mean} = 0,7107 Å. In all cases corrections

were applied to the data for Lorentz and polarisation effects. Empirical absorption corrections were not applied since the small value of μR for all crystals studied obviated this (see Section 3.4.3).

For further details concerning the instrumental setup and data capture practice please refer to section 3.4.3.

The solution of the crystal structure by direct methods using SHELXS-86 and further refinement by least squares refinement using SHELX-76 will be discussed in detail only for the first structure viz. **NITRANN**. All remaining structures solutions will be described only briefly, except where major deviations from that of **NITRANN** occur.

Furthermore crystallographic fundamentals will be assumed. References to general texts on the subject are listed in the bibliography [125,126,127].

5.1.3. Hydrogen Bonds

In contrast to the ubiquitous O-H··O and the common N-H··O hydrogen bonds the O-H··N has not been widely studied [128]. In order to have comparative values against which the observed parameters could be checked all O-H··N hydrogen bonding data stored in the Cambridge Structural Data Base [129] were compiled.

Initially all structures that contained an hydroxyl group and an uncharged nitrogen atom were retrieved. (For the command line used please refer to Appendix 2.) The coordinates were then checked for the presence of O-H··N hydrogen bonds (see Appendix 2 for details)

From the list thus obtained all those values corresponding to entries with O-H-N angles of less than 150° were eliminated. Scatter plots of the parameters for the 170 remaining hydrogen bonds were prepared as these were considered to best illustrate any trend associated with these parameters. These are indicated in figure 5.2. (p 35)

The information incorporated in the scatter plots was used as a guideline for all structures in constraining the hydroxyl hydrogen atoms to within suitable distances of the relevant oxygen and nitrogen atoms.

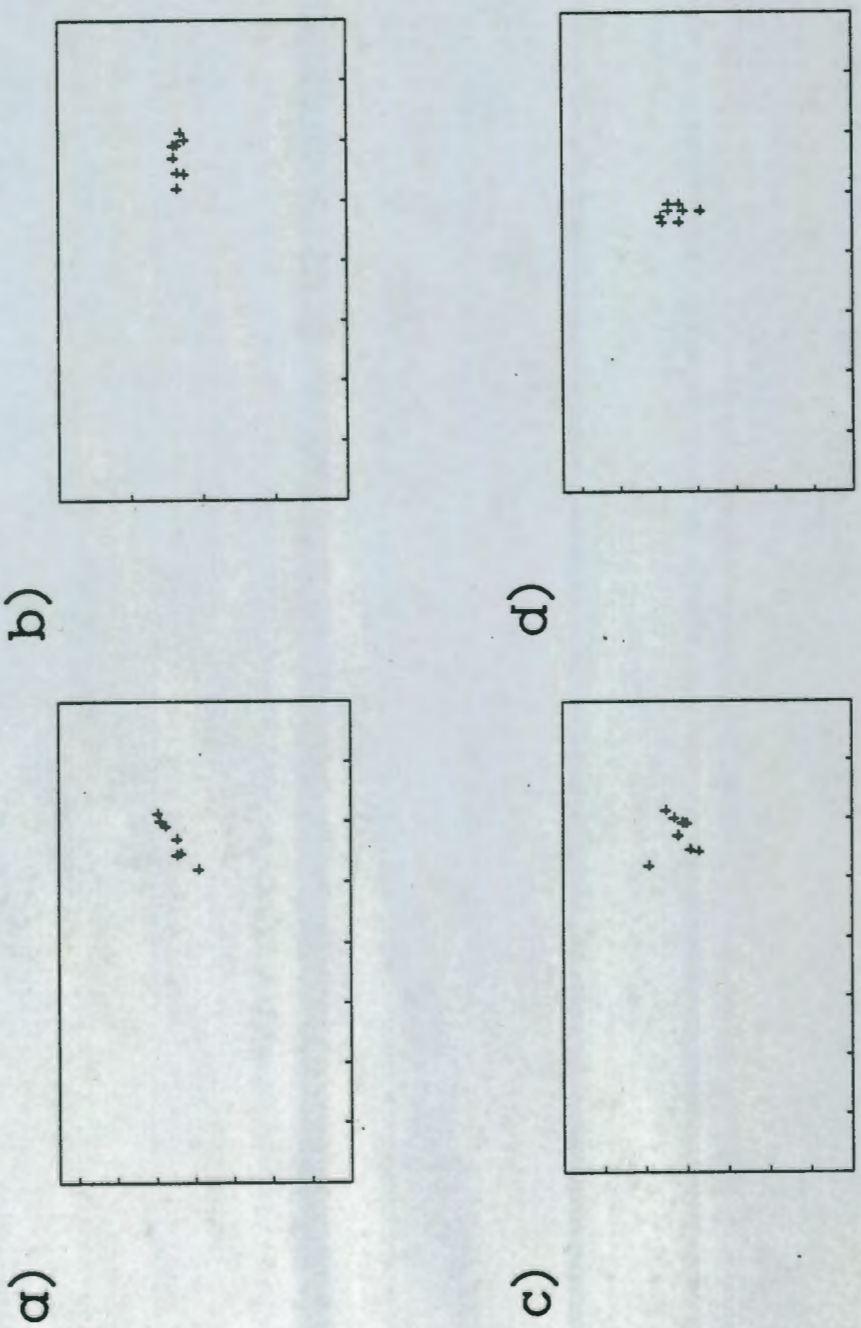

Figure 5.1.3

a) this study

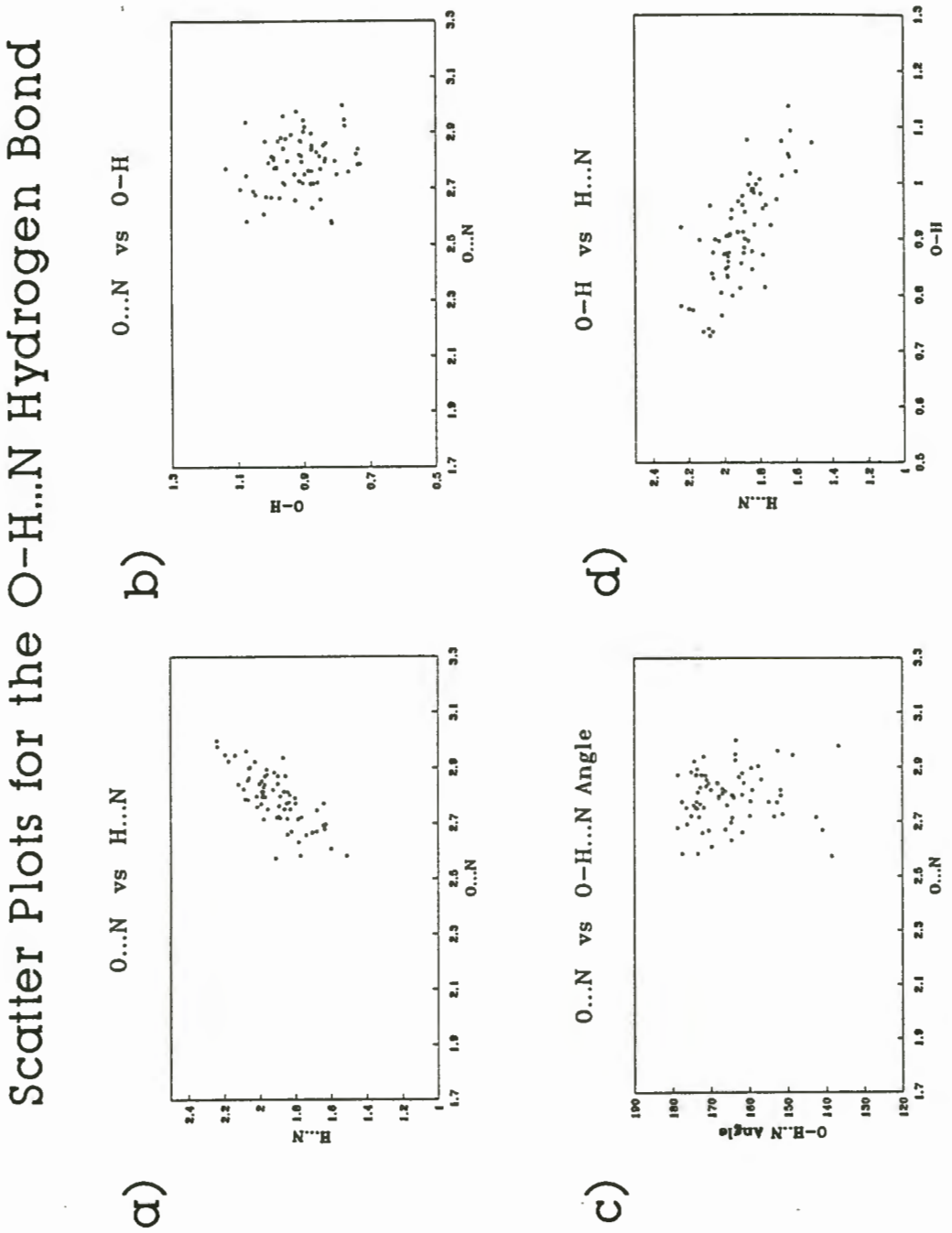

Figure 5.1.2 Scatter Plots relating parameters for the O-H··N hydrogen bond and b) as obtained from the Cambridge Structural Database..

5.2. NITRANN

Preliminary oscillation and Weissenberg photography established that **NITRANN** belonged to the monoclinic space group $P2_1/c$. This was confirmed by the crystal reflection data which exhibited the following non-extinction conditions:

$$h0l : l = 2n$$
$$0k0 : k = 2n$$
$$(00l : l = 2n)$$

The crystal structure for **NITRANN** was solved by direct methods making use of the SHELXS-86 program. The total number of reflections collected was 2415. Of these 91 were rejected as being systematically absent. After merging equivalent reflections (including Friedel opposites) a total of 2177 unique reflections were obtained. Of these, 1363 reflections were considered to be observed, $|F_o| \geq 4\sigma(F_o)$, while the remainder were suppressed. With the $R_{(\sigma)}$ and $R_{(int)}$ (indicating internal consistency of reflection intensities for merged pairs) having values of 0,0320 and 0,0178 respectively the data were considered to be of good quality (R-factor expressions are to be found in Appendix 1).

Analysing the data as a function of resolution in the range of 1,1 to 1,2 Å it was found that 158 of the 323 theoretically possible reflections were actually observed. Since this constitutes a fraction considerably greater than the one quarter required for centrosymmetric structures it was concluded that solution of the structure by direct methods was likely to succeed.

Though the space group $P2_1/c$ is uniquely defined by systematically absent reflections the E-statistics were analysed to test the consistency of the method. The mean $|E^2 - 1|$ values for the *0kl, h0l, hk0* projections and for the remaining reflections were calculated to be 1,034, 1,033, 0,971 and 1,027 respectively. Because they are all close to the theoretical value of 0,986 the crystal is confirmed to be centric. This is consistent with and consequently confirms the space group to be $P2_1/c$ [130].

Subsequently 146 subset reflections were chosen according to their estimated α values as well as their ability to generate a large number of negative quartets (1813 were found of which 1000 were used). The 50 subset phase permutations considered to be the best were refined by 4 cycles of full tangent refinement. The best solution chosen on the basis of its combined figure of merit, CFOM, (see Appendix 1) was extended by

expanding the tangent refinement to include all 535 reflections with E > 1,200 and performing one cycle of E-Fourier refinement.

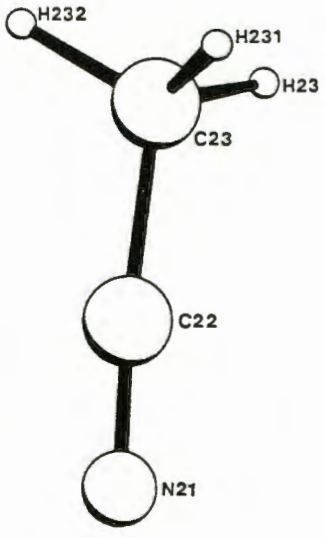

Figure 5.2. The numbering scheme used for the acetonitrile molecule

The 17 highest peaks of the E-map resulted in a chemically reasonable model. Of the 17 peaks 14 could be identified as belonging to the non-hydrogen atoms of the host molecule situated on the Wyckoff special position *d* (½,½,0), which has a site symmetry of $\bar{1}$ (consistent with the host molecule symmetry) and a multiplicity of 2 in the space group $P2_1/c$. The remaining 3 peaks identified the guest non-hydrogen atoms. The R-factor based on the 513 E-values used, R_E, was calculated to be 0,271.

The 17 atom positions thus obtained were employed as the trial model for refinement by full-matrix least-squares using SHELX-76. All atoms were treated isotropically. This resulted in a R value of 0,167.

As a next step all heavy atoms (C, O, N) were refined anisotropically. This permitted a reduction in the R-factor to 0,121 as well as allowing the identification of all hydrogen atoms other than the hydroxyl hydrogens in the difference Fourier synthesis.

The model was therefore updated to include all these hydrogen atoms in geometrically idealised positions, all being constrained to a distance of 1,00 Å from and allowed to ride on their parent atom. The temperature factors of all (aromatic) host hydrogens were linked, as were those of the three methyl hydrogens of the guest. This model realised an R of 0,095. Analysis of the interatomic distances revealed the distance

between the host oxygen O(1) and the nitrogen of the guest N(21) to be 2,880 Å, indicative of the presence of a hydrogen bond.

Though a diffuse peak was observed in this region the hydrogen atom could not be located. It was consequently constrained to within theoretically plausible (see section 5.1.3) distances from the hydrogen bond donor and acceptor atoms. Refinement led to final O(1)-H(1) and N(21)···H(1) distances of 0,970 Å and 1,952 Å . This represented a satisfactory location of the hydroxyl hydrogen H(1).

Two reflections (1,0,4 and -1,0,4) with δ/σ larger than 9 were suppressed to allow for improved refinement. The elimination of these reflections was justified by the fact that both reflections, being reflections at low theta values, suffer seriously from extinction effects, indicated by F_o-values far lower than the corresponding F_c-values.

A weighting scheme based on $\sigma^2(F) + gF^2$ was used to allow a further refinement of the model. The weighting scheme was chosen to yield minimal variation in the parameter $\Sigma\omega(\Delta F)^2$ of reflections with sin θ and $(F/F_{max})^{½}$. Values of g between 0 and 1 were used which led to the conclusion that though unit weights resulted in the smallest Goodness of Fit parameter (S = 1,25), this gave poor analysis of variance. On the other hand minimal variation was obtained when a weighting scheme based on a g = 0,05 was used which yielded an artificially high S-value of 2,62. This weighting scheme was retained even though this caused a slight increase in the R-factor.

The final full-matrix least-squares refinement of the model on F minimizing $\Sigma\omega||F_o| - |F_c||^2$ using 1370 independent reflections realised a clear convergence of parameters and resulted in a final R = 0,096 while R_w = 0,117. The Δ/σ values were all low (<0,1%).

The guest atoms were observed to generally display larger temperature factors than the host atoms, which were ascribed to vibrational effects. Relatively large peaks of electron density [$(\Delta\rho)_{max}$ = 0,40 e.Å^{-3}] in the vicinity of the guest, however, indicate a certain degree of positional disorder in the guest.

(As mentioned in Section 5.1 crystal data and details of data collections and refinements are given in Tables 5.2.1, 2 and 3, while an analysis of variance is given in Table 5.2.4. Table 5.2.5 lists the fractional atomic coordinates while hydrogen-bond data are given in Table 5.2.6. Finally bond lengths, bond angles and torsion angles are supplied at the end of Chapter 5, while information on least-squares planes and tables of observed and calculated structure factors may be found in Appendix 3.)

Table 5.2.1. : NITRANN - Crystal Data

Host : Guest	1 : 2
Molecular formula	$C_{26}H_{20}O_2 \cdot 2C_2H_3N$
Molecular weight ($g.mol^{-1}$)	446,54
Space group	$P2_1/c$
Z	2
a / (Å)	8,530(2)
b / (Å)	16,995(6)
c / (Å)	9,034(1)
α / (°)	90,0
β / (°)	109,15(2)
γ / (°)	90,0
V / ($Å^3$)	1237,1(6)
D_c / ($g.cm^{-3}$)	1,199
D_m / ($g.cm^{-3}$)	1,176(8)
μ(MoKα) (cm^{-1})	0,805
F(000) / e	472,0

Table 5.2.2. : NITRANN - Data collection parameters

Crystal dimensions (mm)	0,5 x 0,5 x 0,5
Range scanned θ (°)	1 - 25
Range of indices (h,k,l)	$-10 \leq h \leq 10$
	$0 \leq k \leq 20$
	$0 \leq l \leq 10$
Reflections for lattice parameters no., θ range (°)	24, 16 - 17
Instability of standard reflections (%)	0,7%
Scan mode	ω-2θ
Scan width in ω (°)	(0,90+0,35tanθ)
Vertical aperture length (mm)	(4)
Aperture width (mm)	(1,20+1,05tanθ)
Number of reflections collected	2415
Number of unique reflections	2177

Table 5.2.3. : NITRANN - Final refinement

Number of observed ($I_{rel} > 2\sigma I_{rel}$) reflections, N,	1363
Number of parameters, NP	163
N / NP	8,4
$R=(R\|\|F_o\|-\|F_c\|\|)/(R\|F_o\|)$	0,096
$wR=(R\|\|F_o\|-\|F_c\|\|\cdot w^{½})/(R\|F_o\|\cdot w^{½})$	0,117
$w=1/(\sigma^2(F)+[g]\cdot F^2)$	$1/(\sigma^2F - 0{,}050F^2)$
S	2,62
Max. shift/esd	≤0,1%
Max. height in difference Fourier map (e.Å^{-3})	0,39
Min. height in difference Fourier map (e.Å^{-3})	-0,29

Table 5.2.4. : NITRANN - Analysis of variance

By parity groups

Group	*ggg*	*ugg*	*gug*	*uug*	*ggu*	*ugu*	*guu*	*uuu*	All
M	195	180	161	177	147	155	185	170	1370
V	89	86	78	73	74	73	81	92	81

As a function of sin θ

SINθ	0,00 - 0,18	0,18 - 0,22	0,22 - 0,26	0,26 - 0,28	0,28 - 0,31	0,31 - 0,33	0,33 - 0,35	0,35 - 0,38	0,38 - 0,40	0,40 - 0,43
M	161	120	174	95	176	126	125	174	113	106
V	79	85	76	81	80	89	84	73	90	84

As a function of $(F/F_{max})^{½}$

$(F/F_{max})^{½}$	0 - 0,15	0,15 - 0,17	0,17 - 0,19	0,19 - 0,21	0,21 - 0,23	0,23 - 0,25	0,25 - 0,28	0,28 - 0,32	0,32 - 0,39	0,39 - 1,00
M	147	152	145	169	130	104	125	128	139	131
V	112	99	73	86	87	64	78	72	66	45

As a function of [Miller indices]

h	0	1	2	3	4	5	6	7	8	9	10	11	12	13	Rest
M	112	229	214	193	168	147	130	88	60	25	4	0	0	0	0
V	73	77	84	92	90	77	76	75	71	78	69	0	0	0	0

k	0	1	2	3	4	5	6	7	8	9	10	11	12	13	Rest
M	58	105	110	109	105	102	94	94	86	90	82	76	57	52	150
V	100	94	100	89	82	84	84	88	82	75	62	64	57	65	67

l	0	1	2	3	4	5	6	7	8	9	10	11	12	13	Rest
M	119	208	221	179	150	140	132	100	77	30	14	0	0	0	0
V	59	60	63	91	122	96	73	77	75	72	98	0	0	0	0

M = Number of reflections in that Group

V = $100[N \Sigma(\omega|F_o - F_c|^2)/(M \Sigma\omega)]$ where M = total number of reflections

TABLE 5.2.5. : NITRANN - Fractional atomic coordinates (x10⁴) and Thermal Parameters (Å² x 10³) with e.s.d.'s in parentheses.

Atom	x/a	y/b	z/c	U_{iso}/U_{eq}(*)
C(1)	6634(5)	4943(2)	1311(5)	40(1) *
O(1)	7927(4)	5525(2)	1901(4)	60(2) *
H(1)	7483(38)	6039(6)	1517(46)	59(14)
C(2)	6452(5)	4756(2)	-350(5)	42(2) *
C(3)	7887(5)	4523(3)	-681(5)	49(2) *
H(3)	8984(5)	4513(3)	177(5)	82(6)
C(4)	7785(7)	4303(3)	-2194(6)	56(2) *
H(4)	8816(7)	4155(3)	-2425(6)	82(6)
C(5)	6305(7)	4291(3)	-3352(6)	60(2) *
H(5)	6229(7)	4105(3)	-4424(6)	82(6)
C(6)	4892(6)	4536(3)	-3050(5)	50(2) *
H(6)	3808(6)	4545(3)	-3925(5)	82(6)
C(7)	4940(5)	4771(2)	-1568(5)	41(2) *
C(11)	7255(6)	4207(2)	2341(5)	44(2) *
C(12)	6337(7)	3516(3)	1936(7)	60(2) *
H(12)	5331(7)	3494(3)	978(7)	82(6)
C(13)	6846(10)	2856(3)	2892(9)	83(3) *
H(13)	6168(10)	2364(3)	2624(9)	82(6)
C(14)	8222(9)	2861(4)	4159(8)	78(3) *
H(14)	8562(9)	2376(4)	4811(8)	82(6)
C(15)	9164(9)	3540(4)	4564(7)	79(3) *
H(15)	10196(9)	3551(4)	5498(7)	82(6)
C(16)	8634(7)	4214(3)	3626(5)	61(2) *
H(16)	9292(7)	4711(3)	3914(5)	82(6)
N(21)	7312(10)	7179(3)	1254(11)	126(4) *
C(22)	7521(8)	7774(4)	1828(8)	81(3) *
C(23)	7753(13)	8544(4)	2499(13)	114(5) *
H(231)	8265(13)	8446(4)	3648(13)	182(25)
H(232)	6637(13)	8791(4)	2287(13)	182(25)
H(233)	8481(13)	8905(4)	2140(13)	182(25)

Anisotropic atoms have thermal parameters ($Å^2 \times 10^3$) of the form :

$\exp(-2\pi^2(U_{11}h^2a^{*2} + U_{22}k^2b^{*2} + U_{33}l^2c^{*2} + 2U_{23}klb^*c^*\cos\alpha + 2U_{13}hla^*c^*\cos\beta + 2U_{12}hla^*b^*\cos\gamma)$

Atom	U11	U22	U33	U23	U13	U12
C(1)	35(2)	33(2)	52(2)	2(2)	15(2)	2(2)
O(1)	54(2)	40(2)	90(3)	-10(2)	29(2)	-11(1)
C(2)	45(2)	31(2)	58(3)	5(2)	29(2)	3(2)
C(3)	42(2)	48(3)	64(3)	12(2)	26(2)	8(2)
C(4)	65(3)	49(3)	70(3)	11(2)	44(3)	16(2)
C(5)	81(4)	55(3)	55(3)	4(2)	39(3)	13(3)
C(6)	58(3)	46(2)	47(3)	3(2)	18(2)	10(2)
C(7)	49(3)	29(2)	54(3)	4(2)	29(2)	4(2)
C(11)	51(3)	39(2)	48(2)	-1(2)	24(2)	7(2)
C(12)	60(3)	44(3)	76(3)	8(2)	22(3)	1(2)
C(13)	98(5)	42(3)	123(6)	20(3)	55(5)	12(3)
C(14)	99(5)	70(4)	76(4)	25(3)	42(4)	36(4)
C(15)	89(4)	96(5)	53(3)	11(3)	24(3)	40(4)
C(16)	70(3)	62(3)	47(3)	-5(2)	14(3)	15(3)
N(21)	131(6)	56(4)	180(7)	-26(4)	38(5)	-17(4)
C(22)	80(4)	57(4)	102(5)	1(3)	24(4)	-8(3)
C(23)	141(7)	65(5)	165(8)	-29(5)	92(6)	-24(5)

TABLE 5.2.6. : NITRANN - Hydrogen bonding data

Donor-H	Donor···Acceptor	H···Acceptor	Donor-H···Acceptor
O(1)-H(1)	O(1)···N(21)	H(1)···N(21)	O(1)-H(1)···N(21)
0,97(2) Å	2,884(6) Å	1,95(1) Å	161(3)°

5.3. PROP

The space group for the crystal structure of **PROP** was identified to be $P2_1/n$. This space group is equivalent to $P2_1/c$ but refers to a different cell choice which causes the c-glide plane to be converted into an n-glide plane. The X-ray data collection of 2569 reflections in the range of $1^\circ \leq \theta \leq 25^\circ$ exhibited the non-extinction reflection conditions consistent with this space group :

$$h0l : h + l = 2n$$
$$(h00 : h = 2n)$$
$$(00l : l = 2n)$$
$$0k0 : k = 2n$$

After 163 systematically absent reflections had been rejected and equivalent reflections merged, 2323 unique reflections remained of which 1567 were considered to be observed. Values for R_{int} = 0,030 and R_σ = 0,036 indicated a data set of moderately good quality.

E-maps were generated using 259 reflections with normalised structure factors ≥ 1,2. The best E-map, chosen because of its combined figure of merit, CFOM = 0,04, had an R-factor calculated on the basis of E-values R_E = 0,228. The highest 18 peaks were found to represent a chemically realistic model showing all host as well as guest non-hydrogen atoms. The host atoms were found to be centered around the Wyckoff special position d $(0,\frac{1}{2},\frac{1}{2})$ which has a site symmetry of $\bar{1}$, as required by the host symmetry, while the guest was found in a general position.

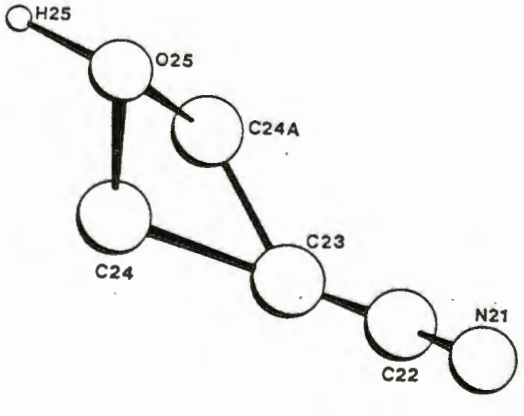

Figure 5.3 The numbering scheme used for the 3-Hydroxypropionitrile molecule.

From the E-map, the γ-carbon on the guest (C(24)) was observed to have an electron density significantly lower than that of the other non-hydrogen atoms. At a distance of 1,57 Å from this peak another peak of electron density significantly above that expected for a hydrogen atom could be distinguished. It was concluded that the C(24) of the guest was positionally disordered between the two sites.

This interpretation was supported by the subsequent difference electron density map. This revealed an arc of electron density in the region of the C(24) with clear maxima at the two extreme positions.

The disordered guest hypothesis was tested by means of the Hamilton test by comparing the R-factors of the two possible models. The first included only one position for C(24) while both were included in the second requiring the sum of the site occupancy factors (s.o.f.) of the alternate peaks C(24) and C(24A) to equal one. All non-hydrogen atoms were varied isotropically. While the first model realised a R = 0,145 the second yielded a corresponding figure of 0,132 after a similar number of cycles of refinement. The Hamilton test indicated that the second model is significantly better than the first (at the 0,005 confidence level) thus vindicating the initial assumption.

The s.o.f.'s of C(24) and C(24A) at this stage were found to be 0,558 and 0,443 respectively. Because of subsequent coupling between the s.o.f.'s and the anisotropic temperature factors of the disordered carbon, it was deemed necessary to refine the s.o.f.'s and the temperature factors independently.

Modelling all non-hydrogen atoms anisotropically caused a reduction of the R to 0,093. The introduction of all non-hydroxyl hydrogens of the host in idealised positions (C-H = 1,00 Å) and of the hydroxyl hydrogens (at constrained distances from both the hydrogen bond donor and acceptor atoms) resulted in a further improvement of the model.

The guest hydrogens were only partially observable due to the disordered nature of the molecular backbone. They were nevertheless initially included in calculated positions with s.o.f.'s linked to their parent atoms and fixed positionally. This necessitated intermittent recalculation of the positional parameters, yielding a residual factor of R = 0,066. However this was not found to be significantly better than the model which did not include the disordered hydrogen atoms and, in addition, resulted in abnormal hydrogen bond parameters. Consequently it was decided not to include these hydrogens in the final model.

An approximate weighting scheme based on a g-value of 0,02 was introduced. At convergence, $(\Delta/\sigma)_{max}$ = 0,056, final R = 0,066 and R_w = 0,082.

The final difference Fourier map showed no indications of incorrectly placed atoms. However, as expected, a maximum residual electron density, $(\Delta\rho)_{max}$, of 0,31 e.Å^{-3} reflected the absence of the methylene hydrogens of the guest. The minimum residual electron density, $(\Delta\rho)_{min}$, by contrast was found to be lower at -0,25 e.Å^{-3}.

The tables below list additional information on crystal data, data collection parameters, final refinement data, analysis of variance, fractional atomic coordinates and hydrogen bonding data. Bond lengths, bond angles, torsion angles appear at the end of the chapter (pp 89), while least-squares planes data and the observed and calculated structure factors may be found in the appendices.

Table 5.3.1. : PROP - Crystal Data

Host : Guest	1 : 2
Molecular formula	$C_{26}H_{20}O_2 \cdot 2C_3H_5NO$
Molecular weight ($g.mol^{-1}$)	506,60
Space group	$P2_1/n$
Z	2
a / (Å)	8,444(1)
b / (Å)	9,7931(7)
c / (Å)	16,558(2)
α / (°)	90,0
β / (°)	104,34(1)
γ / (°)	90,0
V / ($Å^3$)	1326,6(3)
D_c / ($g.cm^{-3}$)	1,268
D_m / ($g.cm^{-3}$)	1,278(8)
μ(MoKα) (cm^{-1})	0,41
F(000) / e	504,0

Table 5.3.2. : PROP - Data collection

Crystal dimensions (mm)	0,34 x 0,38 x 0,41
Range scanned θ (°)	1 - 25
Range of indices (h,k,l)	$-10 \leq h \leq 10$
	$0 \leq k \leq 11$
	$0 \leq l \leq 19$
Reflections for lattice parameters no., θ range (°)	15,96 - 16,78
Instability of standard reflections (%)	1,5%
Scan mode	ω-2θ
Scan width in ω (°)	(0,85 + 0,35tanθ)
Vertical aperture length (mm)	(4)
Aperture width (mm)	(1,12 + 1,05tanθ)
Number of reflections collected	2569
Number of unique reflections	2323

Table 5.3.3. : PROP - Final refinement

Number of observed ($I_{rel} > 2\sigma I_{rel}$)reflections, N	1567
Number of parameters, NP	191
N / NP	8,4
$R = (R\|\|F_o\|-\|F_c\|\|)/(R\|F_o\|)$	0,066
$wR = (R\|\|F_o\|-\|F_c\|\| \cdot w^{½})/(R\|F_o\| \cdot w^{½})$	0,082
$w = 1/(\sigma^2(F) + [g] \cdot F^2)$	$1/(\sigma^2F - 0{,}02F^2)$
S	2,71
Max. shift/esd	0,056
Max. height in difference Fourier map ($e.Å^{-3}$)	0,31
Min. height in difference Fourier map ($e.Å^{-3}$)	-0,25

TABLE 5.3.4. : PROP - Analysis of variance

By parity groups

Group	*ggg*	*ugg*	*gug*	*uug*	*ggu*	*ugu*	*guu*	*uuu*	All
M	227	166	197	198	175	226	192	186	1567
V	90	67	85	70	81	80	69	66	77

As a function of sin θ

SINθ	0,00 - 0,18	0,18 - 0,22	0,22 - 0,26	0,26 - 0,29	0,29 - 0,31	0,31 - 0,34	0,34 - 0,36	0,36 - 0,38	0,38 - 0,40	0,40 - 0,43
M	174	185	131	175	136	218	147	132	139	130
V	113	87	69	65	63	63	76	70	68	78

As a function of $(F/F_{max})^{½}$

$(F/F_{max})^{½}$	,0- 0,15	0,15 - 0,17	0,17 - 0,19	0,19 - 0,20	0,20 - 0,22	0,22 - 0,24	0,24 - 0,27	0,27 - 0,31	0,31 - 0,37	0,37 - 1,00
M	187	174	200	96	145	158	168	150	150	139
V	122	82	92	69	77	56	48	54	44	72

As a function of [Miller indices]

h	0	1	2	3	4	5	6	7	8	9	10	11	12	13	Rest
M	129	255	252	226	211	165	136	102	62	28	1	0	0	0	0
V	107	77	80	70	79	67	68	69	72	67	65	0	0	0	0

k	0	1	2	3	4	5	6	7	8	9	10	11	12	13	Rest
M	118	206	201	211	191	161	145	115	105	63	34	17	0	0	0
V	102	72	78	85	63	66	79	65	80	60	108	79	0	0	0

l	0	1	2	3	4	5	6	7	8	9	10	11	12	13	Rest
M	71	124	124	136	120	132	109	111	100	77	88	72	76	57	170
V	112	91	73	70	103	82	65	63	70	76	74	73	69	64	59

M = Number of reflections in that Group

$V = 100[N \Sigma(\omega|F_o - F_c|^2)/(M \Sigma\omega)]$ where M = total number of reflections

TABLE 5.3.5.: PROP - Fractional atomic coordinates (x 10^4) and Thermal Parameters ($Å^2$ x 10^3) with e.s.d.'s in parentheses

Atom	x/a	y/b	z/c	U_{iso}/U_{eq}(*)
C(1)	765(4)	3790(3)	5532(2)	29(1) *
O(1)	157(3)	3226(2)	6196(1)	39(1) *
H(1)	-345(61)	2322(23)	6118(17)	98(17)
C(2)	1174(4)	5269(3)	5784(2)	31(1) *
C(3)	2304(4)	5507(3)	6542(2)	41(1) *
H(3)	2820(4)	4650(3)	6929(2)	58(4)
C(4)	2771(5)	6814(4)	6808(2)	48(1) *
H(4)	3644(5)	6979(4)	7398(2)	58(4)
C(5)	2114(5)	7914(4)	6309(2)	43(1) *
H(5)	2489(5)	8943(4)	6500(2)	58(4)
C(6)	981(4)	7679(4)	5572(2)	41(1) *
H(6)	445(4)	8542(4)	5195(2)	58(4)
C(7)	500(4)	6371(3)	5291(2)	31(1) *
C(11)	2349(4)	3068(3)	5465(2)	34(1) *
C(12)	3200(5)	3595(4)	4914(2)	46(1) *
H(12)	2741(5)	4490(4)	4549(2)	58(4)
C(13)	4624(5)	2983(5)	4829(3)	57(2) *
H(13)	5273(5)	3398(5)	4399(3)	58(4)
C(14)	5217(5)	1849(4)	5295(3)	58(2) *
H(14)	6321(5)	1362(4)	5223(3)	58(4)
C(15)	4407(5)	1333(4)	5847(3)	59(2) *
H(15)	4890(5)	454(4)	6220(3)	58(4)
C(16)	2955(5)	1940(4)	5932(3)	48(1) *
H(16)	2314(5)	1522(4)	6365(3)	58(4)
N(21)	-4087(5)	5468(4)	8633(2)	62(1) *
C(22)	-3794(5)	4566(4)	8292(3)	53(2) *
C(23)	-3432(8)	3361(5)	7837(4)	88(3) *
C(24)	-2882(14)	3787(14)	7066(7)	89(4) *
C(24A)	-2099(26)	3318(12)	7572(12)	85(8) *
O(25)	-1518(6)	4570(5)	7245(3)	104(2) *
H(25)	-882(67)	4337(20)	6840(29)	120(21)

Anisotropic atoms have thermal parameters ($Å^2 \times 10^3$) of the form :

$$\exp(-2\pi^2(U_{11}h^2a^{*2} + U_{22}k^2b^{*2} + U_{33}l^2c^{*2} + 2U_{23}klb^*c^*\cos\alpha + 2U_{13}hla^*c^*\cos\beta + 2U_{12}hla^*b^*\cos\gamma)$$

Atom	U11	U22	U33	U23	U13	U12
C(1)	33(2)	30(2)	27(2)	7(1)	11(1)	5(1)
O(1)	49(1)	38(1)	33(1)	8(1)	17(1)	1(1)
C(2)	33(2)	30(2)	31(2)	2(1)	11(1)	8(1)
C(3)	41(2)	42(2)	36(2)	-1(2)	5(1)	0(2)
C(4)	42(2)	58(2)	41(2)	-6(2)	7(2)	0(2)
C(5)	44(2)	42(2)	44(2)	-12(2)	12(2)	-6(2)
C(6)	45(2)	34(2)	44(2)	-1(2)	11(2)	2(2)
C(7)	33(2)	32(2)	32(2)	0(1)	15(1)	0(1)
C(11)	37(2)	31(2)	35(2)	2(1)	9(1)	7(1)
C(12)	44(2)	51(2)	49(2)	9(2)	21(2)	6(2)
C(13)	49(2)	66(3)	64(3)	0(2)	28(2)	9(2)
C(14)	41(2)	57(2)	78(3)	-11(2)	19(2)	13(2)
C(15)	47(2)	49(2)	76(3)	9(2)	7(2)	18(2)
C(16)	55(2)	36(2)	56(2)	8(2)	19(2)	7(2)
N(21)	71(2)	50(2)	73(2)	19(2)	34(2)	0(2)
C(22)	59(3)	44(2)	63(3)	1(2)	27(2)	1(2)
C(23)	117(5)	53(3)	119(5)	-25(3)	72(4)	-1(3)
C(24)	77(7)	121(10)	79(7)	-40(7)	37(6)	-11(7)
C(24A)	136(14)	41(6)	105(12)	-9(7)	83(12)	19(8)
O(25)	119(4)	107(3)	114(3)	-40(3)	78(3)	-25(3)

Table 5.3.6. : PROP - Hydrogen Bonding Data

Donor-H	Donor···Acceptor	H···Acceptor	Donor-H···Acceptor
O(25)-H(25)	O(25)···O(1)^{i}	H(25)···O(1)^{i}	O(25)-H(25)···O(1)^{i}
0,99(6) Å	2,823(5) Å	1,89(5) Å	158(2)°
O(1)-H(1)	O(1)···N(21)^{ii}	H(1)···N(21)^{ii}	O(1)-H(1)···N(21)^{ii}
0,98(3) Å	2,883(4) Å	1,95(3) Å	160(2)°

Equivalent positions:
(i) x,y,z
(ii) -1/2-x, -1/2+y, 3/2-z

5.4. PYD

Crystal data as well as data collection parameters are given in Table 5.4.1 i) and ii).

No symmetry (other than $\bar{1}$) being apparent in preliminary photographs (oscillation and zero-level Weissenberg) it was concluded that the crystal structure **PYD** belonged to either of the triclinic space groups P1 or P$\bar{1}$. As the space group was not uniquely determined by systematic absences, analysis of the reflections collected was required to decide whether the crystal is centrosymmetric or not. Were it centrosymmetric this would indicate that it belongs to the space group P$\bar{1}$.

The mean $|E^2-1|$ values[130] for the 0*kl*, *h*0*l*, *hk*0 projections and the remaining data were all found to be close to the centric value of 0,968. This indicated that the structure **PYD** does, in fact, belong to the triclinic space group P$\bar{1}$. Corrections for Lorentz-polarisation effects were applied but no absorption or decay corrections were made to the data.

Of a total of 5093 measured reflections 4163 were found to be unique. A further 988 were suppressed as unobserved ($4\sigma(F) > F$) leaving 3175 observed reflections. All remaining reflections were used in the structure solution by direct methods using SHELX-86. With $R_{(\sigma)}$ = 0,0401 and $R_{(int)}$ = 0,0154 the data were considered to be of good quality.

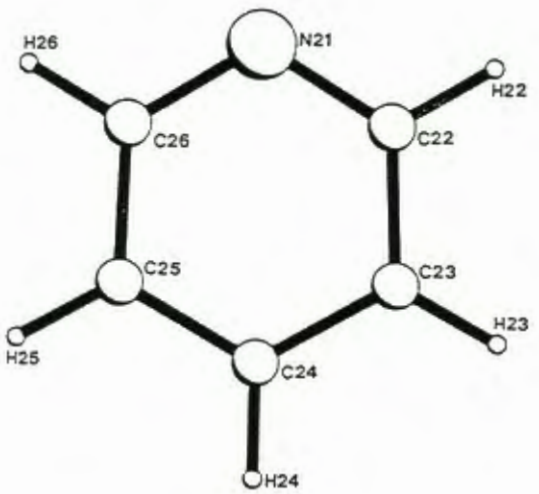

Figure 5.4 The numbering scheme for the Pyridine molecule.

For the 'best' solution obtained, the point atom R-factor based on E-values was calculated to be R_E = 0,260 for 40 peaks. From the E-map calculated on the basis of

these 40 peaks, it was clear that two distinct host molecules centered about two different points of inversion occupied the unit cell and two guest molecules were identified in general positions. With their centrosymmetric opposites, this resulted in two crystallographically distinct host molecules and four guest molecules per unit cell.

The refinement of the 40 non-hydrogen atoms modelled isotropically using SHELX-76 resulted in an initial R = 0,142. The initial refinement was base on a primitive unit cell with a = 9,699(3), b = 9,797(3), c = 17,399(4), α = 105,40(2), β = 92,58(2), γ = 116,80(2). The anisotropic variation of all non-hydrogen atoms, though reducing the R-factor, led to a large degree of coupling between U_{11} and U_{12} as well as U_{22} and U_{12} temperature factors which precluded satisfactory refinement of these parameters. The source of this coupling was traced to the fact that the interaxial angle γ = 116,80° differed appreciably (>10%) from 90° (reference 125 page 366) This problem could only be overcome by refining the structure using a non-reduced unit cell with all angles closer to 90°.

In order to simplify the conversion process it was decided that a new set of axes was to be generated which retained the axes $\underline{b}$ and $\underline{c}$ while replacing $\underline{a}$ by any combination of $\underline{a}$ and $\underline{b}$, thereby moving it in the $\underline{ab}$-plane.

Replacing $\underline{a}$ by $\underline{a}' = \underline{a} + \underline{b}$ produced a cell with $\underline{a}'$ = 10,216 Å, $\underline{b}'$ = 9,797 Å, $\underline{c}'$ = 17,399 Å, α' = 105,41°, β' = 107,31° and γ' = 57,93° ($\underline{b}' = \underline{b}$, $\underline{c}' = \underline{c}$ and $\alpha' = \alpha$ as explained above). However, γ' was now found to be equally far from 90° giving rise to the same problem as before.

Thus, instead, $\underline{a}$ was replaced by $\underline{a}' = 2\underline{a} + \underline{b}$. This results in a C-centered cell (Space group $C\bar{1}$) with a unit cell volume of twice that of the original cell. Now $\underline{a}' = 2\underline{a} + \underline{b}$ = 17,350 Å, β' = 101,56° and γ' = 86,51°.

(For the mathematical basis of the matrix calculations performed below chapter 5 of the International Tables for Crystallography[132] or alternatively any standard text on matrix mathematics may be consulted.)

The Bragg plane transformations are converted by the following matrix calculation:

$$\begin{bmatrix} h' \\ k' \\ l' \end{bmatrix} = \begin{bmatrix} 2 & 1 & 0 \\ 0 & 1 & 0 \\ 0 & 0 & 1 \end{bmatrix} \begin{bmatrix} h \\ k \\ l \end{bmatrix}$$

The corresponding conversion matrix required to transform the fractional coordinates is the transpose of the inverse of the matrix above viz.:

$$\begin{bmatrix} \frac{1}{2} & 0 & 0 \\ -\frac{1}{2} & 1 & 0 \\ 0 & 0 & 1 \end{bmatrix}$$

The equivalent positions for the C-centered cell are :

x',y',z' ; $-x',-y',-z'$; $\frac{1}{2}+x',\frac{1}{2}+y',z'$ and $\frac{1}{2}-x',\frac{1}{2}-y',-z'$.

With this transformation of the unit cell, the parameters for the 40 anisotropic non-hydrogen atoms could refine satisfactorily yielding an R = 0,105. All non-hydroxyl hydrogen atoms were introduced in geometrically idealised positions with linked temperature factors for equivalent hydrogen atoms. This was followed by inclusion of the hydroxyl hydrogens atoms constrained to within suitable distances from the hydrogen bond acceptor and donor atoms. All hydrogen atoms were modelled isotropically thus leading to a further reduction in the R-factor to R = 0,074.

The introduction of a g-parameter for the weighting scheme of g = 0,008 resulted in a final R = 0,072 and a R_W = 0,077. No reflections were excluded since $(\Delta/\sigma)_{max}$ = 4,04. Minimal remaining electron density revealed no further peaks, while all (Δ/σ) values $\leq$ 0,001 indicated excellent convergence.

TABLE 5.4.1. : PYD - Crystal Data

Host : Guest	1 : 2
Molecular formula	$C_{26}H_{20}O_2 \cdot 2C_5H_5N$
Molecular weight ($g.mol^{-1}$)	522,64
Space group	$C\bar{1}$
Z	2 4
a / (Å)	17,350(3)
b / (Å)	9,796(3)
c / (Å)	17,399(4)
α / (°)	105,41(2)
β / (°)	101,56(2)
γ / (°)	86,51(3)
V / ($Å^3$)	2793(1)
D_c / ($g.cm^{-3}$)	1,243
D_m / ($g.cm^{-3}$)	1,239(5)
μ(MoKα) (cm^{-1})	0,42
F(000) / e	1104,0

TABLE 5.4.2. : PYD - Data collection

Crystal dimensions (mm)	0,31 x 0,41 x 0,41
Range scanned θ (°)	1 - 25
Range of indices (h,k,l)	$-33 \leq h \leq 33$
	$-11 \leq k \leq 11$
	$0 \leq l \leq 20$
Reflections for lattice parameters: no., θ range (°)	24; $16,07 \leq \theta \leq 16,88$
Instability of standard reflections (%)	1,4%
Scan mode	ω-2θ
Scan width in ω (°)	$(0,85 + 0,35\tan\theta)$
Vertical aperture length (mm)	(4)
Aperture width (mm)	$(1,20 + 1,05\tan\theta)$
Number of reflections collected	5093
Number of unique reflections	4163

TABLE 5.4.3. : PYD - Final refinement

Number of observed ($I_{rel} > 2\sigma I_{rel}$) reflections, N	3175
Number of parameters, NP	368
N / NP	8,6
$R = (R\|\|F_o\|-\|F_c\|\|)/(R\|F_o\|)$	0,072
$wR = (R\|\|F_o\|-\|F_c\|\|\cdot w^{½})/(R\|F_o\|\cdot w^{½})$	0,077
$w = 1/(\sigma^2(F)+[g]\cdot F^2)$	$1/(\sigma^2F - 0{,}008F^2)$
S	2,02
Max. shift/esd	0,001
Max. height in difference Fourier map ($e.Å^{-3}$)	0,33
Min. height in difference Fourier map ($e.Å^{-3}$)	-0,39

TABLE 5.4.4. : PYD - Analysis of variance

By parity groups

Group	*ggg*	*ugg*	*gug*	*uug*	*ggu*	*ugu*	*guu*	*uuu*	All
M	840	0	0	761	752	0	0	822	3175
V	143	0	0	141	143	0	0	143	142

As a function of sin θ

SINθ	0,00 - 0,18	0,18 - 0,23	0,23 - 0,26	0,26 - 0,29	0,29 - 0,31	0,31 - 0,34	0,34 - 0,36	0,36 - 0,38	0,38 - 0,40	0,40 - 0,43
M	354	371	283	320	278	456	279	294	270	270
V	165	151	151	127	122	127	125	151	142	159

As a function of $(F/F_{max})^{½}$

$(F/F_{max})^{½}$	0 - 0,16	0,16 - 0,18	0,18 - 0,20	0,20 - 0,21	0,21 - 0,23	0,23 - 0,26	0,26 - 0,29	0,29 - 0,32	0,32 - 0,38	0,38 - 1,00
M	341	330	397	206	321	385	328	256	299	312
V	186	155	147	135	138	130	120	129	128	137

As a function of [Miller indices]

h	0	1	2	3	4	5	6	7	8	9	10	11	12	13	Rest
M	125	261	256	245	230	236	220	207	201	191	174	162	131	118	418
V	149	135	151	143	158	150	144	146	135	132	123	129	142	137	146

k	0	1	2	3	4	5	6	7	8	9	10	11	12	13	Rest
M	212	424	428	399	380	352	299	242	188	135	85	31	0	0	0
V	179	159	143	134	141	142	125	125	128	129	137	173	0	0	0

l	0	1	2	3	4	5	6	7	8	9	10	11	12	13	Rest
M	143	267	257	247	255	227	215	206	207	195	174	154	145	127	356
V	130	136	143	150	139	143	131	131	155	145	131	147	152	146	150

M = Number of reflections in that Group

V = $100[N \Sigma(\omega|F_o - F_c|^2)/(M \Sigma\omega)]$ where M = total number of reflections

TABLE 5.4.5. : PYD - Fractional atomic coordinates (x 10^4) and Thermal Parameters ($Å^2$ x 10^3) with e.s.d.'s in parentheses

Atom	x/a	y/b	z/c	U_{iso}/U_{eq}(*)
C(1)	385(1)	4668(3)	5804(2)	27(1) *
O(1)	1039(1)	5298(2)	6407(1)	36(1) *
H(1)	1181(18)	6105(23)	6240(14)	69(2)
C(2)	643(2)	3990(3)	5003(2)	27(1) *
C(3)	1261(2)	3001(3)	5014(2)	37(1) *
H(3)	1546(2)	2855(3)	5546(2)	69(2)
C(4)	1481(2)	2233(3)	4311(2)	41(1) *
H(4)	1920(2)	1525(3)	4331(2)	69(2)
C(5)	1095(2)	2437(3)	3571(2)	40(1) *
H(5)	1244(2)	1861(3)	3054(2)	69(2)
C(6)	502(2)	3444(3)	3553(2)	36(1) *
H(6)	234(2)	3611(3)	3021(2)	69(2)
C(7)	272(1)	4231(3)	4268(2)	27(1) *
C(11)	89(2)	3511(3)	6124(2)	31(1) *
C(12)	-319(2)	2357(3)	5580(2)	41(1) *
H(12)	-414(2)	2281(3)	4983(2)	69(2)
C(13)	-592(2)	1311(4)	5856(3)	54(1) *
H(13)	-894(2)	494(4)	5462(3)	69(2)
C(14)	-451(2)	1395(4)	6668(3)	56(2) *
H(14)	-637(2)	626(4)	6865(3)	69(2)
C(15)	-54(2)	2528(4)	7215(2)	53(1) *
H(15)	39(2)	2592(4)	7809(2)	69(2)
C(16)	223(2)	3598(3)	6942(2)	39(1) *
H(16)	515(2)	4420(3)	7341(2)	69(2)
C(1B)	-367(2)	10610(3)	-717(2)	32(1) *
O(1B)	103(1)	8275(2)	983(1)	44(1) *
H(1B)	-238(18)	7674(29)	508(12)	69(2)
C(2B)	-236(2)	10590(3)	768(2)	34(1) *
C(3B)	-464(2)	11144(4)	1517(2)	46(1) *
H(3B)	-245(2)	10725(4)	1982(2)	69(2)
C(4B)	-992(2)	12271(4)	1623(2)	49(1) *
H(4B)	-1152(2)	12654(4)	2161(2)	69(2)
C(5B)	-1294(2)	12857(3)	992(2)	48(1) *
H(5B)	-1668(2)	13678(3)	1070(2)	69(2)
C(6B)	-1079(2)	12311(3)	253(2)	44(1) *

Table 5.4.5 cont.

H(6B)	-1305(2)	12733(3)	-208(2)	69(2)	
C(7B)	-548(2)	11173(3)	133(2)	33(1)	*
C(11B)	1139(2)	9926(3)	1298(2)	32(1)	*
C(12B)	1482(2)	11145(3)	1263(2)	45(1)	*
H(12B)	1212(2)	11690(3)	873(2)	69(2)	
C(13B)	2193(2)	11618(4)	1761(2)	50(1)	*
H(13B)	2431(2)	12502(4)	1731(2)	69(2)	
C(14B)	2575(2)	10880(4)	2298(2)	49(1)	*
H(14B)	3091(2)	11215(4)	2656(2)	69(2)	
C(15B)	2237(2)	9678(4)	2334(2)	46(1)	*
H(15B)	2508(2)	9140(4)	2727(2)	69(2)	
C(16B)	1527(2)	9193(3)	1838(2)	40(1)	*
H(16B)	1297(2)	8306(3)	1870(2)	69(2)	
N(21)	1688(2)	7766(3)	6301(2)	55(1)	*
C(22)	2386(2)	7805(4)	6118(3)	69(2)	*
H(22)	2676(2)	6892(4)	5962(3)	69(2)	
C(23)	2735(3)	9035(5)	6133(3)	80(2)	*
H(23)	3271(3)	9025(5)	6003(3)	69(2)	
C(24)	2327(3)	10269(4)	6329(3)	80(2)	*
H(24)	2560(3)	11184(4)	6340(3)	69(2)	
C(25)	1602(2)	10255(4)	6510(3)	69(2)	*
H(25)	1292(2)	11150(4)	6650(3)	69(2)	
C(26)	1307(2)	8985(4)	6494(2)	55(1)	*
H(26)	778(2)	8974(4)	6635(2)	69(2)	
N(21B)	-950(2)	6249(3)	-149(2)	69(2)	*
C(22B)	-835(3)	5560(4)	-875(3)	71(2)	*
H(22B)	-305(3)	5619(4)	-1007(3)	69(2)	
C(23B)	-1395(3)	4769(4)	-1459(3)	74(2)	*
H(23B)	-1282(3)	4297(4)	-2010(3)	69(2)	
C(24B)	-2109(3)	4632(5)	-1285(3)	82(2)	*
H(24B)	-2529(3)	4048(5)	-1700(3)	69(2)	
C(25B)	-2239(3)	5301(5)	-538(4)	84(2)	*
H(25B)	-2758(3)	5217(5)	-390(4)	69(2)	
C(26B)	-1650(3)	6099(4)	17(3)	76(2)	*
H(26B)	-1753(3)	6589(4)	570(3)	69(2)	

Anisotropic atoms have thermal parameters ($Å^2 \times 10^3$) of the form :

$\exp(-2\pi^2(U_{11}h^2a^{*2} + U_{22}k^2b^{*2} + U_{33}l^2c^{*2} + 2U_{23}klb^*c^*\cos\alpha + 2U_{13}hla^*c^*\cos\beta + 2U_{12}hla^*b^*\cos\gamma)$

Atom	U11	U22	U33	U23	U13	U12
C(1)	24(1)	26(1)	32(2)	13(1)	1(1)	0(1)
O(1)	32(1)	34(1)	40(1)	13(1)	-3(1)	-7(1)
C(2)	25(1)	21(1)	41(2)	11(1)	10(1)	-2(1)
C(3)	32(2)	34(2)	49(2)	20(1)	9(1)	6(1)
C(4)	34(2)	29(2)	70(2)	19(2)	23(2)	10(1)
C(5)	40(2)	31(2)	53(2)	6(1)	22(2)	0(1)
C(6)	39(2)	29(2)	40(2)	7(1)	10(1)	0(1)
C(7)	25(1)	20(1)	36(2)	10(1)	6(1)	-2(1)
C(11)	29(1)	28(1)	40(2)	17(1)	10(1)	5(1)
C(12)	40(2)	35(2)	53(2)	16(2)	10(2)	-6(1)
C(13)	54(2)	35(2)	83(3)	21(2)	23(2)	-9(2)
C(14)	61(2)	41(2)	87(3)	34(2)	37(2)	6(2)
C(15)	60(2)	55(2)	61(2)	35(2)	32(2)	17(2)
C(16)	43(2)	37(2)	44(2)	19(1)	13(1)	6(1)
C(1B)	37(2)	29(2)	31(2)	11(1)	5(1)	0(1)
O(1B)	54(1)	38(1)	44(1)	17(1)	9(1)	-10(1)
C(2B)	29(1)	35(2)	35(2)	6(1)	4(1)	-1(1)
C(3B)	42(2)	58(2)	36(2)	10(2)	8(1)	3(2)
C(4B)	41(2)	55(2)	42(2)	-4(2)	13(2)	6(2)
C(5B)	46(2)	39(2)	53(2)	0(2)	15(2)	12(2)
C(6B)	47(2)	35(2)	47(2)	9(1)	7(2)	7(1)
C(7B)	31(2)	34(2)	34(2)	6(1)	5(1)	-2(1)
C(11B)	36(2)	30(2)	33(2)	8(1)	9(1)	3(1)
C(12B)	44(2)	40(2)	51(2)	21(2)	0(2)	-4(1)
C(13B)	45(2)	43(2)	61(2)	12(2)	5(2)	-8(2)
C(14B)	31(2)	51(2)	56(2)	5(2)	4(2)	5(2)
C(15B)	38(2)	50(2)	46(2)	17(2)	0(1)	14(1)
C(16B)	41(2)	37(2)	42(2)	16(1)	7(1)	8(1)
N(21)	53(2)	44(2)	72(2)	23(2)	8(2)	-7(1)
C(22)	61(3)	46(2)	102(4)	17(2)	26(2)	4(2)

Table 5.4.5. cont.

C(23)	51(2)	69(3)	130(4)	27(3)	39(3)	-3(2)
C(24)	65(3)	53(2)	131(4)	32(3)	26(3)	-14(2)
C(25)	62(3)	40(2)	108(4)	14(2)	27(2)	0(2)
C(26)	45(2)	52(2)	69(3)	13(2)	16(2)	-9(2)
N(21B)	77(3)	49(2)	81(3)	19(2)	2(2)	-15(2)
C(22B)	62(3)	50(2)	98(4)	15(2)	17(3)	0(2)
C(23B)	86(3)	44(2)	87(3)	7(2)	20(3)	4(2)
C(24B)	71(3)	52(3)	109(4)	15(3)	-9(3)	-5(2)
C(25B)	62(3)	60(3)	135(5)	32(3)	23(3)	-7(2)
C(26B)	96(4)	50(2)	90(3)	20(2)	33(3)	0(2)

TABLE 5.4.6. : PYD - Hydrogen bonding data

Donor-H	Donor···Acceptor	H···Acceptor	Donor-H···Acceptor
O(1)-H(1)	O(1)···N(21)	H(1)···N(21)	O(1)-H(1)···N(21)
0,97(3) Å	2,793(4) Å	1,87(3) Å	159(3)°
O(1B)-H(21)	O(1B)···N(21B)	H(1B)···N(21B)	O(1B)-H(1B)···N(21B)
0,98(2) Å	2,842(3) Å	1,89(3) Å	162(2)°

5.5. 3PIC

Despite the fact that the crystal used to collect the data set for **3PIC** was sealed in a Lindemann tube, the total decay observed for the three standard reflections, used to monitor the stability of the crystal, was 46,2% over the 36,9 hours of data collection. On the assumption that the decay was linear and isotropic, decay corrections were applied to the data.

On the basis of preliminary oscillation and Weissenberg photographs **3PIC** had been assigned the monoclinic space group $P2_1/c$. This was supported by analysis of the 5804 reflections measured by the Enraf-Nonius CAD-4 diffractometer.

1473 of the reflections were rejected as being systematically absent or non-unique, while, of the 4331 unique reflections remaining after equivalent reflections had been merged, a further 1151 were suppressed as being unobserved. Notwithstanding the large decay observed for **3PIC**, an $R_{(int)}$ = 0,017 and an $R_{(\sigma)}$ = 0,043 so the data were still considered satisfactory.

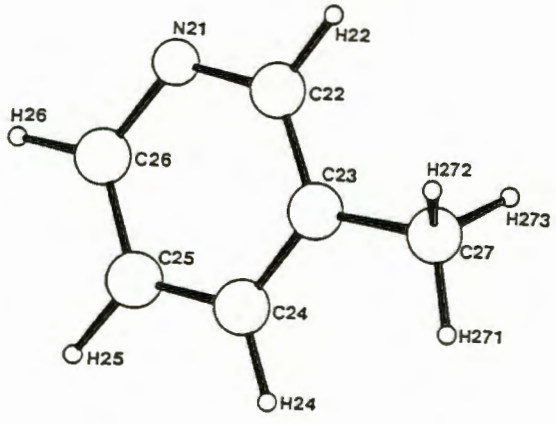

Figure 5.5 The numbering scheme employed for the 3-Methylpyridine molecule.

Analysis of the number of unique data as a function of resolution in the range of 1,1 to 1,2 Å revealed that 390 of the 546 reflections theoretically observable were actually observed, indicating that the structure should solve. .

The best solution obtained, with a combined figure of merit of 0,039 and an R-factor based on E-values R_E = 0,225 for the highest 42 peaks, supplied a chemically sound model for the structure. Two crystallographically distinct host molecules were

observed. The first of these was centered about the centre of inversion situated at ½,0,½ (Wyckoff position d, multiplicity 2). The second was located about the Wyckoff position c (0,0,½) which also has a multiplicity of 2.

Two distinct guest molecules were found to occupy general positions. Thus, because of the number of symmetry operations in the space group $P2_1/c$, the number of formula units per unit cell, Z, was determined to be 4.

Employing the 42 peaks, identified by the direct methods, as the initial model for refinement and treating all non-hydrogen atoms isotropically an initial R = 0,114 was obtained. This was reduced to R = 0,060 by anisotropic modelling of all non-hydrogen atoms and the introduction of all non-hydroxyl hydrogen atoms, with coupled temperature factors, in idealised positions. The methyl group for the guest was modelled as a rigid group.

Further refinement of the model was achieved by the incorporation of the hydroxyl hydrogen atoms. They were restricted to suitable distances from their parent atoms and the hydrogen bond acceptor atoms. Finally the g-value for the weighting scheme was allowed to refine. With a g = 0,005 and a reflection to parameter ratio of 8,0, a R = 0,044, a R_W = 0,053 and a S = 0,881 were achieved. Shift/Esd values ≤ 0,001 indicated excellent convergence of parameters, while minimal residual electron density in the difference Fourier map (Maximum = 0,18, Minimum = 0,22 e.$Å^{-3}$) implied that neither was any peak incorrectly assigned nor had any peaks gone undetected.

Table 5.5.1. : 3PIC - Crystal Data

Host : Guest	1 : 2
Molecular formula	$C_{26}H_{20}O_2 \cdot 2C_6H_7N$
Molecular weight ($g.mol^{-1}$)	550,70
Space group	$P2_1/c$
Z	4
a / (Å)	17,129(4)
b / (Å)	8,2150(5)
c / (Å)	22,066(5)
α / (°)	90,0
β / (°)	106,03(1)
γ / (°)	90,0
V / (Å^3)	2984(2)
D_c / ($g.cm^{-3}$)	1,225
D_m / ($g.cm^{-3}$)	1,226(3)
μ(MoKα) (cm^{-1})	0,41
F(000) / e	1168,0

Table 5.5.2. : 3PIC - Data Collection Parameters

Crystal dimensions (mm)	0,34 x 0,34 x 0,38
Range scanned θ (°)	1 - 23
Range of indices (h,k,l)	$-18 \leq h \leq 18$
	$0 \leq k \leq 9$
	$0 \leq l \leq 24$
Reflections for lattice parameters no., θ range (°)	24; 16,11≤θ≤16,71
Stability of standard reflections (%)	-46,2%
Scan mode	ω-2θ
Scan width in ω (°)	(0,80+0,35tanθ)
Vertical aperture length (mm)	(4)
Aperture width (mm)	(1,12+1,05tanθ)
Number of reflections collected	5804
Number of unique reflections	4331

Table 5.5.3. : 3PIC - Final Refinement

Number of observed ($I_{rel} > 2\sigma I_{rel}$) reflections, N	3180
Number of parameters, NP	396
N / NP	8,0
$R = (R\|\|F_o\|-\|F_c\|\|)/(R\|F_o\|)$	0,044
$wR = (R\|\|F_o\|-\|F_c\|\|\cdot w^{½})/(R\|F_o\|\cdot w^{½})$	0,053
$w = 1/(\sigma^2(F) + [g]\cdot F^2)$	$1/(\sigma^2F - 0{,}005F^2)$
S	0,881
Max. shift/esd	≤ 0,001
Max. height in difference Fourier map (e.Å^{-3})	0,18
Min. height in difference Fourier map (e.Å^{-3})	-0,22

Table 5.5.4. : 3PIC - Analysis of Variance

By parity groups

Group	*ggg*	*ugg*	*gug*	*uug*	*ggu*	*ugu*	*guu*	*uuu*	All
M	483	498	395	412	299	314	404	375	3180
V	83	92	77	77	74	79	77	78	81

As a function of sin θ

SINθ	0,0 -	0,18 -	0,22 -	0,26 -	0,29 -	0,31 -	0,33 -	0,36 -	0,38 -	0,40 -	0,43
M	375	289	377	344	274	295	292	422	266	246	
V	95	83	80	63	61	72	81	76	87	102	

As a function of $(F/F_{max})^{½}$

$(F/F_{max})^{½}$	0,0 -	0,15 -	0,17 -	0,19 -	0,21 -	0,22 -	0,24 -	0,27 -	0,30 -	0,40 -	1,00
M	378	330	337	359	295	284	312	291	304	290	
V	121	86	90	79	80	64	62	62	74	49	

As a function of [Miller indices]

h	0	1	2	3	4	5	6	7	8	9	10	11	12	13	Rest
M	120	246	248	250	237	252	248	237	209	182	165	159	136	125	366
V	77	71	73	76	70	76	86	89	82	83	73	90	78	81	92

k	0	1	2	3	4	5	6	7	8	9	10	11	12	13	Rest
M	303	550	505	476	415	330	268	192	103	38	0	0	0	0	0
V	103	74	80	82	77	73	75	80	85	92	0	0	0	0	0

l	0	1	2	3	4	5	6	7	8	9	10	11	12	13	Rest
M	113	182	215	166	205	171	210	155	191	161	185	142	158	116	810
V	95	85	81	68	105	75	83	83	76	75	74	77	74	78	79

M = Number of reflections in that Group

V = $100[N \Sigma(\omega|F_o - F_c|^2)/(M \Sigma\omega)]$ where M = total number of reflections

TABLE 5.5.5. : 3PIC - Fractional atomic coordinates (x 10^4) and Thermal Parameters (Å² x 10^3) with e.s.d.'s in parentheses

Atom	x/a	y/b	z/c	U_{iso}/U_{eq}(*)
C(1)	5650(1)	-552(3)	4685(1)	34(1) *
O(1)	5965(1)	411(2)	4263(1)	43(1) *
H(1)	5601(19)	1297(31)	4104(10)	103(13)
C(2)	4744(1)	-814(3)	4396(1)	34(1) *
C(3)	4497(1)	-1608(3)	3811(1)	44(1) *
H(3)	4919(1)	-1992(3)	3609(1)	66(2)
C(4)	3693(2)	-1873(3)	3512(1)	51(1) *
H(4)	3529(2)	-2447(3)	3096(1)	66(2)
C(5)	3109(2)	-1336(4)	3791(1)	50(1) *
H(5)	2521(2)	-1507(4)	3573(1)	66(2)
C(6)	3334(1)	-568(3)	4366(1)	43(1) *
H(6)	2906(1)	-201(3)	4566(1)	66(2)
C(7)	4155(1)	-290(3)	4677(1)	34(1) *
C(11)	6081(1)	-2203(3)	4760(1)	36(1) *
C(12)	5850(2)	-3415(3)	5111(1)	46(1) *
H(12)	5405(2)	-3192(3)	5312(1)	66(2)
C(13)	6219(2)	-4922(4)	5190(1)	54(1) *
H(13)	6041(2)	-5776(4)	5446(1)	66(2)
C(14)	6836(2)	-5254(3)	4914(1)	55(1) *
H(14)	7105(2)	-6345(3)	4966(1)	66(2)
C(15)	7072(2)	-4062(4)	4568(1)	56(1) *
H(15)	7516(2)	-4292(4)	4367(1)	66(2)
C(16)	6705(2)	-2540(3)	4492(1)	48(1) *
H(16)	6893(2)	-1683(3)	4242(1)	66(2)
C(1B)	906(1)	-410(3)	5228(1)	36(1) *
O(1B)	1552(1)	-107(2)	4950(1)	50(1) *
H(1B)	1301(11)	129(36)	4519(5)	73(10)
C(2B)	280(1)	-1539(3)	4813(1)	35(1) *
C(3B)	551(2)	-3017(3)	4627(1)	48(1) *
H(3B)	1146(2)	-3267(3)	4754(1)	66(2)
C(4B)	18(2)	-4127(4)	4275(1)	58(1) *
H(4B)	222(2)	-5177(4)	4148(1)	66(2)
C(5B)	-804(2)	-3786(4)	4097(1)	56(1) *
H(5B)	-1198(2)	-4594(4)	3844(1)	66(2)
C(6B)	-1078(2)	-2334(3)	4269(1)	48(1) *
H(6B)	-1673(2)	-2092(3)	4135(1)	66(2)
C(7B)	-544(1)	-1188(3)	4628(1)	36(1) *
C(11B)	1298(1)	-1279(3)	5854(1)	37(1) *
C(12B)	820(2)	-1667(3)	6249(1)	45(1) *

Table 5.5.5 cont.

H(12B)	234(2)	-1353(3)	6124(1)	66(2)	
C(13B)	1138(2)	-2473(3)	6809(1)	53(1)	*
H(13B)	781(2)	-2745(3)	7085(1)	66(2)	
C(14B)	1944(2)	-2904(4)	6989(1)	61(1)	*
H(14B)	2175(2)	-3498(4)	7395(1)	66(2)	
C(15B)	2429(2)	-2517(4)	6609(1)	62(1)	*
H(15B)	3016(2)	-2829(4)	6740(1)	66(2)	
C(16B)	2110(2)	-1688(3)	6039(1)	50(1)	*
H(16B)	2470(2)	-1394(3)	5769(1)	66(2)	
N(21)	4902(1)	2973(3)	3569(1)	60(1)	*
C(22)	4166(2)	2538(4)	3225(1)	59(1)	*
H(22)	3872(2)	1693(4)	3403(1)	95(4)	
C(23)	3776(2)	3165(4)	2639(1)	59(1)	*
C(27)	2958(2)	2531(7)	2268(2)	112(2)	*
H(271)	2775(2)	3131(7)	1858(2)	272(17)	
H(272)	2555(2)	2699(7)	2515(2)	272(17)	
H(273)	3001(2)	1342(7)	2183(2)	272(17)	
C(24)	4185(2)	4347(5)	2408(1)	70(1)	*
H(24)	3938(2)	4835(5)	1983(1)	95(4)	
C(25)	4927(2)	4846(5)	2761(2)	82(2)	*
H(25)	5222(2)	5726(5)	2602(2)	95(4)	
C(26)	5273(2)	4140(4)	3340(2)	71(1)	*
H(26)	5820(2)	4520(4)	3594(2)	95(4)	
N(21B)	1203(1)	986(3)	3708(1)	61(1)	*
C(22B)	1514(2)	2471(4)	3746(1)	64(1)	*
H(22B)	1812(2)	2881(4)	4175(1)	95(4)	
C(23B)	1459(2)	3493(4)	3242(1)	71(1)	*
C(27)	1832(3)	5174(6)	3341(2)	127(2)	*
H(271)	1733(3)	5739(6)	2925(2)	272(17)	
H(272)	2430(3)	5080(6)	3541(2)	272(17)	
H(273)	1579(3)	5815(6)	3623(2)	272(17)	
C(24B)	1060(2)	2893(5)	2656(1)	71(1)	*
H(24B)	1005(2)	3574(5)	2271(1)	95(4)	
C(25B)	739(2)	1360(5)	2603(2)	74(1)	*
H(25B)	446(2)	908(5)	2181(2)	95(4)	
C(26B)	826(2)	450(4)	3140(2)	70(2)	*
H(26B)	591(2)	-672(4)	3097(2)	95(4)	

Anisotropic atoms have thermal parameters ($Å^2 \times 10^3$) of the form :

$EXP(-2\pi^2(U_{11}h^2a^{*2} + U_{22}k^2b^{*2} + U_{33}l^2c^{*2} + 2U_{23}klb^*c^*\cos\alpha + 2U_{13}hla^*c^*\cos\beta + 2U_{12}hla^*b^*\cos\gamma)$

Atom	U11	U22	U33	U23	U13	U12
C(1)	33(1)	38(1)	33(1)	4(1)	11(1)	0(1)
O(1)	43(1)	47(1)	43(1)	11(1)	19(1)	0(1)
C(2)	34(1)	35(1)	32(1)	5(1)	5(1)	0(1)
C(3)	44(1)	49(2)	38(1)	0(1)	7(1)	1(1)
C(4)	51(2)	52(2)	43(1)	-4(1)	1(1)	-1(1)
C(5)	37(1)	49(2)	54(2)	-1(1)	-2(1)	-3(1)
C(6)	33(1)	40(1)	53(2)	0(1)	8(1)	-2(1)
C(7)	32(1)	30(1)	37(1)	3(1)	6(1)	0(1)
C(11)	32(1)	39(1)	35(1)	0(1)	7(1)	0(1)
C(12)	46(1)	47(2)	48(1)	9(1)	17(1)	4(1)
C(13)	55(2)	46(2)	61(2)	12(1)	14(1)	2(1)
C(14)	50(2)	43(2)	71(2)	0(1)	13(1)	4(1)
C(15)	48(2)	51(2)	76(2)	-2(2)	28(1)	6(1)
C(16)	45(1)	45(2)	60(2)	2(1)	26(1)	-1(1)
C(1B)	34(1)	40(1)	35(1)	2(1)	10(1)	-1(1)
O(1B)	39(1)	65(1)	50(1)	4(1)	20(1)	-5(1)
C(2B)	38(1)	37(1)	31(1)	4(1)	9(1)	1(1)
C(3B)	53(2)	42(2)	45(1)	-4(1)	10(1)	7(1)
C(4B)	74(2)	42(2)	55(2)	-8(1)	14(1)	5(1)
C(5B)	62(2)	43(2)	57(2)	-11(1)	4(1)	-7(1)
C(6B)	43(1)	44(2)	51(1)	-2(1)	2(1)	-7(1)
C(7B)	39(1)	37(1)	32(1)	1(1)	8(1)	-3(1)
C(11B)	36(1)	35(1)	37(1)	-4(1)	5(1)	1(1)
C(12B)	49(1)	46(2)	40(1)	3(1)	15(1)	2(1)
C(13B)	67(2)	52(2)	41(1)	2(1)	14(1)	4(2)
C(14B)	80(2)	51(2)	39(1)	2(1)	-2(1)	8(2)
C(15B)	49(2)	63(2)	60(2)	-3(2)	-8(1)	15(2)
C(16B)	41(1)	55(2)	53(2)	-3(1)	7(1)	2(1)
N(21)	63(2)	67(2)	48(1)	9(1)	12(1)	2(1)

Table 5.5.5 cont.

C(22)	63(2)	60(2)	58(2)	8(1)	24(2)	-4(2)
C(23)	54(2)	68(2)	54(2)	0(2)	16(1)	11(2)
C(27)	72(2)	153(5)	98(3)	-8(3)	3(2)	-12(3)
C(24)	89(3)	70(2)	52(2)	18(2)	20(2)	14(2)
C(25)	100(3)	72(2)	81(2)	18(2)	37(2)	-15(2)
C(26)	67(2)	75(2)	72(2)	4(2)	19(2)	-12(2)
N(21B)	58(2)	70(2)	59(2)	6(1)	22(1)	-3(1)
C(22B)	64(2)	74(2)	51(2)	2(2)	10(1)	-7(2)
C(23B)	75(2)	76(2)	56(2)	16(2)	8(2)	-10(2)
C(27)	165(5)	94(3)	101(3)	27(3)	5(3)	-55(3)
C(24B)	68(2)	95(3)	49(2)	14(2)	12(2)	5(2)
C(25B)	69(2)	101(3)	51(2)	-12(2)	14(2)	8(2)
C(26B)	66(2)	69(2)	78(2)	-14(2)	25(2)	-7(2)

TABLE 5.5.6. : 3PIC - Hydrogen Bonding Data

Donor-H	Donor···Acceptor	H···Acceptor	Donor-H···Acceptor
O(1)-H(1)	O(1)···N(21)	H(1)···N(21)	O(1)-H(1)···N(21)
0,96(3) Å	2,925(3) Å	1,99(3) Å	165(2)°
O(1B)-H(1B)	O(1B)···N(21B)	H(1B)···N(21B)	O(1B)-H(1B)···N(21B)
0,95(1) Å	2,788(3) Å	1,89(2) Å	157(2)°

5.6. 24LU

Preliminary X-ray oscillation and Weissenberg photography indicated that **24LU** was triclinic and belonged either to the space group P1 or to $P\bar{1}$. Analysis of the E-statistics[130], as calculated from the reflections collected, indicated that the crystal was centric and consequently could be assigned to the triclinic space group $P\bar{1}$. Accurate cell dimensions, obtained from the diffractometer, indicated that the cell was very similar to that observed for the inclusion complex of the host (**1**) with the guest 2-methylpyridine[124]. Although the difference in cell dimensions and consequently in cell volume was significant, reflecting the larger size of the 2,4-dimethylpyridine as compared to 2-methylpyridine, it was expected that they would be structurally closely related. The similarity of the structures was partly to be expected since both complexes were found to possess the unusual, for the present group of compounds, host to guest ratio of 1:1. (Reference to the close correspondence of these complexes will again be made at the end of this and other relevant sections dealing with the complex **24LU**.)

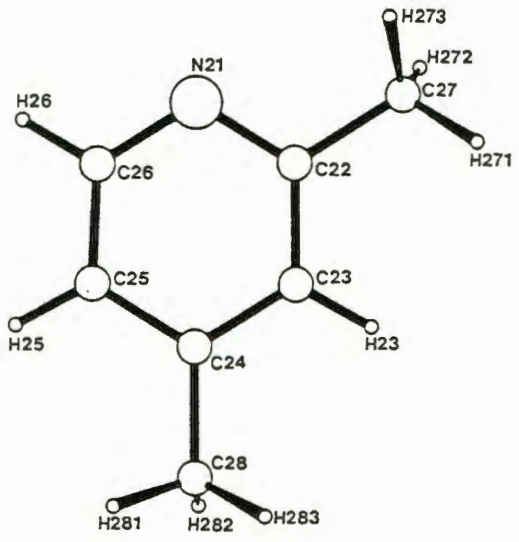

Figure 5.6 The numbering scheme employed for the 2,4-Dimethylpyridine molecule.

As was the case in all previous complexes, the reflection data for **24LU** were collected by irradiating a crystal of this compound, sealed in a Lindemann tube, with MoKα radiation. The reflections were recorded with the aid of an Enraf-Nonius CAD-4 diffractometer. The total exposure time for the crystal was 34,2 hours and the change in intensity over that time was 1,4%. Lorentz and polarisation corrections, but no absorption corrections were applied to the data.

Of a total of 4513 reflections 3722 were unique of which 780 were suppressed ($4\sigma(F) > F$) leaving 2942 reflections. Of the 1075 reflections with $E > 1,20$, 402 with large E-values were used in an initial search for the 'best' solution of this structure.

The best solution obtained by direct methods for 36 peaks was calculated to have a $R_E = 0,195$. It revealed a guest molecule in a general position and 2 host molecules centered about the special Wyckoff positions *e* and *g*. The 36 peaks thus identified were used as the first model for further refinement using SHELX-76. An initial $R = 0,111$ was obtained when all heavy atoms (C, O and N) were treated isotropically.

Anisotropic modelling of all non-hydrogen atoms ($R = 0,085$) and the introduction of all non-hydroxyl hydrogens ($R = 0,048$) were the next steps in the refinement of the structure. This was followed by the inclusion of the hydroxyl hydrogen atoms, initially in observed positions but tied to H-bond donor and acceptor atoms within theoretically plausible distances (see section 5.1.3) and allowing these to refine. This resulted in an $R = 0,046$. Finally a weighting scheme was chosen to minimise the variance of reflections by parity groups, $\sin\theta$, $(F/F_{max})^{½}$ and Miller indices. With a $g = 0,001$, a reflection to parameter ratio of 8,8 a final $R = 0,041$, $R_W = 0,046$ and a $S = 1,26$ were obtained. The maximum and minimum electron densities for the difference Fourier map were found to be 0,16 and -0,25 $e.Å^{-3}$ respectively.

TABLE 5.6.1. : 24LU - Crystal Data

Host : Guest	1 : 1
Molecular formula	$C_{26}H_{20}O_2 \cdot C_7H_9N$
Molecular weight ($g.mol^{-1}$)	471,60
Space group	$P\bar{1}$
Z	2
a / (Å)	9,178(1)
b / (Å)	10,739(2)
c / (Å)	13,589(2)
α / (°)	71,94(1)
β / (°)	88,24(1)
γ / (°)	75,03(1)
V / ($Å^3$)	1228,4(9)
D_c / ($g.cm^{-3}$)	1,275
D_m / ($g.cm^{-3}$)	1,259(9)
μ(MoKα) (cm^{-1})	0,21
F(000) / e	250

TABLE 5.6.2. : 24LU - Data collection

Crystal dimensions (mm)	0,34 x 0,34 x 0,44
Range scanned θ (°)	1 - 25
Range of indices (h,k,l)	$-10 \leq h \leq 10$
	$-12 \leq k \leq 12$
	$0 \leq l \leq 16$
Reflections for lattice parameters no., θ range (°)	24; $15,97 \leq \theta \leq 16,93$
Stability of standard reflections (%)	1,4%
Scan mode	ω-2θ
Scan width in ω (°)	$(0,85 + 0,35\tan\theta)$
Vertical aperture length (mm)	(4)
Aperture width (mm)	$(1,12 + 1,05\tan\theta)$
Number of reflections collected	4513
Number of unique reflections	3722

TABLE 5.6.3. : 24LU - Final refinement

Number of observed ($I_{rel} > 2\sigma I_{rel}$) reflections, N	2942
Number of parameters, NP	339
N / NP	8,7
$R = (R\|\|F_o\|-\|F_c\|\|)/(R\|F_o\|)$	0,041
$wR = (R\|\|F_o\|-\|F_c\|\| \cdot w^{½})/(R\|F_o\| \cdot w^{½})$	0,046
$w = 1/(\sigma^2(F) + [g] \cdot F^2)$	$1/(\sigma^2F - 0{,}001F^2)$
S	1,26
Max. shift/esd	±10%
Max. height in difference Fourier map (e.Å^{-3})	0,16
Min. height in difference Fourier map (e.Å^{-3})	-0,25

TABLE 5.6.4. : 24LU - Analysis of Variance

By parity groups

Group	*ggg*	*ugg*	*gug*	*uug*	*ggu*	*ugu*	*guu*	*uuu*	All
M	361	360	382	370	364	366	365	374	2942
V	46	43	46	45	44	45	51	46	46

As a function of sin θ

SINθ	0,00 - 0,18	0,18 - 0,23	0,23 - 0,27	0,27 - 0,29	0,29 - 0,32	0,32 - 0,34	0,34 - 0,36	0,36 - 0,38	0,38 - 0,40	0,40 - 0,43
M	311	301	338	234	366	262	295	276	273	286
V	52	52	49	40	37	43	45	43	40	52

As a function of $(F/F_{max})^{½}$

$(F/F_{max})^{½}$	0,0- 0,16	0,16 - 0,18	0,18 - 0,20	0,20 - 0,22	0,22 - 0,24	0,24 - 0,26	0,26 - 0,29	0,29 - 0,33	0,33 - 0,39	0,39 - 1,00
M	326	319	340	327	267	229	298	294	268	274
V	54	52	47	48	46	46	42	41	36	41

As a function of [Miller indices]

h	0	1	2	3	4	5	6	7	8	9	10	11	12	13	Rest
M	218	445	416	379	359	318	271	223	161	105	47	0	0	0	0
V	51	43	48	47	49	45	43	43	40	45	49	0	0	0	0

k	0	1	2	3	4	5	6	7	8	9	10	11	12	13	Rest
M	184	368	360	347	320	306	273	239	187	156	109	75	18	0	0
V	46	49	50	47	39	45	43	42	40	51	45	52	67	0	0

l	0	1	2	3	4	5	6	7	8	9	10	11	12	13	Rest
M	156	277	293	282	247	263	250	231	208	178	162	127	105	83	80
V	51	53	49	42	44	50	45	46	40	46	40	40	41	44	44

M = Number of reflections in that Group

V = $100[N\,\Sigma(\omega|F_o - F_c|^2)/(M\,\Sigma\omega)]$ where M = total number of reflections

TABLE 5.6.5. : 24LU - Fractional atomic coordinates (x 10^4) and Thermal Parameters ($Å^2$ x 10^3) with e.s.d.'s in parentheses

Atom	x/a	y/b	z/c	U_{iso}/U_{eq}(*)
C(1)	653(2)	4607(2)	6115(1)	31(1) *
O(1)	-76(1)	4839(1)	7013(1)	36(1) *
H(1)	-1045(13)	5498(17)	6822(16)	61(1)
C(2)	622(2)	5952(2)	5292(1)	31(1) *
C(3)	1213(2)	6872(2)	5585(2)	40(1) *
H(3)	1603(2)	6633(2)	6317(2)	61(1)
C(4)	1265(2)	8095(2)	4887(2)	45(1) *
H(4)	1673(2)	8746(2)	5114(2)	61(1)
C(5)	753(2)	8424(2)	3869(2)	45(1) *
H(5)	807(2)	9304(2)	3352(2)	61(1)
C(6)	165(2)	7526(2)	3573(2)	40(1) *
H(6)	-208(2)	7769(2)	2837(2)	61(1)
C(7)	79(2)	6287(2)	4276(1)	31(1) *
C(11)	2292(2)	3807(2)	6470(1)	34(1) *
C(12)	3368(2)	3721(2)	5728(2)	43(1) *
H(12)	3078(2)	4228(2)	4979(2)	61(1)
C(13)	4830(2)	2940(2)	6020(2)	54(1) *
H(13)	5590(2)	2879(2)	5482(2)	61(1)
C(14)	5248(3)	2247(2)	7050(2)	57(1) *
H(14)	6310(3)	1688(2)	7259(2)	61(1)
C(15)	4204(3)	2325(2)	7789(2)	52(1) *
H(15)	4505(3)	1812(2)	8535(2)	61(1)
C(16)	2731(2)	3113(2)	7504(2)	42(1) *
H(16)	1983(2)	3180(2)	8049(2)	61(1)
C(1B)	574(2)	6157(2)	9275(1)	34(1) *
O(1B)	740(2)	6454(1)	8175(1)	45(1) *
H(1B)	510(26)	5766(15)	7923(12)	61(1)
C(2B)	1599(2)	4767(2)	9836(1)	34(1) *
C(3B)	3147(2)	4550(2)	9667(2)	45(1) *
H(3B)	3525(2)	5303(2)	9191(2)	61(1)
C(4B)	4152(2)	3326(2)	10143(2)	50(1) *

Table 5.6.5 cont.

H(4B)	5250(2)	3189(2)	10009(2)	61(1)	
C(5B)	3637(3)	2280(2)	10811(2)	52(1)	*
H(5B)	4365(3)	1389(2)	11167(2)	61(1)	
C(6B)	2127(2)	2473(2)	10979(2)	45(1)	*
H(6B)	1762(2)	1712(2)	11456(2)	61(1)	
C(7B)	1082(2)	3721(2)	10495(1)	35(1)	*
C(11B)	1088(2)	7245(2)	9580(1)	34(1)	*
C(12B)	1194(2)	7159(2)	10614(2)	44(1)	*
H(12B)	926(2)	6391(2)	11156(2)	61(1)	
C(13B)	1666(3)	8120(2)	10907(2)	52(1)	*
H(13B)	1750(3)	8035(2)	11658(2)	61(1)	
C(14B)	2020(3)	9195(2)	10171(2)	53(1)	*
H(14B)	2362(3)	9891(2)	10383(2)	61(1)	
C(15B)	1902(3)	9299(2)	9146(2)	56(1)	*
H(15B)	2151(3)	10081(2)	8607(2)	61(1)	
C(16B)	1439(3)	8333(2)	8844(2)	47(1)	*
H(16B)	1360(3)	8423(2)	8092(2)	61(1)	
N(21)	-2775(2)	6778(2)	6691(1)	44(1)	*
C(22)	-4116(2)	6529(2)	6957(2)	44(1)	*
C(27)	-4156(3)	5089(2)	7343(3)	74(1)	*
H(271)	-5183(3)	4977(2)	7243(3)	122(5)	
H(272)	-3836(3)	4717(2)	8098(3)	122(5)	
H(273)	-3420(3)	4589(2)	6951(3)	122(5)	
C(23)	-5407(2)	7571(2)	6878(2)	44(1)	*
H(23)	-6391(2)	7350(2)	7082(2)	61(1)	
C(24)	-5353(2)	8907(2)	6523(2)	43(1)	*
C(28)	-6754(3)	10046(2)	6434(2)	56(1)	*
H(281)	-6731(3)	10815(2)	5796(2)	122(5)	
H(282)	-6693(3)	10334(2)	7061(2)	122(5)	
H(283)	-7717(3)	9779(2)	6418(2)	122(5)	
C(25)	-3959(3)	9145(2)	6260(2)	51(1)	*
H(25)	-3854(3)	10095(2)	6001(2)	61(1)	
C(26)	-2726(3)	8070(2)	6355(2)	53(1)	*
H(26)	-1729(3)	8266(2)	6164(2)	61(1)	

Anisotropic atoms have thermal parameters ($Å^2 \times 10^3$) of the form :

$\exp(-2\pi^2(U_{11}h^2a^{*2} + U_{22}k^2b^{*2} + U_{33}l^2c^{*2} + 2U_{23}klb^*c^*\cos\alpha + 2U_{13}hla^*c^*\cos\beta + 2U_{12}hla^*b^*\cos\gamma)$

Atom	U11	U22	U33	U23	U13	U12
C(1)	25(1)	39(1)	29(1)	-12(1)	2(1)	-5(1)
O(1)	32(1)	45(1)	30(1)	-14(1)	4(1)	-3(1)
C(2)	24(1)	36(1)	35(1)	-14(1)	3(1)	-5(1)
C(3)	37(1)	47(1)	42(1)	-17(1)	4(1)	-15(1)
C(4)	40(1)	46(1)	59(1)	-23(1)	7(1)	-18(1)
C(5)	39(1)	38(1)	56(1)	-7(1)	5(1)	-12(1)
C(6)	33(1)	42(1)	42(1)	-6(1)	1(1)	-10(1)
C(7)	22(1)	35(1)	34(1)	-11(1)	3(1)	-4(1)
C(11)	29(1)	38(1)	40(1)	-18(1)	-1(1)	-7(1)
C(12)	34(1)	53(1)	48(1)	-23(1)	5(1)	-8(1)
C(13)	31(1)	65(2)	72(2)	-35(1)	7(1)	-6(1)
C(14)	33(1)	60(2)	80(2)	-36(1)	-15(1)	2(1)
C(15)	47(1)	51(1)	56(2)	-20(1)	-16(1)	0(1)
C(16)	38(1)	46(1)	43(1)	-17(1)	-5(1)	-4(1)
C(1B)	39(1)	40(1)	29(1)	-12(1)	4(1)	-14(1)
O(1B)	60(1)	54(1)	31(1)	-18(1)	7(1)	-23(1)
C(2B)	35(1)	41(1)	35(1)	-19(1)	3(1)	-13(1)
C(3B)	38(1)	51(1)	53(1)	-22(1)	9(1)	-15(1)
C(4B)	35(1)	62(2)	62(2)	-31(1)	2(1)	-11(1)
C(5B)	43(1)	49(1)	62(2)	-22(1)	-10(1)	-1(1)
C(6B)	45(1)	44(1)	47(1)	-13(1)	-3(1)	-11(1)
C(7B)	35(1)	40(1)	35(1)	-16(1)	0(1)	-11(1)
C(11B)	32(1)	38(1)	35(1)	-12(1)	2(1)	-10(1)
C(12B)	49(1)	53(1)	38(1)	-17(1)	6(1)	-23(1)
C(13B)	55(1)	65(2)	50(1)	-32(1)	5(1)	-22(1)
C(14B)	51(1)	50(1)	71(2)	-31(1)	5(1)	-19(1)
C(15B)	69(2)	42(1)	62(2)	-13(1)	10(1)	-26(1)
C(16B)	57(1)	46(1)	42(1)	-12(1)	7(1)	-21(1)
N(21)	38(1)	48(1)	46(1)	-19(1)	4(1)	-4(1)
C(22)	44(1)	45(1)	44(1)	-18(1)	2(1)	-8(1)
C(27)	67(2)	48(2)	107(2)	-22(2)	16(2)	-14(1)
C(23)	37(1)	51(1)	48(1)	-21(1)	4(1)	-12(1)
C(24)	42(1)	47(1)	39(1)	-17(1)	2(1)	-3(1)
C(28)	47(1)	52(1)	62(2)	-19(1)	6(1)	0(1)
C(25)	50(1)	42(1)	60(2)	-14(1)	12(1)	-10(1)
C(26)	41(1)	54(1)	65(2)	-19(1)	12(1)	-13(1)

TABLE 5.6.6. : 24LU - Hydrogen Bonding Data

Donor-H	Donor···Acceptor	H···Acceptor	Donor-H···Acceptor
O(1)-H(1)	O(1)···N(21)	H(1)···N(21)	O(1)-H(1)···N(21)
0,97(1) Å	2,739(2) Å	1,78(1) Å	169(2)°
O(1B)-H(1B)	O(1B)···O(1)	H(1B)···O(1)	O(1B)-H(1B)···O(1)
0,97(2) Å	2,916(3) Å	1,97(2) Å	162(1)°

5.7. 26LU

Crystals of **26LU** form within days of preparation of an appropriately concentrated solution of host (1) in 2,6-dimethylpyridine (2,6-Lutidine). They are colourless, translucent parallelepipeds with sharply defined edges. However, when exposed to air their surfaces turn opaque within a few minutes. Consequently, they need to be sealed in Lindemann tubes for X-ray photography and Data collection.

X-ray photography indicated that **26LU** was triclinic. The space group (either P1 or $P\bar{1}$) could not be determined uniquely from systematic absences. However, later analysis of the $|E^2-1|_{mean}$ statistics[130] for the *hk*0, *h*0*l* and 0*kl* projections as well as the rest of the reflection data indicated that the unit cell contained a centre of inversion. Thus 26LU was identified as belonging to the triclinic space group $P\bar{1}$.

In all, 3058 reflections were measured for the complex **26LU** during the 19,6 h that the data collection was in progress. Of these, 2062 unique reflections with $4\sigma(F) < F$ were used in the structure solution. Direct methods (SHELXS-86) produced an E-map with R_E = 0,249. This revealed all 22 atoms required to locate half the host molecule and the guest in the asymmetric unit.

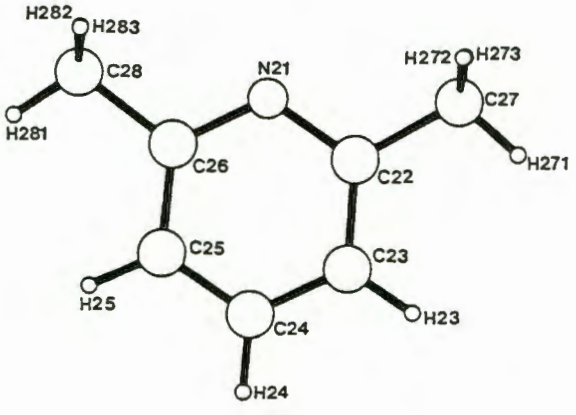

Figure 5.7 The numbering scheme used for the 2,6-Dimethylpyridine molecule.

The host was observed to occupy the Wyckoff special position *g* (0,½,½) while the guest, not having a centre of inversion, was found in a general position.

Refinement of the atomic positions obtained from direct methods was carried out by full-matrix least-squares refinement using SHELX-76. All atoms were varied isotropically (R = 0,254). Modelling all carbon, nitrogen and oxygen atoms anisotropically and introducing all non-hydroxyl hydrogens (aromatic C-H : 1,00 Å) in

idealised positions effected a significant improvement in the model, resulting in a R = 0,059.

The inclusion of the hydroxyl hydrogen atom, H(1), confined to within theoretical distances from O(1) and N(21), followed by the introduction of a weighting scheme brought about a final R = 0,054, a R_W = 0,064 and a S = 1,08. The maximum and minimum electron densities in the final difference Fourier synthesis were negligible at 0,19 and -0,28 e.$Å^{-3}$ respectively. For further final refinement statistics refer to tables 5.7.1 to 3 below.

TABLE 5.7.1 : 26LU - Crystal Data

Host : Guest	1 : 2
Molecular formula	$C_{26}H_{20}O_2 \cdot 2C_7H_9N$
Molecular weight ($g.mol^{-1}$)	578,76
Space group	$P\bar{1}$
Z	1
a / (Å)	8,620(4)
b / (Å)	8,986(3)
c / (Å)	11,353(2)
α / (°)	85,33(2)
β / (°)	81,11(2)
γ / (°)	71,69(3)
V / ($Å^3$)	824,4(5)
D_c / ($g.cm^{-3}$)	1,166
D_m / ($g.cm^{-3}$)	1,175(8)
μ(MoKα) (cm^{-1})	0,38
F(000) / e	308,0

TABLE 5.7.2. : 26LU - Data collection

Crystal dimensions (mm)	0,38 x 0,41 x 0,41
Range scanned θ (°)	1 - 25
Range of indices (h,k,l)	$-10 \leq h \leq 10$
	$-10 \leq k \leq 10$
	$0 \leq l \leq 13$
Reflections for lattice parameters: no., θ range (°)	24; 15,97≤θ≤16,91
Instability of standard reflections (%)	3,0%
Scan mode	ω-2θ
Scan width in ω (°)	(0,85 + 0,35tanθ)
Vertical aperture length (mm)	(4)
Aperture width (mm)	(1,12 + 1,05tanθ)
Number of reflections collected	3058
Number of unique reflections	2180

TABLE 5.7.1. : 26LU - Final Refinement

Number of observed ($I_{rel} > 2\sigma I_{rel}$) reflections, N	2062
Number of parameters, NP	212
N / NP	9,7
$R = (R\|\|F_o\|-\|F_c\|\|)/(R\|F_o\|)$	0,054
$wR = (R\|\|F_o\|-\|F_c\|\| \cdot w^{½})/(R\|F_o\| \cdot w^{½})$	0,064
$w = 1/(\sigma^2(F) + [g] \cdot F^2)$	$1/(\sigma^2F - 0{,}005F^2)$
S	1,08
Max. shift/esd	±12%
Max. height in difference Fourier map (e $Å^{-3}$)	0,19
Min. height in difference Fourier map (e $Å^{-3}$)	-0,28

TABLE 5.7.4. : 26LU - Analysis of Variance

By parity groups

Group	*ggg*	*ugg*	*gug*	*uug*	*ggu*	*ugu*	*guu*	*uuu*	All
M	262	259	259	260	261	246	255	260	2062
V	31	35	37	32	35	31	36	34	34

As a function of sin θ

SINθ	0,00 - 0,18	0,18 - 0,23	0,23 - 0,27	0,27 - 0,29	0,29 - 0,32	0,32 - 0,34	0,34 - 0,36	0,36 - 0,38	0,38 - 0,40	0,40 - 0,43
M	214	226	237	151	252	198	198	194	202	190
V	41	36	38	28	33	31	31	30	32	34

As a function of $(F/F_{max})^{½}$

$(F/F_{max})^{½}$	,0- 0,16	0,16 - 0,18	0,18 - 0,20	0,20 - 0,23	0,23 - 0,25	0,25 - 0,28	0,28 - 0,31	0,31 - 0,36	0,36 - 0,44	0,44 - 1,00
M	211	201	214	275	172	232	179	187	205	186
V	44	39	44	35	32	31	29	26	22	27

As a function of [Miller indices]

h	0	1	2	3	4	5	6	7	8	9	10	11	12	13	Rest
M	169	322	312	295	261	230	192	137	95	41	8	0	0	0	0
V	30	33	35	33	34	32	37	32	38	36	40	0	0	0	0

k	0	1	2	3	4	5	6	7	8	9	10	11	12	13	Rest
M	154	307	303	281	247	220	190	156	110	70	24	0	0	0	0
V	32	37	33	39	36	31	29	28	32	32	33	0	0	0	0

l	0	1	2	3	4	5	6	7	8	9	10	11	12	13	Rest
M	131	247	226	217	221	204	191	158	145	118	91	67	35	11	0
V	37	38	38	34	30	34	32	33	33	30	31	28	25	36	0

M = Number of reflections in that Group

V = $100[N \Sigma(\omega|F_o - F_c|^2)/(M \Sigma\omega)]$ where M = total number of reflections

TABLE 5.7.5. : 26LU - Fractional atomic coordinates (x 10^4) and Thermal Parameters ($Å^2$ x 10^3) with e.s.d.'s in parentheses

Atom	x/a	y/b	z/c	U_{iso}/U_{eq}(*)
C(1)	6637(2)	3677(2)	4988(2)	35(1) *
O(1)	7968(2)	3258(2)	4037(1)	43(1) *
H(1)	7706(25)	3931(21)	3361(8)	87(9)
C(2)	5093(2)	3471(2)	4619(2)	35(1) *
C(3)	5184(3)	1987(2)	4258(2)	47(1) *
H(3)	6251(3)	1119(2)	4238(2)	78(2)
C(4)	3840(3)	1706(2)	3930(2)	53(1) *
H(4)	3928(3)	637(2)	3680(2)	78(2)
C(5)	2366(3)	2894(2)	3944(2)	51(1) *
H(5)	1384(3)	2693(2)	3704(2)	78(2)
C(6)	2257(2)	4357(2)	4292(2)	45(1) *
H(6)	1188(2)	5219(2)	4299(2)	78(2)
C(7)	3612(2)	4664(2)	4636(1)	34(1) *
C(11)	7155(2)	2538(2)	6038(2)	38(1) *
C(12)	6053(3)	2612(2)	7066(2)	54(1) *
H(12)	4935(3)	3407(2)	7117(2)	78(2)
C(13)	6484(4)	1590(3)	8033(2)	68(1) *
H(13)	5681(4)	1656(3)	8778(2)	78(2)
C(14)	8022(4)	483(3)	7960(2)	70(1) *
H(14)	8335(4)	-264(3)	8649(2)	78(2)
C(15)	9102(3)	413(3)	6949(2)	64(1) *
H(15)	10225(3)	-386(3)	6897(2)	78(2)
C(16)	8688(3)	1439(2)	5989(2)	50(1) *
H(16)	9507(3)	1380(2)	5254(2)	78(2)
N(21)	2232(2)	5089(3)	8265(2)	63(1) *
C(22)	2600(3)	5788(4)	9141(2)	72(1) *
C(27)	2954(5)	7313(4)	8809(3)	108(2) *
H(271)	3419(5)	7829(4)	9355(3)	208(10)
H(272)	1875(5)	8045(4)	8617(3)	208(10)
H(273)	3740(5)	7046(4)	8056(3)	208(10)
C(23)	2642(4)	5119(5)	10285(2)	94(2) *
H(23)	2929(4)	5643(5)	10928(2)	78(2)
C(24)	2290(5)	3744(5)	10524(3)	109(2) *
H(24)	2328(5)	3242(5)	11342(3)	78(2)

Table 5.7.5 cont.

C(25)	1883(5)	3054(4)	9637(3)	102(2) *
H(25)	1588(5)	2059(4)	9807(3)	78(2)
C(26)	1882(3)	3743(4)	8507(2)	73(1) *
C(28)	1464(6)	3035(5)	7501(3)	112(2) *
H(281)	851(6)	2253(5)	7726(3)	208(10)
H(282)	2466(6)	2567(5)	6919(3)	208(10)
H(283)	732(6)	3993(5)	7127(3)	208(10)

Anisotropic atoms have thermal parameters ($Å^2 \times 10^3$) of the form :

$\exp(-2\pi^2(U_{11}h^2a^{*2} + U_{22}k^2b^{*2} + U_{33}l^2c^{*2} + 2U_{23}klb^*c^*\cos\alpha + 2U_{13}hla^*c^*\cos\beta + 2U_{12}hla^*b^*\cos\gamma)$

Atom	U11	U22	U33	U23	U13	U12
C(1)	39(1)	30(1)	35(1)	0(1)	-6(1)	-6(1)
O(1)	43(1)	45(1)	36(1)	0(1)	-2(1)	-5(1)
C(2)	46(1)	29(1)	31(1)	2(1)	-8(1)	-13(1)
C(3)	63(1)	31(1)	50(1)	-2(1)	-13(1)	-14(1)
C(4)	83(2)	39(1)	51(1)	1(1)	-19(1)	-31(1)
C(5)	65(1)	53(1)	49(1)	5(1)	-18(1)	-34(1)
C(6)	47(1)	45(1)	47(1)	5(1)	-13(1)	-19(1)
C(7)	41(1)	31(1)	31(1)	2(1)	-6(1)	-13(1)
C(11)	50(1)	27(1)	38(1)	0(1)	-13(1)	-10(1)
C(12)	70(1)	47(1)	40(1)	2(1)	-6(1)	-12(1)
C(13)	105(2)	65(2)	38(1)	9(1)	-12(1)	-30(2)
C(14)	115(2)	47(1)	57(2)	19(1)	-43(2)	-28(1)
C(15)	80(2)	40(1)	72(2)	8(1)	-36(1)	-6(1)
C(16)	57(1)	35(1)	54(1)	2(1)	-17(1)	-5(1)
N(21)	59(1)	91(2)	40(1)	5(1)	-4(1)	-25(1)
C(22)	76(2)	97(2)	41(1)	-3(1)	-8(1)	-23(2)
C(27)	164(4)	105(3)	72(2)	-2(2)	-30(2)	-56(3)
C(23)	112(3)	135(3)	40(1)	-1(2)	-14(2)	-42(2)
C(24)	130(3)	159(4)	47(2)	38(2)	-18(2)	-64(3)
C(25)	131(3)	134(3)	60(2)	34(2)	-20(2)	-73(3)
C(26)	77(2)	105(2)	48(1)	19(1)	-9(1)	-47(2)
C(28)	163(4)	144(3)	71(2)	19(2)	-30(2)	106(3)

TABLE 5.7.6. : 26LU - Hydrogen Bonding Data

Donor-H	Donor···Acceptor	H···Acceptor	Donor-H···Acceptor
O(1)-H(1) 0,948(1) Å	O(1)···N(21)^{i} 2,901(3) Å	H(1)···N(21)^{i} 1,98(1) Å	O(1)-H(1)···N(21)^{i} 163(2)°

Equivalent Positions:
(^{i})1-x,1-y,1-z

TABLE 5.1 : Bond lengths (Å) with e.s.d.'s in Parentheses

COMPOUND			NITRANN	PROP	PYD(A)	PYD(B)	3PIC(A)	3PIC(B)	24LU(A)	24LU(B)	26LU
C(1)	-	O(1)	1,447(5)	1,434(4)	1,426(3)	1,425(4)	1,436(3)	1,427(3)	1,433(2)	1,441(2)	1,427(2)
C(1)	-	C(2)	1,491(6)	1,523(4)	1,519(5)	1,522(4)	1,522(2)	1,519(3)	1,522(3)	1,519(3)	1,523(3)
C(1)	-	C(7')	1,516(7)	1,517(4)	1,531(3)	1,524(5)	1,521(3)	1,522(3)	1,526(3)	1,523(3)	1,525(3)
C(1)	-	C(11)	1,545(5)	1,541(5)	1,543(5)	1,534(4)	1,531(3)	1,536(3)	1,533(2)	1,535(4)	1,532(3)
O(1)	-	H(1)	0,970(16)	0,976(29)	0,972(27)	0,984(22)	0,960(27)	0,950(12)	0,967(15)	0,975(21)	0,948(12)
C(2)	-	C(3)	1,409(7)	1,395(4)	1,401(5)	1,398(5)	1,402(3)	1,401(4)	1,401(4)	1,403(3)	1,402(3)
C(2)	-	C(7)	1,394(5)	1,387(4)	1,385(5)	1,378(5)	1,390(3)	1,387(2)	1,388(3)	1,384(3)	1,384(2)
C(3)	-	C(4)	1,392(7)	1,379(5)	1,368(5)	1,389(5)	1,371(4)	1,370(4)	1,373(3)	1,371(3)	1,371(4)
C(4)	-	C(5)	1,350(7)	1,387(5)	1,386(5)	1,370(5)	1,383(5)	1,382(5)	1,382(4)	1,387(4)	1,378(3)
C(5)	-	C(6)	1,384(8)	1,371(4)	1,383(5)	1,372(5)	1,374(3)	1,373(4)	1,381(4)	1,370(3)	1,374(3)
C(6)	-	C(7)	1,385(7)	1,389(5)	1,398(5)	1,401(4)	1,403(2)	1,397(3)	1,397(3)	1,406(3)	1,398(3)
C(11)	-	C(12)	1,392(6)	1,393(6)	1,391(4)	1,387(5)	1,385(4)	1,388(4)	1,396(3)	1,384(3)	1,378(3)
C(11)	-	C(16)	1,355(6)	1,373(5)	1,376(5)	1,378(5)	1,385(4)	1,377(4)	1,387(3)	1,385(3)	1,375(3)
C(12)	-	C(13)	1,395(8)	1,382(6)	1,386(6)	1,384(4)	1,379(4)	1,375(3)	1,380(2)	1,381(4)	1,391(3)
C(13)	-	C(14)	1,344(9)	1,374(6)	1,364(7)	1,374(5)	1,385(5)	1,374(5)	1,379(4)	1,378(4)	1,380(4)
C(14)	-	C(15)	1,385(10)	1,367(7)	1,372(5)	1,368(6)	1,370(4)	1,371(5)	1,373(4)	1,368(4)	1,354(3)
C(15)	-	C(16)	1,408(8)	1,400(6)	1,405(6)	1,383(4)	1,389(4)	1,400(3)	1,390(3)	1,388(4)	1,384(3)
N(21)	-	C(22)	1,125(9)	1,110(6)	1,317(6)	1,312(6)	1,329(3)	1,325(4)	1,342(3)		1,345(4)
N(21)	-	C(26)			1,324(5)	1,329(7)	1,325(5)	1,318(4)	1,332(3)		1,334(5)
C(22)	-	C(23)	1,427(10)	1,472(7)	1,374(7)	1,362(6)	1,381(3)	1,376(4)	1,385(3)		1,387(4)
C(22)	-	C(27)							1,481(3)		1,502(5)
C(23)	-	C(24)		1,521(15)	1,361(6)	1,355(8)	1,375(5)	1,377(3)	1,379(3)		1,359(7)
C(23)	-	C(24A)		1,306(25)							
C(23)	-	C(27)					1,507(5)	1,512(6)			
C(24)	-	C(25)			1,358(7)	1,348(8)	1,358(5)	1,366(6)	1,384(3)		1,367(6)
C(24)	-	O(25)		1,353(13)							
C(24)	-	C(28)							1,507(3)		
C(24A)	-	O(25)		1,472(17)							
C(25)	-	C(26)			1,365(6)	1,374(7)	1,379(6)	1,374(6)	1,368(3)		1,379(4)
O(25)	-	H(25)		0,985(57)							
C(26)	-	C(28)									1,492(6)

TABLE 5.2 : Bond angles (°) with e.s.d.'s in parentheses

COMPOUND	NITRANN	PROP	PYD(A)	PYD(B)	3PIC(A)	3PIC(B)	24LU(A)	24LU(B)	26LU
C(7')- C(1) - C(11)	108,3(4)	108,6(3)	108,4(3)	109,1(3)	109,1(2)	108,4(2)	107,5(3)	109,0(2)	108,4(2)
C(2) -C(1) - C(11)	109,6(3)	108,3(3)	109,4(3)	109,0(3)	109,0(2)	108,7(2)	109,9(2)	109,4(2)	109,0(2)
C(2) -C(1) - C(7')	114,7(4)	114,0(3)	113,0(3)	112,6(3)	113,0(2)	113,1(2)	112,7(2)	113,2(2)	113,1(2)
O(1) -C(1) - C(11)	105,2(3)	111,1(3)	105,6(3)	106,6(3)	107,6(2)	105,6(2)	106,6(2)	106,0(2)	106,5(2)
O(1) -C(1) - C(7')	109,3(3)	110,0(3)	109,8(3)	110,4(3)	108,9(2)	110,4(2)	109,6(2)	109,6(2)	109,8(2)
O(1) -C(1) - C(2)	109,4(3)	104,8(3)	110,5(3)	110,0(3)	109,2(2)	110,5(2)	110,3(3)	109,4(2)	109,9(2)
C(1) -O(1) - H(1)	108,9(22)	118,4(16)	105,4(14)	106,5(13)	109,4(19)	106,0(11)	111,0(12)	111,5(10)	109,8(12)
C(1) -C(2) - C(7)	123,7(4)	123,1(3)	123,7(3)	124,1(3)	123,4(2)	122,9(2)	123,5(3)	123,4(2)	123,4(2)
C(1) -C(2) - C(3)	117,6(4)	117,6(3)	117,1(3)	117,0(3)	117,8(2)	118,0(2)	117,3(2)	117,5(3)	117,8(2)
C(3) -C(2) - C(7)	118,7(4)	119,3(3)	119,0(3)	118,9(4)	118,8(2)	119,1(2)	119,2(3)	119,1(3)	118,8(2)
C(2) -C(3) - C(4)	120,3(4)	121,3(3)	121,2(3)	120,7(3)	121,8(2)	121,3(3)	121,3(3)	121,3(2)	121,2(2)
C(3) -C(4) - C(5)	120,4(5)	119,3(3)	119,9(4)	120,2(4)	119,2(2)	119,6(3)	119,8(3)	119,7(2)	120,1(2)
C(4) -C(5) - C(6)	119,7(5)	119,2(3)	119,4(4)	119,5(4)	120,3(3)	119,8(3)	119,4(3)	119,7(4)	119,5(3)
C(5) -C(6) - C(7)	121,7(5)	122,3(3)	121,0(3)	121,2(3)	121,0(2)	121,5(3)	121,7(3)	121,3(3)	121,3(2)
C(2) -C(7) - C(6)	119,0(4)	118,5(3)	119,2(3)	119,5(3)	119,0(2)	118,8(2)	118,7(3)	118,9(2)	119,2(2)
C(1') -C(7) - C(6)	119,1(5)	118,6(3)	117,7(3)	117,3(3)	117,5(2)	117,3(2)	117,7(2)	117,7(2)	117,3(2)
C(1') -C(7) - C(2)	121,4(4)	122,8(3)	123,1(3)	123,1(3)	123,5(2)	123,9(2)	123,6(3)	123,4(2)	123,5(2)
C(1) -C(11) - C(16)	122,6(4)	122,5(3)	121,1(3)	121,8(3)	122,5(2)	122,5(2)	122,1(2)	121,8(2)	122,1(2)
C(1) -C(11) - C(12)	118,2(4)	118,4(3)	119,8(3)	120,0(3)	119,6(2)	118,9(2)	119,2(2)	119,8(3)	119,2(2)
C(12) -C(11) - C(16)	119,2(4)	119,1(4)	119,2(3)	118,2(4)	117,9(3)	118,6(2)	118,6(2)	118,4(3)	118,7(2)
C(11) -C(12) - C(13)	118,8(6)	120,6(4)	120,6(4)	120,9(3)	121,6(3)	121,3(3)	120,5(3)	120,8(3)	120,5(2)
C(12) -C(13) - C(14)	122,0(6)	119,9(4)	120,1(4)	120,4(4)	120,0(3)	120,1(3)	120,3(3)	120,4(3)	119,8(2)
C(13) -C(14) - C(15)	119,9(6)	120,1(4)	120,3(4)	118,8(4)	118,9(3)	119,6(2)	119,9(3)	119,2(4)	119,5(3)
C(14) -C(15) - C(16)	118,4(6)	120,4(4)	120,2(4)	121,3(4)	121,2(3)	120,6(3)	120,3(3)	120,8(3)	121,0(3)
C(11) -C(16) - C(15)	121,7(5)	119,9(4)	119,7(3)	120,4(4)	120,4(3)	119,9(3)	120,4(3)	120,3(3)	120,4(2)
C(22) -N(21) - C(26)			117,3(4)	116,4(4)	117,1(3)	116,8(3)	117,5(3)		119,3(2)
N(21) -C(22) - C(23)	177,8(8)	179,1(5)	123,4(4)	123,9(5)	124,9(3)	125,0(3)	121,6(3)		121,0(3)
N(21) -C(22) - C(27)							117,1(3)		116,4(2)
C(27) -C(22) - C(23)							121,3(2)		122,6(3)
C(22) -C(23) - C(24)		110,8(6)	117,9(5)	119,2(5)	116,5(3)	116,5(3)	120,7(2)		119,4(3)
C(22) -C(23) - C(24A)		120,2(7)							
C(22) -C(23) - C(27)					121,1(3)	120,6(3)			
C(24) -C(23) - C(27)					122,4(3)	122,9(3)			
C(23) -C(24) - C(25)			119,9(5)	118,4(5)	119,5(3)	119,6(3)	117,0(4)		119,5(3)
C(23) -C(24) - O(25)		113,1(8)							
C(23) -C(24) - C(28)							121,0(2)		120,3(5)
C(28) -C(24) - C(25)							122,0(4)		
C(23) -C(24A)- O(25)		119(1)							
C(24) -O(25) - H(25)		107(2)							
C(24A) -O(25) - H(25)		110(1)							
C(24) -C(25) - C(26)			118,2(4)	119,3(6)	120,0(4)	118,8(4)	119,4(4)		119,4(4)
N(21) -C(26) - C(25)			123,4(4)	122,9(5)	121,9(3)	123,2(4)	123,9(3)		121,5(3)
C(25) -C(26) - C(28)									121,7(3)
N(21) -C(26) - C(28)									116,8(3)

TABLE 5.3 : Torsion angles (°) with e.s.d.'s in parentheses

COMPOUND	NITRANN	PROP	PYD(A)	PYD(B)	3PIC(A)	3PIC(B)	24LU(A)	24LU(B)	26LU
C(7') - C(1) - C(11) - C(12)	69,9(5)	66,1(4)	87,7(4)	70,5(4)	66,5(3)	58,8(3)	78,2(4)	68,1(5)	65,7(3)
C(2) - C(1) - C(11) - C(12)	-55,8(5)	-58,2(4)	-35,9(5)	-52,2(5)	-57,3(3)	-64,5(3)	-44,9(5)	-56,1(5)	-57,8(3)
O(1) - C(1) - C(11) - C(12)	-173,3(4)	-172,8(3)	-154,8(3)	-171,0(3)	-175,6(2)	177,0(2)	-164,4(4)	-174,0(4)	-176,2(2)
C(7') - C(1) - C(11) - C(16)	-109,0(5)	-114,6(4)	-92,5(4)	-106,6(4)	-113,1(3)	-121,1(3)	-98,9(4)	-111,2(4)	-114,4(2)
C(2) - C(1) - C(11) - C(16)	125,2(5)	121,2(4)	144,0(4)	130,8(4)	123,1(3)	115,6(3)	138,0(4)	124,6(4)	122,2(2)
O(1) - C(1) - C(11) - C(16)	7,8(6)	6,5(5)	25,1(4)	12,0(5)	4,9(3)	-2,9(3)	18,5(5)	6,7(5)	3,7(3)
C(11) - C(1) - C(7') - C(2')	-117,4(4)	-118,4(3)	-115,2(4)	-116,6(4)	-123,4(3)	-115,9(3)	-117,1(4)	-121,6(3)	-120,3(2)
C(2) - C(1) - C(7') - C(2')	5,3(6)	2,4(5)	6,2(5)	4,0(5)	-2,0(3)	4,7(3)	4,2(5)	0,4(4)	0,7(3)
O(1) - C(1) - C(7') - C(2')	128,6(4)	119,8(3)	129,9(4)	127,4(4)	119,5(3)	129,0(3)	127,4(4)	122,8(3)	123,8(2)
O(1) - C(1) - C(2) - C(3)	53,9(5)	58,4(4)	54,5(4)	54,0(4)	59,8(3)	53,0(3)	54,7(5)	57,0(5)	57,0(3)
O(1) - C(1) - C(2) - C(7)	-128,7(4)	-122,8(3)	-129,6(4)	-127,6(4)	-119,4(3)	-128,9(2)	-127,0(4)	-122,9(4)	-123,7(2)
C(2) - C(1) - O(1) - H(1)	78,7(20)	170,2(24)	69,1(16)	85,6(17)	44,1(17)	46,1(14)	48,6(12)	57,7(13)	61,9(11)
C(7') - C(1) - O(1) - H(1)	-47,6(20)	47,3(24)	-56,1(16)	-39,3(17)	-79,7(17)	-79,7(14)	-76,1(12)	-66,9(13)	-63,1(11)
C(11) - C(1) - O(1) - H(1)	-163,7(20)	-73,0(24)	-172,7(16)	-156,0(17)	162,2(17)	163,3(14)	167,9(12)	175,6(13)	179,8(11)
C(7') - C(1) - C(2) - C(7)	-5,5(6)	-2,4(5)	-6,2(5)	-4,1(5)	2,0(3)	-4,7(3)	-4,2(5)	-0,4(5)	-0,7(3)
C(7') - C(1) - C(2) - C(3)	177,0(4)	178,8(3)	177,9(3)	177,7(3)	-178,9(2)	177,2(2)	177,5(3)	179,5(3)	-179,9(2)
C(11) - C(1) - C(2) - C(7)	116,5(4)	118,5(3)	114,6(4)	115,6(4)	123,4(3)	115,8(3)	115,7(3)	121,3(4)	119,9(2)
C(11) - C(1) - C(2) - C(3)	-61,0(5)	-60,3(4)	-61,3(4)	-62,7(4)	-57,5(3)	-62,3(3)	-62,6(4)	-58,8(4)	-59,3(3)
C(2') - C(1') - C(7) - C(6)	178,8(3)	179,0(3)	174,0(3)	178,1(3)	-179,1(2)	177,6(2)	177,6(3)	179,8(3)	179,4(2)
C(1) - C(2) - C(7) - C(1')	3,3(5)	2,6(5)	6,8(5)	4,5(6)	-2,2(4)	5,2(4)	4,7(6)	0,5(6)	0,7(3)
C(3) - C(2) - C(7) - C(1')	-178,2(3)	-178,6(3)	-177,4(3)	-177,3(4)	178,7(2)	-176,8(2)	-177,1(4)	-179,4(4)	180,0(2)
C(1) - C(2) - C(7) - C(6)	-175,7(4)	-178,7(3)	-173,3(3)	-177,7(4)	178,9(2)	-177,2(2)	-177,2(4)	-179,8(4)	-179,4(2)
C(1) - C(2) - C(3) - C(4)	176,8(4)	178,5(3)	173,4(3)	177,9(4)	-178,9(2)	177,2(3)	178,4(4)	179,9(4)	179,0(2)
C(3) - C(2) - C(7) - C(6)	1,8(6)	0,1(5)	2,5(5)	0,6(6)	-0,2(4)	0,9(4)	1,1(6)	0,3(6)	-0,1(3)
C(7) - C(2) - C(3) - C(4)	-0,8(7)	-0,4(5)	-2,8(6)	-0,5(6)	0,3(4)	-1,0(4)	0,0(6)	-0,1(6)	-0,2(4)
C(2) - C(3) - C(4) - C(5)	-1,7(8)	-0,5(5)	0,7(6)	-0,2(6)	0,3(4)	0,2(5)	-1,2(6)	-0,4(6)	0,4(4)
C(3) - C(4) - C(5) - C(6)	3,2(8)	1,7(6)	1,6(6)	0,8(6)	-0,9(5)	0,6(5)	1,4(6)	0,8(6)	-0,2(4)
C(4) - C(5) - C(6) - C(7)	-2,2(8)	-2,1(6)	-1,8(6)	-0,8(6)	1,0(4)	-0,7(5)	-0,3(6)	-0,7(6)	-0,2(4)
C(5) - C(6) - C(7) - C(2)	-0,3(7)	1,2(5)	-0,3(5)	0,0(6)	-0,4(4)	-0,1(4)	-1,0(6)	0,2(6)	0,3(3)

Table 5.3. (cont.)

COMPOUND	NITRANN	PROP	PYD(A)	PYD(B)	3PIC(A)	3PIC(B)	24LU(A)	24LU(B)	26LU
C(5) - C(6) - C(7) - C(1')	178,5(5)	179,9(3)	179,6(3)	178,0(4)	-179,4(2)	177,7(3)	177,3(4)	179,9(4)	-179,7(2)
C(1) - C(11) - C(16) - C(15)	178,9(5)	-179,6(4)	180,0(3)	177,7(4)	-179,4(3)	-178,4(3)	175,7(4)	-179,9(4)	-179,0(2)
C(1) - C(11) - C(12) - C(13)	-177,4(5)	-179,8(4)	-179,7(4)	-177,6(4)	179,8(3)	178,7(3)	-176,1(4)	179,5(4)	179,7(2)
C(12) - C(11) - C(16) - C(15)	0,0(8)	-0,3(6)	-0,1(6)	0,6(6)	1,1(4)	1,7(4)	-1,5(6)	0,8(6)	1,0(4)
C(16) - C(11) - C(12) - C(13)	1,6(8)	0,8(6)	0,4(6)	-0,5(6)	-0,6(4)	-1,4(4)	1,1(6)	-1,2(6)	-0,2(4)
C(11) - C(12) - C(13) - C(14)	-2,2(10)	-0,4(6)	-1,0(6)	0,4(6)	-0,1(5)	0,3(5)	-0,6(6)	0,9(6)	-0,6(4)
C(12) - C(13) - C(14) - C(15)	1,2(11)	-0,6(7)	1,4(7)	-0,4(6)	0,60(54)	0,4(5)	0,4(6)	-0,1(6)	0,6(5)
C(13) - C(14) - C(15) - C(16)	0,4(10)	1,1(7)	-1,2(7)	0,6(6)	-0,89(52)	0,1(5)	-0,7(6)	-0,4(6)	0,2(4)
C(14) - C(15) - C(16) - C(11)	-1,0(9)	-0,7(7)	0,5(6)	-0,7(6)	1,37(49)	-0,9(5)	1,3(6)	0,1(6)	-1,0(4)
C(22) - N(21) - C(26) - C(28)									179,3(3)
C(22) - N(21) - C(26) - C(25)			0,2(6)	-1,6(7)	-2,0(5)	-0,8(5)	-0,7(6)		0,2(5)
C(26) - N(21) - C(22) - C(27)							-179,1(4)		-179,0(3)
C(26) - N(21) - C(22) - C(23)			1,0(7)	2,7(7)	2,7(5)	1,3(5)	0,7(6)		0,9(5)
N(21) - C(22) - C(23) - C(27)					176,7(3)	179,5(3)			
N(21) - C(22) - C(23) - C(24)			-1,4(8)	-2,3(8)	-1,2(5)	-1,2(5)	-0,2(6)		-0,6(5)
C(27) - C(22) - C(23) - C(24)							179,6(4)		179,3(4)
C(22) - C(23) - C(24) - C(28)							179,9(4)		
C(22) - C(23) - C(24) - O(25)		59,9(10)							
C(22) - C(23) - C(24A) - O(25)		-37,8(14)							
C(22) - C(23) - C(24) - C(25)			0,6(8)	0,7(8)	-1,0(5)	0,6(5)	-0,3(6)		-0,7(6)
C(27) - C(23) - C(24) - C(25)					-178,8(4)	179,9(4)			
C(23) - C(24) - O(25) - H(25)		145,4(28)							
C(23) - C(24A) - O(25) - H(25)		-152,9(30)							
C(23) - C(24) - C(25) - C(26)			0,5(7)	0,3(8)	1,6(6)	-0,2(6)	0,3(6)		1,8(6)
C(28) - C(24) - C(25) - C(26)							-179,9(4)		
C(24) - C(25) - C(26) - N(21)			-0,9(7)	0,2(9)	0,0(6)	0,3(6)	0,2(7)		-1,6(5)
C(24) - C(25) - C(26) - C(28)									179,4(4)

(Right-hand Rule, Klyne & Prelog (1960) Experientia 16,521) (E.S.D.'s Following Stanford & Waser, Acta Cryst (1972) a28,213)

CHAPTER 6.

DISCUSSION :

CRYSTAL STRUCTURES

6. DISCUSSION : CRYSTAL STRUCTURES

6.1. HOST CONFORMATION

6.1.1. Introduction

The host molecule *trans*-9,10-dihydroxy-9,10-diphenyl-9,10-dihydroanthracene is an essentially rigid structure. Due to the *anti* nature of its hydroxyl and phenyl substituents it fulfils the requirements for a centrosymmetric molecule. Thus it has been observed to occupy a centre of inversion in all crystal structures. This is true, not only for all its inclusion compounds whose structures have been solved to date, but also for the host in its uncomplexed form, the so-called α-phase [102].

Because the host molecule consists of a central, (essentially planar) tricyclic nucleus, flanked on either side by phenyl rings, the majority of C-C bonds are aromatic in nature. As a result, bar grave distortions of the molecule in response to an unfavourable packing scheme, major deviations from theoretical values for bond lengths and bond angles are not expected. Thus a simple comparison of bond lengths and angles while excluding torsion angles and other parameters is not particularly informative.

However, three features of the host molecule dictate its absolute spatial configuration. Investigating these is correspondingly important in comparing and analysing the stresses which the host is subjected to. They include the degree of planarity of the tricyclic nucleus, the orientation of the phenyl ring to the central nucleus and, thirdly, the relative position of the hydroxyl substituents as compared to the molecule as a whole.

In the discussion below the following convention regarding the naming of the rings was used:
A - The central 1,4-cyclohexadiene ring
B - The benzene rings adjacent to A
C - The phenyl rings

As mentioned previously, tables giving a complete listing of all bond lengths, bond angles and torsion angles have been included at the end of chapter 5 (pp 89). Parallel columns for each crystallographically distinct molecule for all of the structures allows for comparison of these values.

6.1.2. Bond Lengths and Bond Angles

In total nine distinct host molecules have been described as part of the six crystal structures presented here - three of the structures contain two distinct host molecules per asymmetric unit. As a result of vibrational effects, a certain degree of fluctuation in the values of the bond lengths and angles for the nine molecules would be expected and this is indeed observed. Generally, however, these parameters were found to conform well to theoretical values as well as to the corresponding parameters reported for the uncomplexed host molecule and other inclusion compounds.

The parameters displaying the largest variation were generally associated with those parts of the molecule particularly exposed to external forces. Bond lengths belonging to this category include those between the tricyclic nucleus and the substituents (C(1)-O(1) and C(1)-C(11)) and to a lesser degree the single bonds of the 1,4-cyclohexadiene ring (C(1) - C(2) and C(1) - C(7')).

The bond lengths and bond angles defined by the atoms of ring A reflect the fact that C(1) is not sp^2- but rather sp^3-hybridised. The C(2) - C(1) - C(7') angle is strained at approximately 113° (significantly different from the ideal sp^3-hybridisation angle of 109,5°). Concomitantly the C(1) - C(2) - C(7) and C(1') - C(7) - C(2) bond angles are forced to expand from their theoretical 120° to values nearer 123-4°.

6.1.3. The Conformation of the Tricyclic Nucleus

As discussed in the introduction (Chapter 1) the conformation adopted by the central 1,4-cyclohexadiene ring of the host molecule is of interest to structural chemists following the uncertainty that reigned for so long over the conformation adopted by this ring in various molecules.

With only one exception [101] to date, the 1,4-cyclohexadiene ring in the host molecule has generally been reported to be planar [100,101,102,114,133]. Though 'perfect' planarity is never achieved in practice, small deviations from the ideal state may often be insignificant in comparison to the accuracy of the experimental method used. In such cases a ring would be termed planar. So when is the deviation from planarity significant enough for the ring to be described as non-planar ?

In discussing the conformation of six-membered rings various tests have been applied in the past. The simplest of these involves comparing the sum of the internal angles of the ring to the planar value of 720°. Deviation from planarity lead to sums of less than

720° being obtained. Other conformations can, however, not be described using this method.

In contrast a technique introduced by Duax and Norton [134] was found to be more useful. In addition to indicating the degree of puckering of a ring, it also defines the conformation adopted by the ring.

The method is based on the fact that two torsion angles of a ring are additive inverses if they are related by a mirror plane perpendicular to the plane of the ring but passing through its centre. On the other hand, they are equal if related by a twofold axis lying in the plane of the ring (see fig. 6.1).

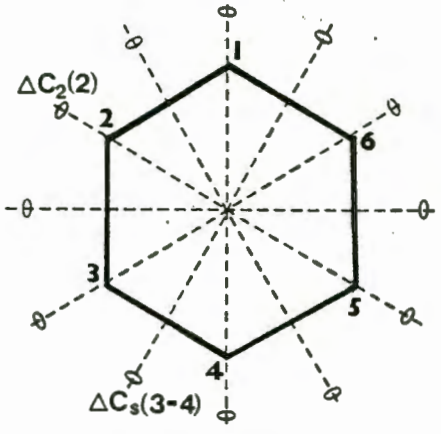

Figure 6.1 The symmetry elements of a six-membered ring

Two 'asymmetry parameters' - ΔC_s for mirror planes, ΔC_2 for two-fold axes - are defined by the authors. These can be used to fully describe the conformation of any ring. A value close to 0 for either parameter indicates the presence of the symmetry element being tested for.

For a ring to be planar all 12 symmetry elements indicated in fig. 6.1 must be present. By contrast a chair conformation is defined by the three mirror planes passing through two opposite atoms and the three two-fold axes bisecting two mutually opposite bonds. The boat, twist, sofa and half-chair conformations correspondingly are indicated by the presence respectively of two mirrors, two two-fold axes, one mirror and one two-fold axis.

For the present thesis a cut-off value for the asymmetry parameters of 5° is assumed (Duax and Norton suggest 4). Thus values below 5° were taken to indicate the presence of the symmetry element.

Interestingly the *trans*-9,10-dihydroxy-9,10-diphenyl-9,10-dihydroanthracene molecule has been found to invariably occupy a centre of inversion. The consequence of this is that the 1,4-cyclohexadiene ring must have one of only two possible conformations: Only the planar and chair-shaped conformations of six-membered rings are centrosymmetric.

Thus, since planarity is never attained, all central rings of (1) could be said to be chair-shaped but flattened to various degrees.

As a result of the centrosymmetry of the host molecule the two double bonds of the 1,4-cyclohexadiene ring are always coplanar and in addition the benzene rings on either side of the central ring are parallel (but not coplanar). The first of these properties is particularly useful as this allows deviation from perfect planarity of the central ring to be quantified by simply determining the distance (h) of C(1) from the plane defined by the four sp^2-hybridised atoms of the ring. (See figure 6.2)

Geometrical calculation indicates that for the present case the cut-off value of 5° for the asymmetry parameters translates into a corresponding value for h = 0,03 Å. This value has consequently been used here as the standard by which a ring is judged to be either planar or not.

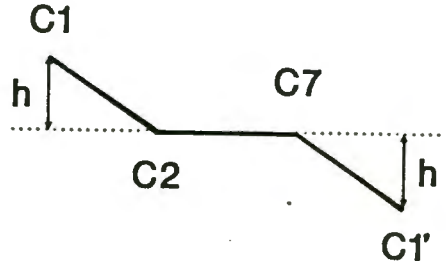

Figure 6.2 The Centrosymmetric 1,4-cyclohexadiene ring viewed along the plane defined by the double bonds.

Table 6.1.3 lists the deviation parameter defined above for all host molecules crystallographically described to date and categorises their conformational shape according to the specified cut-off value.

Analysis of the information listed leads one to conclude that the central 1,4-cyclohexadiene ring of the compound *trans*-9,10-dihydroxy-9,10-diphenyl-9,10-dihydroanthracene deviates very slightly but significantly from planarity. Its conformation could therefore most accurately be described as a 'nearly planar chair'.

To complete the discussion of the shape of the tricyclic nucleus the dihedral angle defined by the central double-bond plane and the adjacent benzene ring must be

considered. The appropriate angles are listed in table 6.1.3.a) (98. The dihedral angles are generally observed to be small (<3°), indicating that the tricyclic nucleus as a whole - with the possible exception of the C(1) atoms - is essentially planar. Only in the case of the **PYD(A)** molecule does the dihedral angle approach the significant 3°. In all cases the benzene rings of the nucleus can be considered to be planar with deviations from their least squares planes well below 0,02 Å.

6.1.4. Phenyl and Hydroxyl Group Orientation

Other aspects of the conformation of the host molecule, clearly linked to the conformation of the central 1,4-cyclohexadiene ring, which need to be considered involve the orientation of the phenyl and hydroxyl substituents in relation to the central tricyclic nucleus.

The exposed position of these substituents relative to the molecule as a whole, implies that their orientation must influence, and be influenced by, the conformation of the molecular nucleus. In fact their orientation, dictated as it is by the surrounding molecules must be considered the root cause of the distortion of the central ring.

As Table 6.1.4 (p99) below indicates, the relative position of both substituents is variable. As expected, the hydroxyl hydrogen is most flexible in its relative orientation, having to align itself with the guest heteroatom.

The phenyl substituent orientation is more difficult to describe. The dihedral angle it forms with the central ring A, though useful, is not definitive. A more precise method of defining its relative position requires the non-bonded angle C(1)'-C(1)-C(11) and corresponding torsion angle C(1)'-C(1)-C(11)-C(12) to be given in addition to the dihedral angle.

Analysis of these values (Table 6.1.4.b) indicates that, whereas the C(1)-C(11) direction is essentially invariant, the non-bonded torsion angle C(1')-C(1)-C(11)-C(12) reveals that this parameter is highly dependent on external forces.

An attempt at determining the energetically most favourable orientation of the phenyl substituent was made utilising the potential energy program EENY [135]. However, these met with only limited success, owing to the oversimplified approach of accounting for non-bonded interactions. By contrast a molecule like (1) represents a complicated and yet flexible structure in which a variation of one parameter would induce changes throughout the system.

Table 6.1.3 : Central Ring Conformation

a) Host molecules reported in this study:

Compound	C(1) deviation (Å)	Conformation	Dihedral angle sp^2-plane/benzene ring
NITRANN	0,056(4)	near-planar chair	1,0(2)
PROP	0,029(3)	near-planar chair	0,3(1)
PYD(A)	0,076(3)	near-planar chair	2,8(2)
PYD(B)	0,050(4)	near-planar chair	0,3(2)
3PIC(A)	0,024(3)	planar	0,2(1)
3PIC(B)	0,057(2)	near-planar chair	0,3(1)
24LU(A)	0,051(4)	near-planar chair	0,6(1)
24LU(B)	0,006(4)	planar	0,2(2)
26LU	0,008(2)	planar	0,4(1)

b) Host molecules previously reported:

Compound	C(1) deviation (Å)	Conformation	Reference
Host	0,037(2)	near-planar chair	100
H:2(2-butanone)	0,028(2)	planar	102
H:2(4-vinylpy$^+$)	0,027(2)	planar	124
H:2(4-methylpy$^+$)	0,021(3)	planar	124
H:2-methylpy$^+$) (A)	0,026(3)	planar	124
(B)	0,029(4)	planar	124
H:2(Acetophenone)	0,032(2)	near-planar chair	114
H:2(3-methylcp*)	0,013(2)	planar	114
H:2(4-methylch$^\#$)	0,039(3)	near-planar chair	133
H:2(2-methylch$^\#$)	0,014(2)	planar	133
H:2(methanol)	0,035(3)	near-planar chair	100
H:Ethanol (A)	0,106(4)	chair	101
(B)	0,027(3)	planar	101
H:1,4-Butanediol	0,046(3)	near-planar chair	102

$^+$ pyridine
* cyclopentanone
$^\#$ cyclohexanone

Treating the phenyl substituent and the tricyclic nucleus as rigid groups it was possible to identify the orientation adopted by the phenyl substituent as corresponding to a broad potential minimum. The determination of an absolute preferred orientation was, however, not possible.

As expected, all phenyl substituent rings were observed to be planar with deviations from the least-squares planes significantly less than 0,02 Å.

Table 6.1.4: The Orientation of a) the Hydroxyl and b) the Phenyl Substituents

a)

Compound name	Torsion angles O(1)-C(1)-C(7')-C(2')	C(2)-C(1)-O(1)-H(1)
NITRANN	128,8(5)	65(3)
PROP	120,1(3)	173(2)
PYD(A)	129,9(4)	69(2)
PYD(B)	127,4(4)	86(2)
3PIC(A)	119,5(3)	46(2)
3PIC(B)	129,0(3)	44(2)
24LU(A)	127,4(3)	48(1)
24LU(B)	122,8(3)	56(2)
26LU	123,8(2)	63(1)

b)

Compound name	Dihedral angle α	Non-bonded angle C(1)'-C(1)-C(11)	Non-bonded Torsion angle C(1)'-C(1)-C(11)-C(12)
NITRANN	88,0(2)	124,8	7,3(4)
PROP	87,8(1)	124,6	3,7(4)
PYD(A)	102,5(1)	123,5	26,2(5)
PYD(B)	92,8(1)	123,4	8,2(4)
3PIC(A)	86,9(1)	127,0	4,6(3)
3PIC(B)	90,7(1)	123,4	-2,5(3)
24LU(A)	84,6(1)	123,8	17,5(5)
24LU(B)	93,7(2)	126,5	6,2(6)
26LU	87,7(1)	125,3	4,2(3)

6.2. CRYSTAL STRUCTURES AND MOLECULAR PACKING

6.2.1. NITRANN

The numbering scheme employed for NITRANN is included in the perspective view of a portion of the structure depicted in figure 6.1.1.

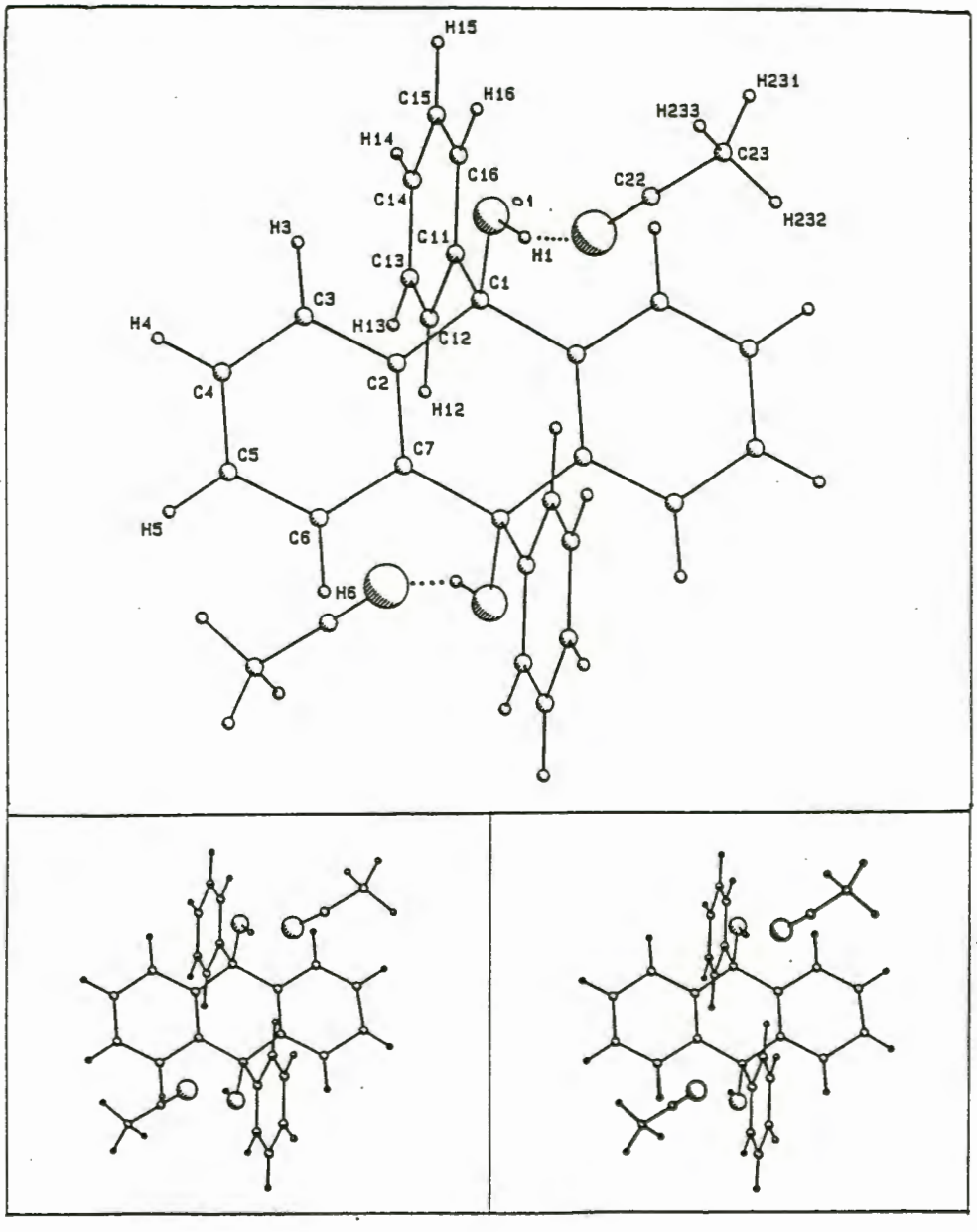

Figure 6.1.1 NITRANN - a perspective view of the structure a) indicating the numbering scheme employed and b) in a stereoscopic view.

As required by the space group symmetry, two host molecules, each situated on a centre of inversion and related to each other by a *c*-glide plane, occupy the unit cell. Associated with each of these host molecules, we found two acetonitrile molecules similarly related by the centre of symmetry.

An interatomic distance between O(1) and N(21) of 2,893(8) Å and a O(1)-H(1)-N(21) angle of 155,5(2,0)° are clearly indicative of a hydrogen bond existing between the two. No further hydrogen bonds occur in the structure and thus the general hydrogen bonding scheme is analogous to that reported for the crystalline adducts formed by (1) with ketones [114,133] and some substituted pyridines [124].

No evidence for stacked aromatic rings can be found. This precludes intermolecular π-interactions as the source of cohesion between molecules. It must therefore be concluded that apart from the hydrogen bond between host and guest, only van der Waals interactions are responsible for crystal stability.

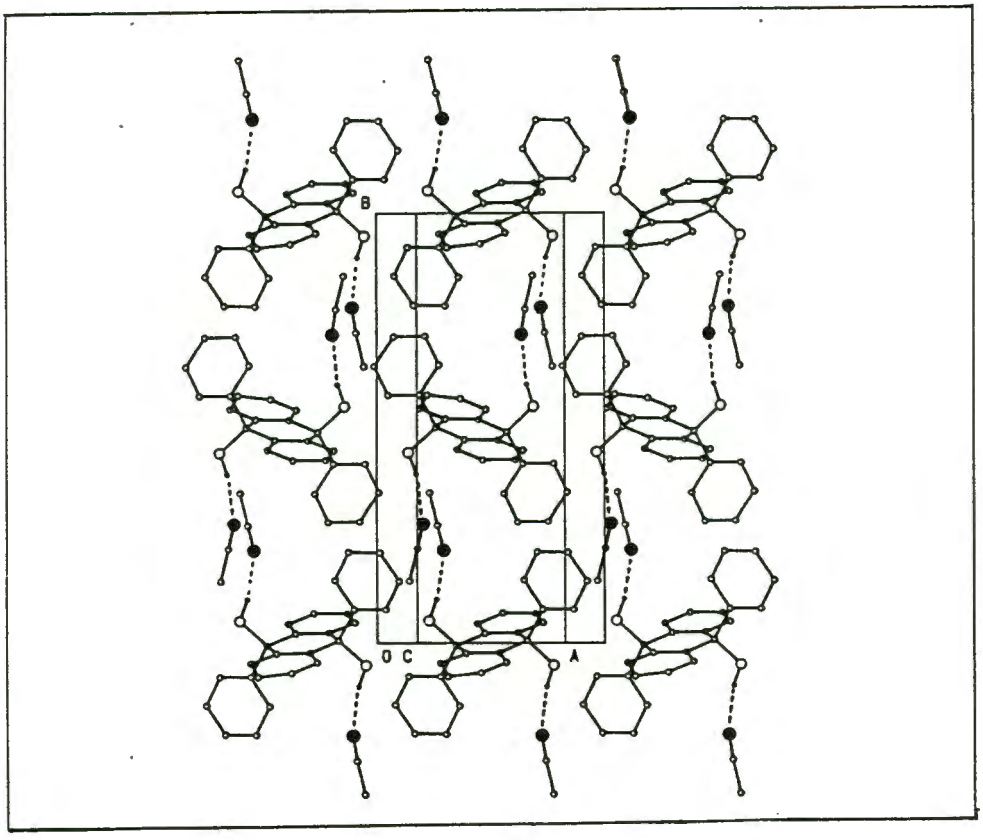

Figure 6.1.2 **NITRANN** - The packing mode as viewed along the [010] direction.

Closer inspection of the packing of **NITRANN** (figure 6.1.2) reveals that the acetonitrile molecules lie in channels that permeate the structure in the direction [001]. These

channels are clearly visible in figure 6.1.3, a stereoscopic view of the host lattice parallel to [001]. The guest molecules have been removed while the host atoms have been assigned van der Waals radii. The two channels visible in the diagram are related by a centre of inversion situated at the centre of the cell and are therefore crystallographically equivalent. It must be stressed, however, that even though the channels occupied by the guest molecules can be represented graphically (as seen in figure 6.1.3) the host lattice is not, in reality, sufficiently stable to exist in this form. Instead, removal of the guest, as will be demonstrated in Chapter 7, causes the host lattice to collapse to the energetically preferred α-phase.

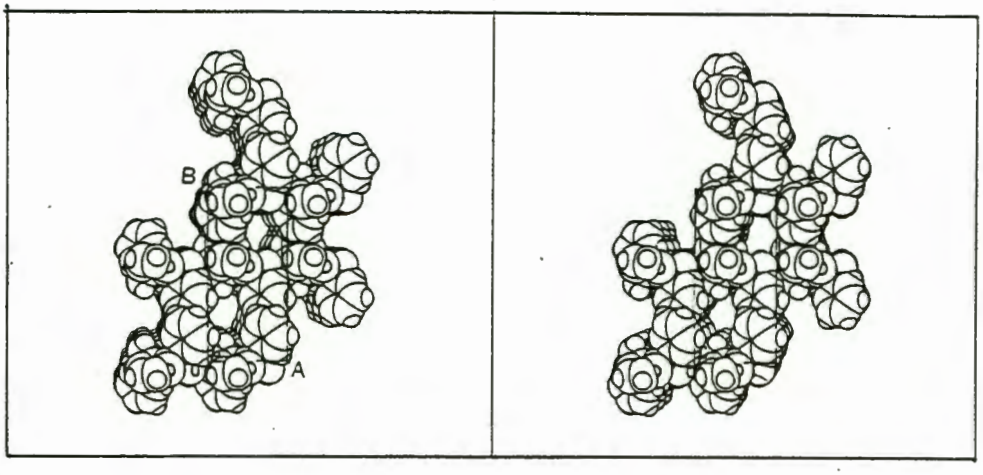

Figure 6.1.3 **NITRANN** - A stereoview of the channels occupied by the acetonitrile molecules (guest molecules are omitted to give an impression of the host lattice)

A computer program OPEC[136] allows the channels to be further investigated. Making use of van der Waals radii[137] assigned to each atom in the unit cell and dividing up the unit cell into small 'elementary volumes' ($V_{el,i}$) - typically 0,2 to 0,5 Å^3 - the fractional occupation D_i of each elementary volume can be calculated. Inspection of the resultant three dimensional map of D_i allows channels and cavities to be identified and their approximate dimensions to be determined.

In the case of **NITRANN** the channels parallel to [001] were clearly discernible. The cross-sectional dimensions of the channels were found to range from a maximum 5,9 x 3,8 Å at the widest point to a minimum of 4,2 x 3,4 Å.

Figure 6.1.4 depicting the *xz*-plane at ½b clearly portrays the close fit of the guest molecules and the channels in which they lie.

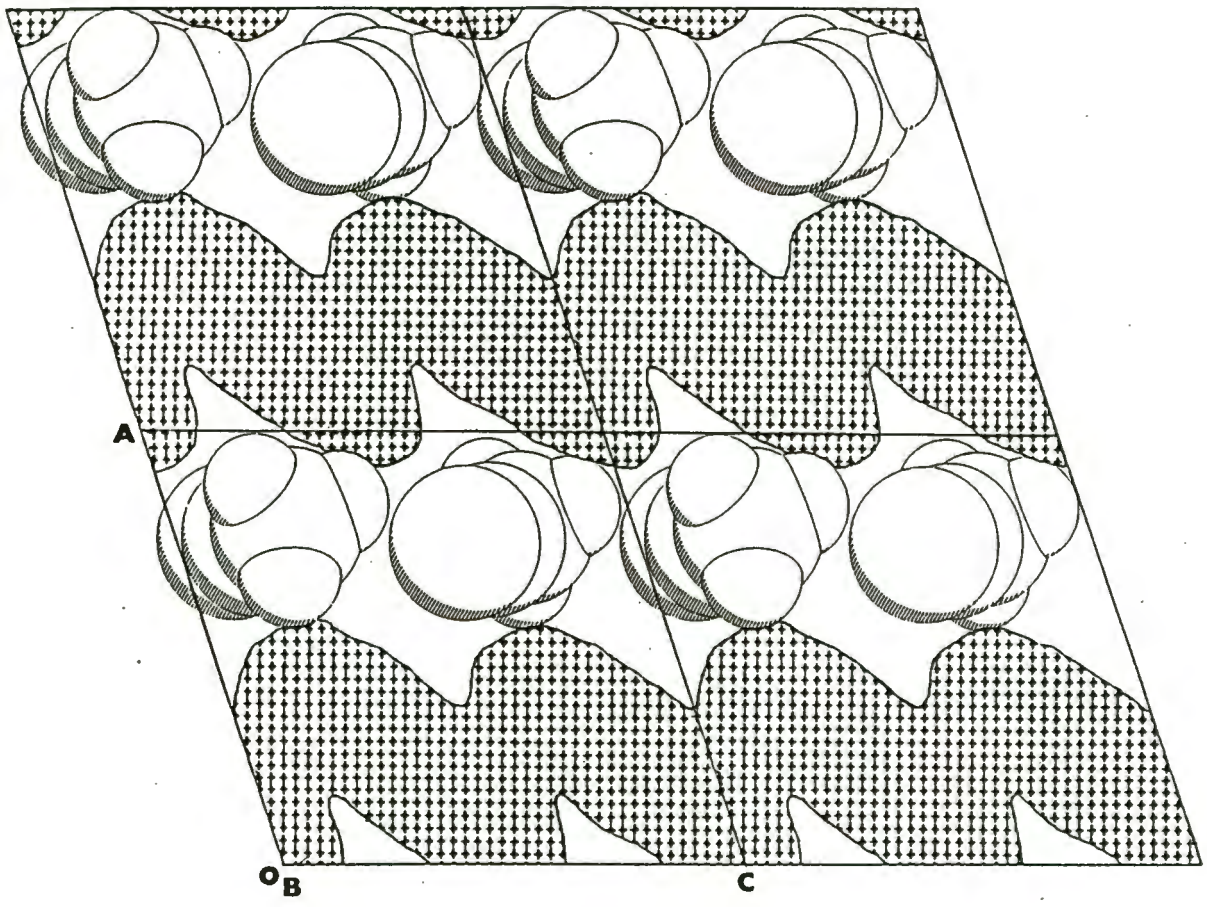

Figure 6.1.4 **NITRANN** - An impression of the close fit between the guest and the host channels.

6.2.2. PROP

The space group in which the complex **PROP** was solved was $P2_1/n$, equivalent to, but a different cell choice of, $P2_1/c$. As in all the crystal structures containing the host molecule solved to date, the host occupies a centre of inversion.

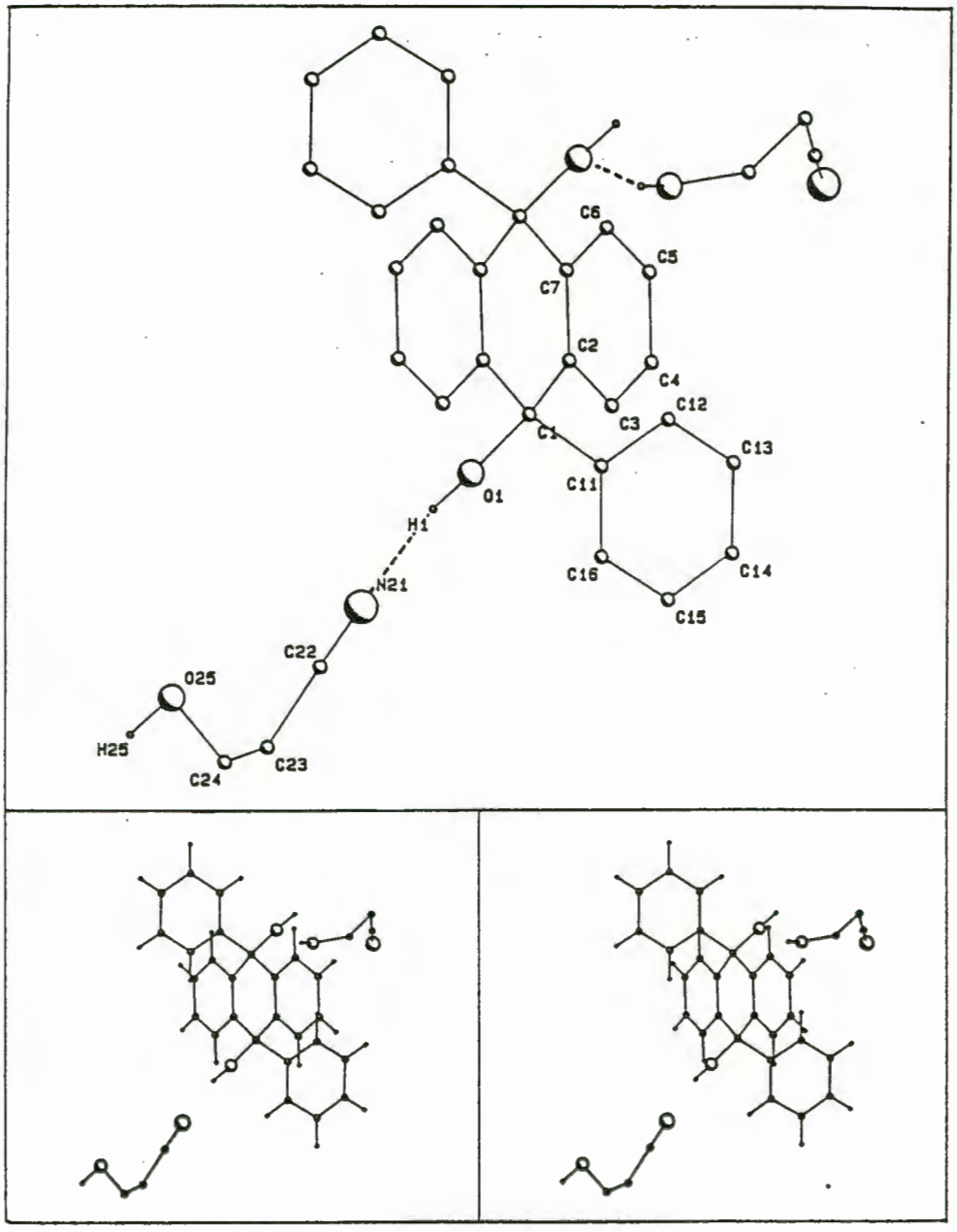

Figure 6.2.1 **PROP** - A perspective view a) indicating the numbering scheme used and b) in stereoscopic view. For clarity only the dominant C(24) position is included and all hydrogen atoms other than the hydroxyl H's are omitted in a).

Associated with each half of the host molecule found to occupy the asymmetric unit is a 3-hydroxypropionitrile molecule in a general crystallographic position. This results in a host to guest ratio of 1:2 . Because of the symmetry operations of $P2_1/n$ this in turn means that a total of two formula units, Z, occupy the unit cell.

A perspective view of the structure in figure 6.2.1 indicates the numbering scheme employed in the case of **PROP**. For clarity, the hydrogen atoms with the exception of the hydroxyl hydrogens, have not been included, while only the dominant position for the statistically disordered C(24) is shown. Hydrogen bonds are indicated by dotted lines.

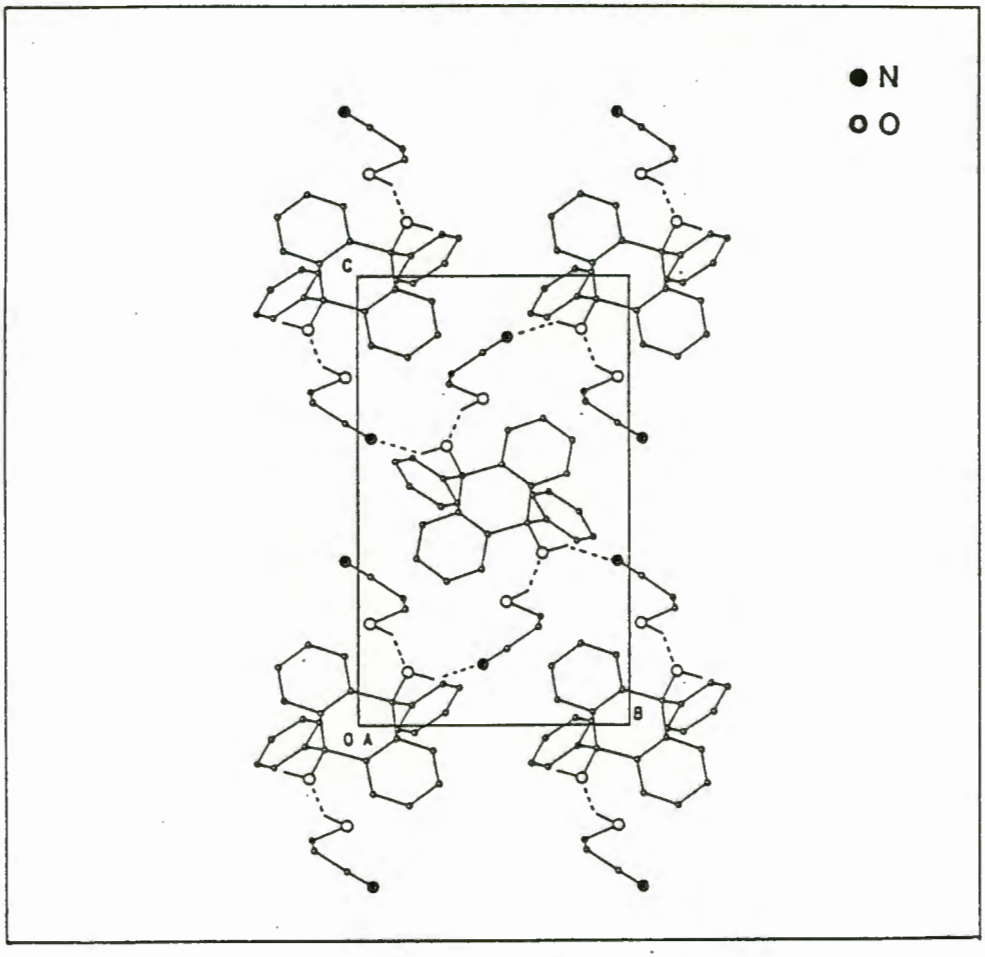

Figure 6.2.2 **PROP** - Packing diagram viewed down [100]

As may be seen from figure 6.2.2, each guest molecule is hydrogen bonded to two alternative host molecules, the host hydroxyl group not only acting as a hydrogen bond donor through its hydrogen atom, but also as an acceptor through oxygen. As a consequence, **PROP** can be described as consisting of infinite two-dimensional molecular layers lying parallel to the (101) plane.

Figure 6.2.2 a view along [100] indicates the manner in which alternative host molecules in the plane are connected by hydrogen bonded guests, while figure 6.2.3 shows the orientation of the planes in relation to the unit cell.

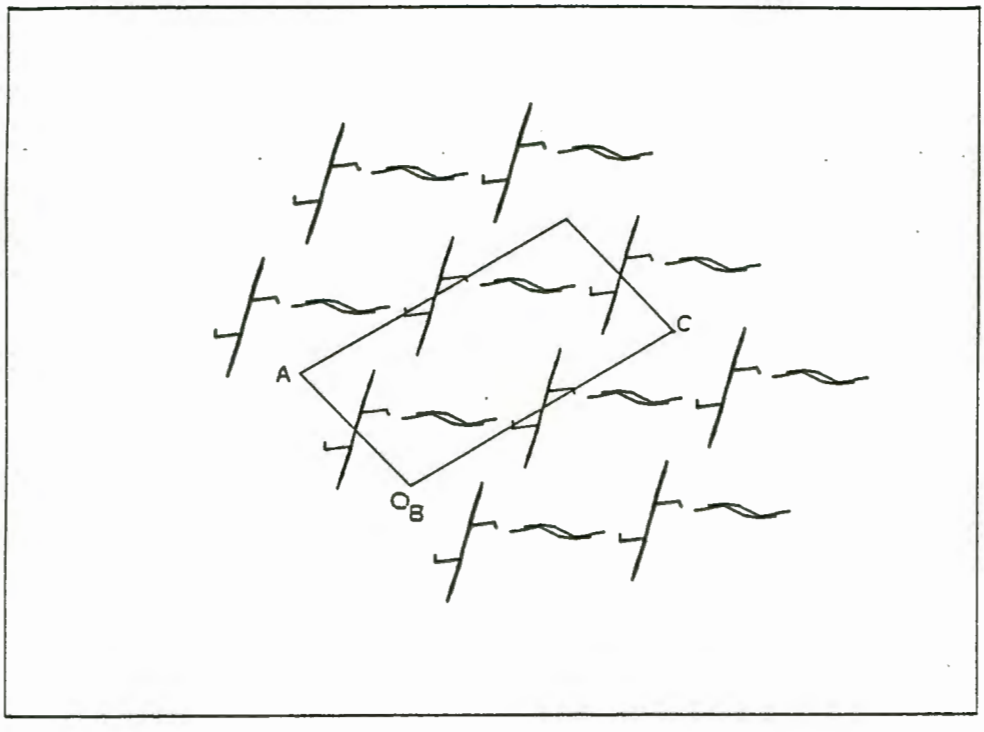

Figure 6.2.3 **PROP** - Packing diagram viewed down [010] (the phenyl substituents have been omitted to emphasise the layered nature of the complex).

Closer analysis of figures 6.2.2 and 6.2.3 indicate that since the guest molecules all lie near ¼a and ¼c (alternatively ¾a and ¾c) their positions describe channels in the direction [010] situated at (¼,y,¼) and centrosymmetrically at (¾,y,¾)

With the help of OPEC this channel is clearly visible. The narrowest point of this channel occurs at ¼,¼,¼ and has a cross-sectional area of 4,22 x 4,9 Å - sufficiently large for a guest molecule to pass through. Figure 6.2.4 (p 107) shows a longitudinal view along the channel at ¼a with the superimposed guest molecules plotted using van der Waals radii, demonstrating the close relationship between the guest molecules and the channel.

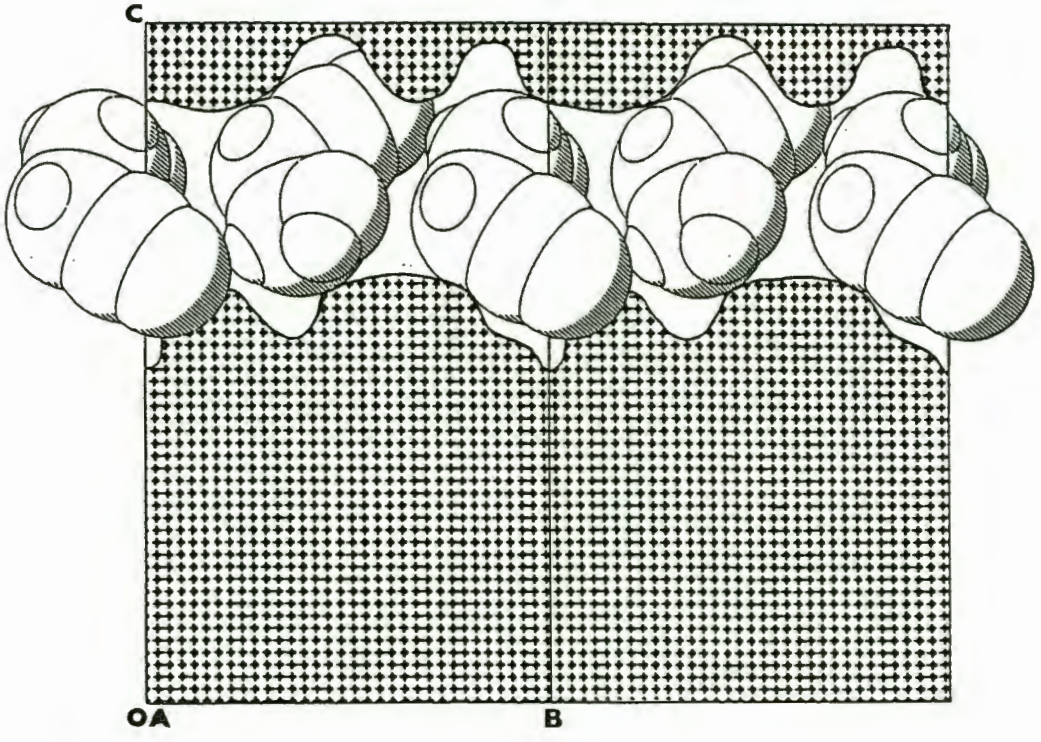

Figure 6.2.4 **PROP** - A cross-sectional view of the guest channel at ¾a. The superimposed guest molecules give an impression of the close relationship between the guest molecules and the channel.

6.2.3. PYD

In the case of the crystal structure **PYD** the original primitive unit cell of the space group $P\bar{1}$ was exchanged in favour of a C-centered cell belonging to the non-primitive space group $C\bar{1}$ for computational reasons (cf. Section 5.3). For consistency this unit cell has been retained and all fractional coordinates, observed and calculated structure factors and all plots refer to this new unit cell.

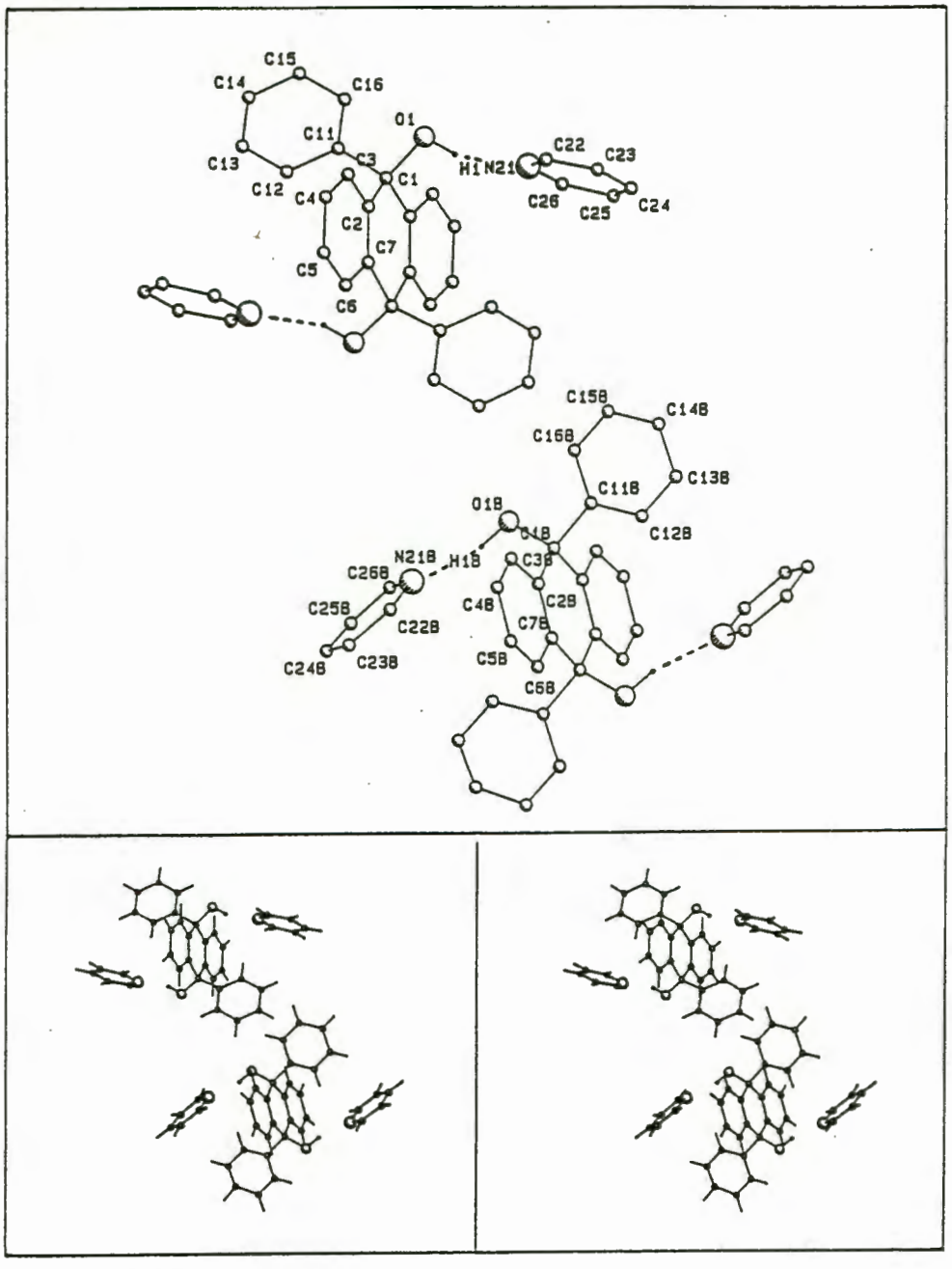

Figure 6.3.1 **PYD** - A perspective view a) indicating the numbering scheme and b) in stereo. Dotted lines indicate hydrogen bonds between host and guest molecules.

Figure 6.3.1, a perspective view of two formula units of **PYD**, indicates the numbering scheme for this crystalline adduct and also indicates the presence of hydrogen bonds (dotted lines) which bind two guest molecules to each host molecule.

As a result of the four symmetry operations for the space group $C\bar{1}$, four asymmetric units occur per unit cell. Because each asymmetric unit contains two crystallographically distinct half host-molecules and two similarly distinct guest molecules, in general positions but associated with the host molecules, the unit cell is found to contain a total of 4 formula units (Z = 4).

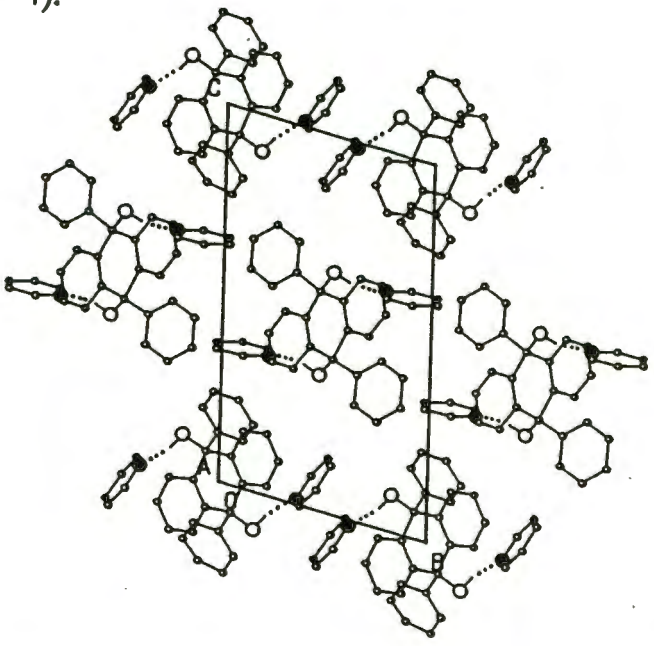

Figure 6.3.2. **PYD** - A packing diagram viewed down [100]. (● and o are used to indicate Nitrogen and Oxygen atoms respectively)

A packing diagram of **PYD** is shown in figure 6.3.2. Hetero atoms have been emphasised and hydrogen bonds are indicated by dotted lines. The hydrogen bonding scheme for **PYD** is comparable to that observed for **NITRANN**, in that each host hydroxyl group is associated with one guest. Details of hydrogen bonding for all six structures are summarised in table 6.1 at the end of this chapter.

Both pyridine rings are found to be planar within experimental accuracy, with maximal deviations from the least-squares planes amounting to 0,008(5) Å and 0,014(5) Å respectively. Since there is no evidence for stacking of aromatic rings, this leaves only van der Waals interactions to supply cohesive forces to the macrostructure. Dihedral angles defined by guest pyridine rings on the one hand and host aromatic rings on the other lie in the range 68,6 to 128,6°, and that spanned by the two distinct guest molecules is observed to be 60,46°, precluding π-interactions.

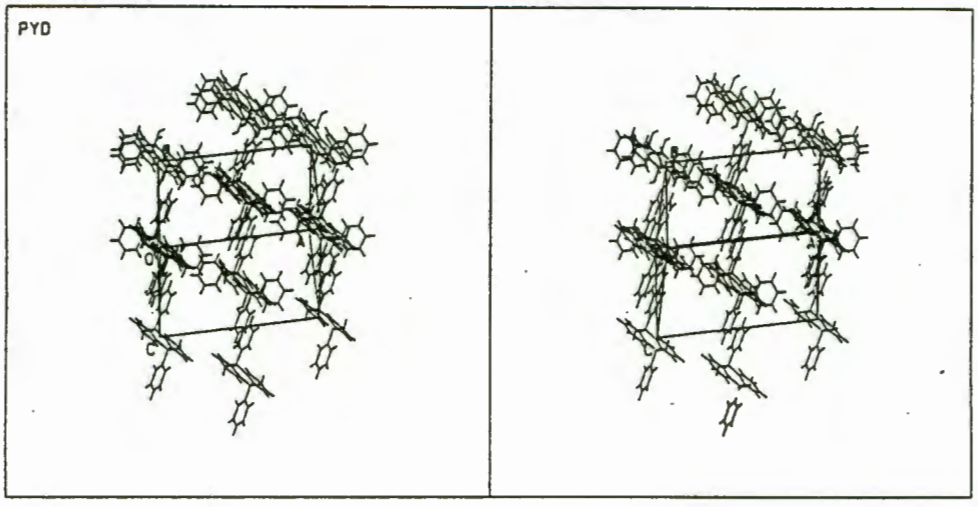

Figure 6.3.3. **PYD** - The guest channels parallel to the line of sight, are clearly visible in this stereo stick diagram down [011].

Figure 6.3.3 is a diagram of the host lattice (guest molecules have been omitted) in the direction [011]. This reveals a set of four identical pairs of 'half-channels' per unit cell. The channels making up each pair are crystallographically distinct and each is occupied by one of the two groups of pyridine molecules. However, the channels are linked and figure 6.3.4 - sketched with data obtained from OPEC and showing a section through the host lattice at ¼a - indicates that the opening between the 'half-channels' is sufficiently large to permit pyridine molecules to pass from one half to the other. On the other hand a minimum for the cross-sectional size of the channel of 4,4 x 3,4 Å indicates that the movement of guest molecules through the channel is not hindered sterically.

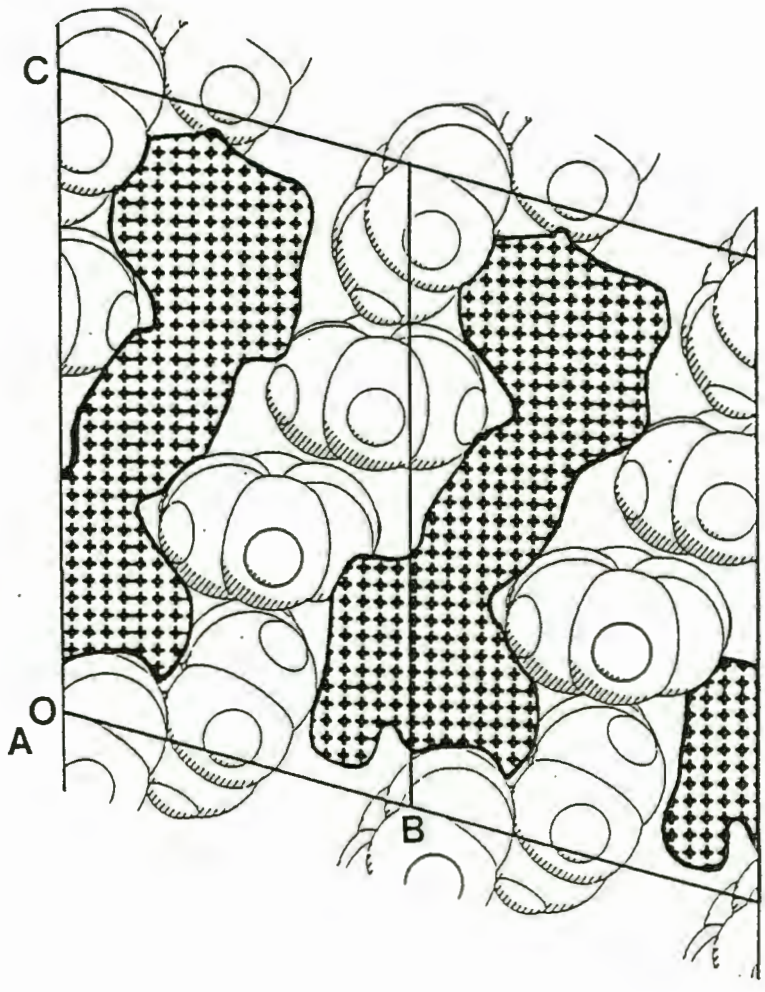

Figure 6.3.4 **PYD** - A cross-section through the host lattice at ¼a indicating the packing of the guest molecules in the channels (Guest molecules are plotted with van der Waals radii while the hatched area indicates the host lattice.)

6.2.4. 3PIC

The complex **3PIC** shares a number of structural features with **PYD**. A perspective view (figure 6.4.1) demonstrates the hydrogen bonding (dotted lines) and the numbering scheme for this structure.

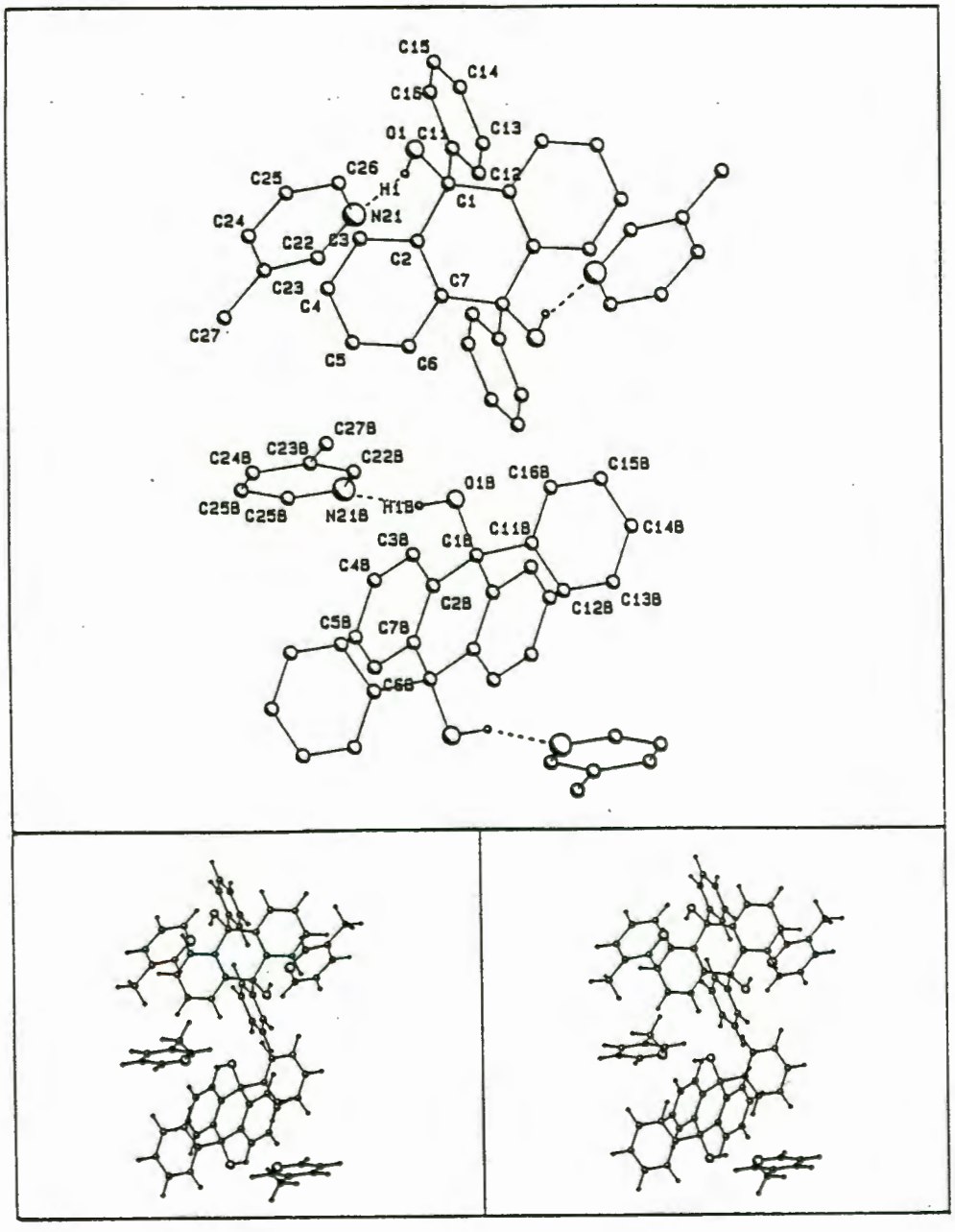

Figure 6.4.1 **3PIC** - A perspective view a) indicating the numbering scheme used (hydrogen atoms have been omitted) and b) in a stereoview.

Though the reduced cell of **3PIC** belongs to the space group $P2_1/c$ (unlike **PYD** which was initially assigned to the space group P1) its asymmetric unit also contains two half host molecules which are crystallographically distinct. The second half of each host

molecule is generated by a centre of inversion. Large unit cell dimensions in comparison to the other structures are required in order to accommodate the four formula units generated by the symmetry operations of the space group.

Each half molecule is associated with a planar 3-methylpyridine molecule. The two are connected by a hydrogen bond involving the hydroxyl group of the host as the donor, while the nitrogen atom of the pyridine ring acts as the acceptor. The absence of π-interactions means that the structure relies on the weak van der Waals forces for its stability, implying that the host lattice is unstable and would be expected to collapse if the guest were removed (see Chapter 7 for more detail).

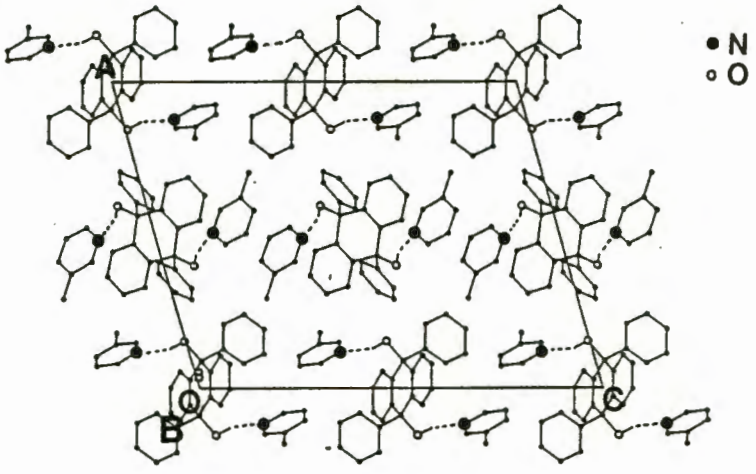

Figure 6.4.2 **3PIC** - A packing diagram viewed parallel to the *b*-axis. Hydrogen bonds are indicated by dotted lines.

A packing diagram (figure 6.4.2) viewed down the short, unique axis b indicates that the two groups of symmetry-related guest molecules are located in two different channels centered about two-fold screw axes at 0,y,¼ (0,y,¾) and ½,y,¼ (½,y,¾). While the second of these channels is essentially linear the first can best be described as undulating, with the widest part of the channel alternatively moving to include either guest position.

In addition, because both sets of guest molecules have z coordinates of approximately ¼, the spaces not occupied by the host also interconnect to create secondary channels which lie close to the (0,0,¼) plane. However, because the resulting web of guest spaces does not lie exactly in the (0,0,¼) plane, it is difficult to depict graphically. Instead a sketch giving an essentially qualitative view of the space net near the crystallographic (0,0,¼) plane is given in figure 6.4.3. The thickness of the net is remarkably constant

with an approximate width along c of 4,4 Å, thus posing no steric hindrance to the movement of the guest molecules.

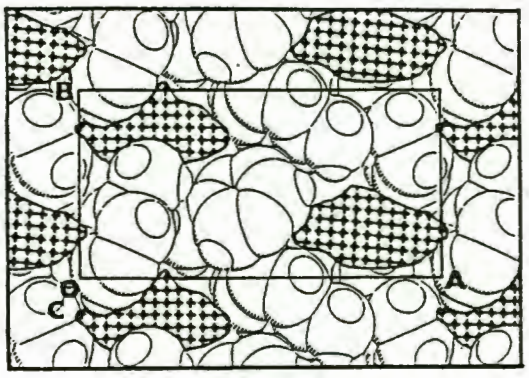

Figure 6.4.3 3PIC - A cross-sectional view of the host at ¼c revealing the guest channel web, parallel to the xy-plane. The guest molecules, drawn with van der Waals radii, are superimposed over the cross-section of the host (hatched area).

6.2.5. 24LU

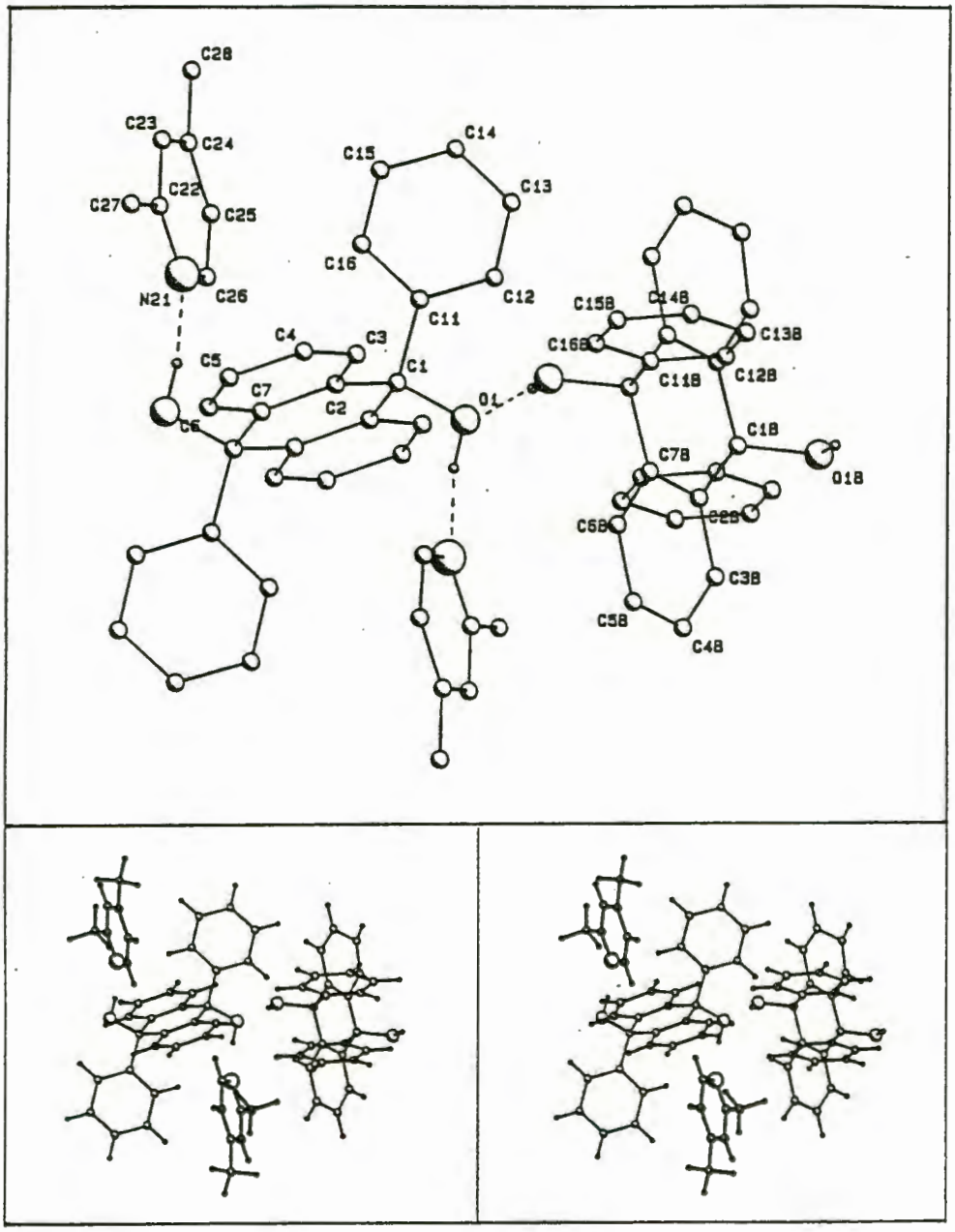

Figure 6.5.1 24LU - A perspective view a) indicating the hydrogen bonding scheme and the numbering scheme, and b) in stereo.

Analysis of the perspective view of the structure 24LU given in figure 6.5.1, indicates that the relative arrangement of molecules in this structure is significantly different from that observed for NITRANN, PYD and 3PIC in a number of respects. The origin of this new packing mode may be traced to the fact that the host to guest ratio for this complex is 1:1, in contrast to the 1:2 ratio observed for the other four adducts described in the preceding sections. As before, the host molecules occupy centres of inversion. But, since each host molecule possesses two hydrogen bonding sites a 1:1 host to guest

ratio implies that, unless each guest molecule acts as hydrogen bond acceptor to two host hydroxyl groups, no guest molecules are available for bonding to the second host molecule located in the asymmetric unit.

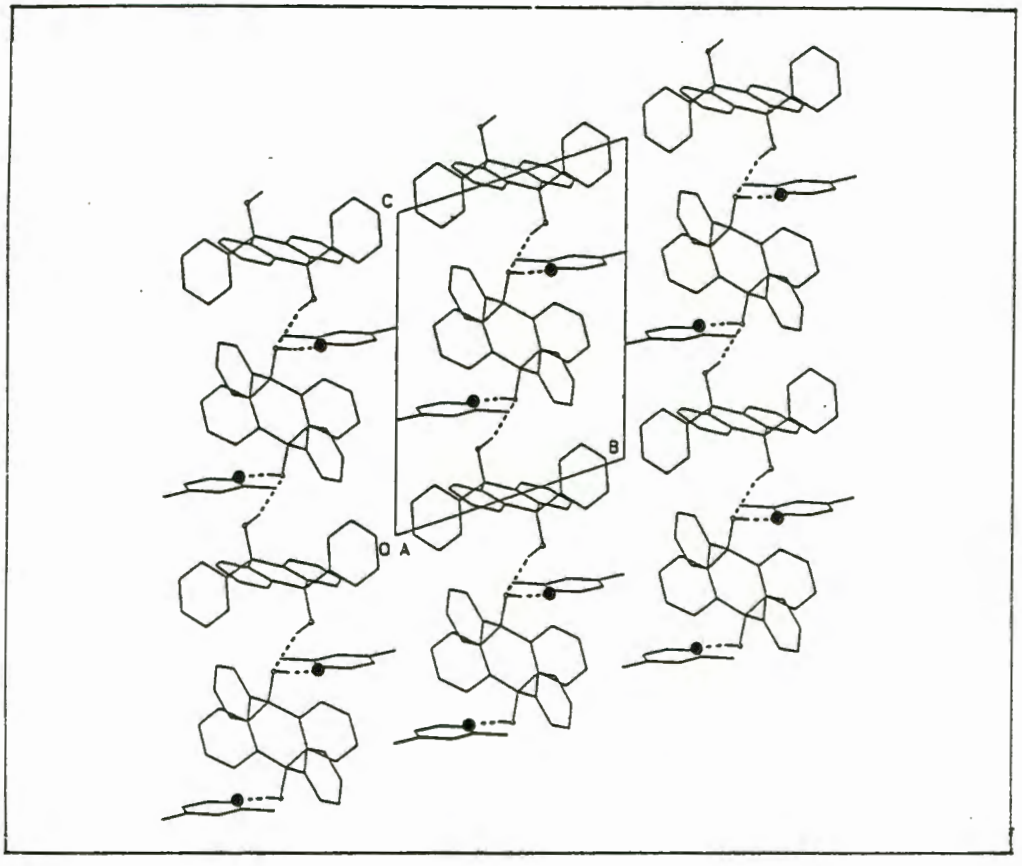

Figure 6.5.2. **24LU** - A packing diagram down [100] indicating infinite strings of hydrogen bonded molecules parallel to [001]. Hydrogen bonds are indicated by dotted lines while o and ● represent O and N atoms respectively.

This hydrogen bond acceptor deficiency, in the form of guest nitrogen atoms, is overcome by hydrogen bonding between the two sets of host molecules. The resulting hydrogen bonding scheme is elucidated by figure 6.5.2. The hydroxyl substituents of one set of host molecules do not only act as hydrogen bond donors to the nitrogen atoms of the 2,4-dimethylpyridine molecules but, simultaneously, provide hydrogen bond acceptor sites to hydroxyl groups of the second group of host molecules. This results in 'strings' of linked host molecules running through the structure parallel to the c-axis with laterally attached guest molecules situated on every alternate host molecule.

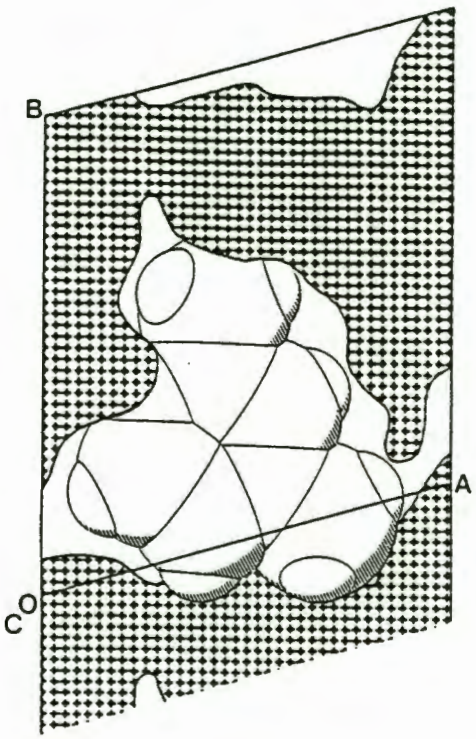

Figures 6.5.3 24LU : A cross-sectional view through the host lattice (hatched area) at *c*/3 indicating the cavity inside which the guest molecule is enclosed.

As a result of the large proportion of host molecules, the guest molecules are isolated from each other and lie in cavities enclosed by host molecules. Figures 6.5.3 a) and b) indicate the close confinement in which the guest molecules are held by the host lattice.

The fact that the guest molecules occupy cavities rather than channels means that, in order for the guest to escape from the complex, the host lattice would first need to be disrupted. This, in turn, leads one to expect the guest to be more firmly held by the host than in other complexes and thus a higher ratio of the desorption onset temperature to the boiling point of the guest as compared to other complexes could be expected.

As was mentioned in Section 5.6, the structure of 24LU (Host:2,4-dimethylpyridine) was found to be virtually isomorphous with that reported for the crystalline complex of (1) with 2-methylpyridine. A comparative listing of unit cell parameters as well as other values for the two structures is given below in Table 6.2.5. Comparison of the atomic coordinates indicated a close correspondence between the two sets of values.

The molecular packing scheme observed for these two complexes was found to be similar to that reported for the ethanol inclusion compound of this host [101]. However, though all belong to the triclinic space group $P\bar{1}$, the unit cell of the ethanol complex differs significantly from the others.

Table 6.2.5: Comparative Data for the Inclusion Complexes of (1) with 2-Methylpyridine and 2,4-Dimethylpyridine.

Guest Solvent	2-Methylpyridine [124]	2,4-Dimethylpyridine [this study]
Space group	$P\bar{1}$	$P\bar{1}$
a / (Å)	9,337(2)	9,178(1)
b / (Å)	10,407(3)	10,739(2)
c / (Å)	13,470(9)	13,589(2)
α / (°)	70,75(3)	71,94(1)
β / (°)	87,65(3)	88,24(1)
γ / (°)	73,58(2)	75,03(1)
Z	2	2
V / (Å^3)	1183,2(9)	1228,4(9)
D_c / (g.cm^{-3})	1,284	1,275

The structure of the complex of the host and 2-methylpyridine was reported to be disordered and, at the time, it was speculated that the cavity in the host structure could be expected to accommodate larger guest molecules. However, because the guest was found to be disordered about a pseudo-mirror plane roughly passing through the N(21) and C(24) atoms, it was expected that 2,6-dimethylpyridine would take the place of the 2-methylpyridine. The methyl substituents of 2,6-dimethylpyridine would then occupy the positions of the two alternate methyl groups of the disordered structure.

However, instead of 2,6-dimethylpyridine, 2,4-dimethylpyridine replaces the 2-methylpyridine guest, roughly coinciding with one of the two disordered guests positions (instead of occupying an intermediate position). The γ-methyl group extending the N(21)-C(24) axis is accommodated by a fractional increase in the unit cell parameters which, in turn, is reflected by a small but significant increase in the unit cell volume. Figure 6.5.4 gives an impression of the positional coincidence of the guest molecules. While the disordered 2-methylpyridine molecules are depicted on page 120, the 2,4-dimethylpyridine guest appears on page 119 in the form of an overlay to emphasise the similarities in the respective guest positions.

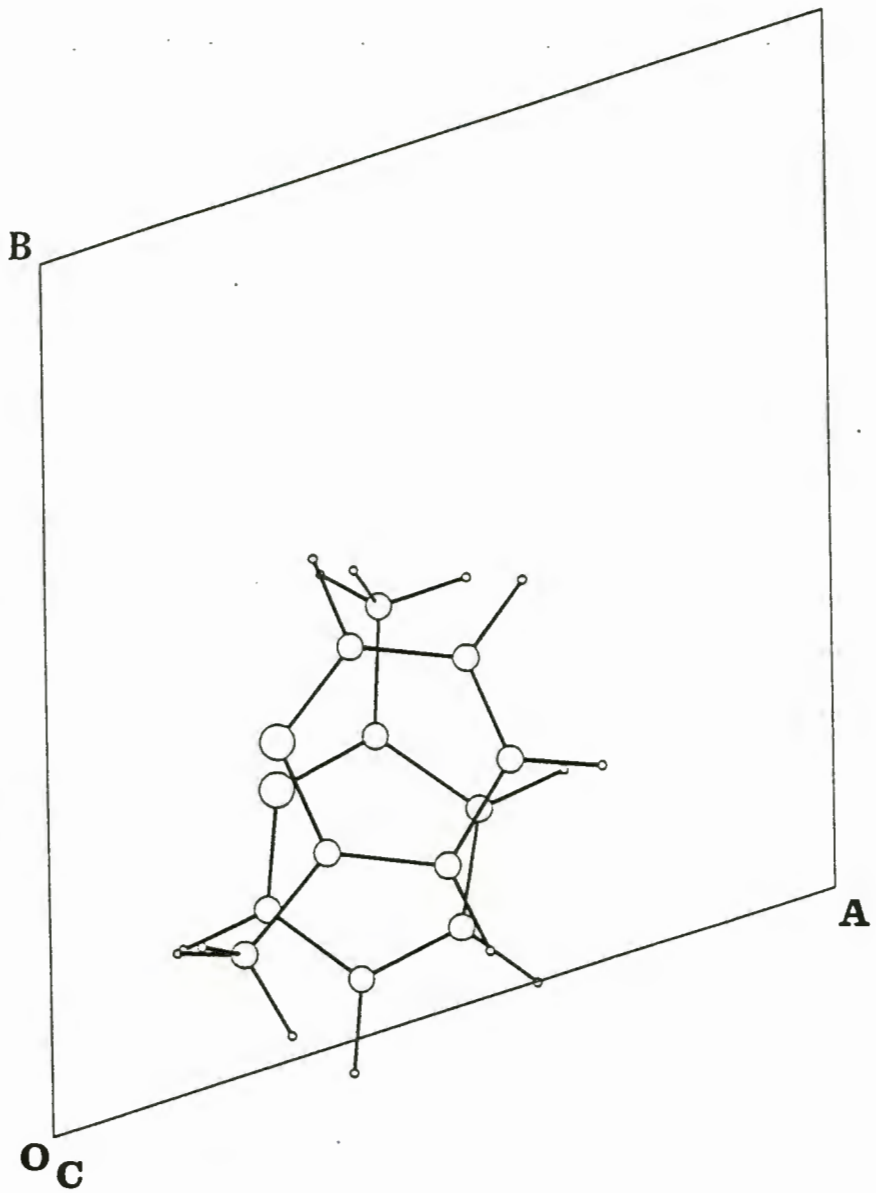

Figure 6.5.4. - The position occupied by the guest in the inclusion compound of (1) with and with
b) 2-methylpyridine (disordered).

6.2.6. 26LU

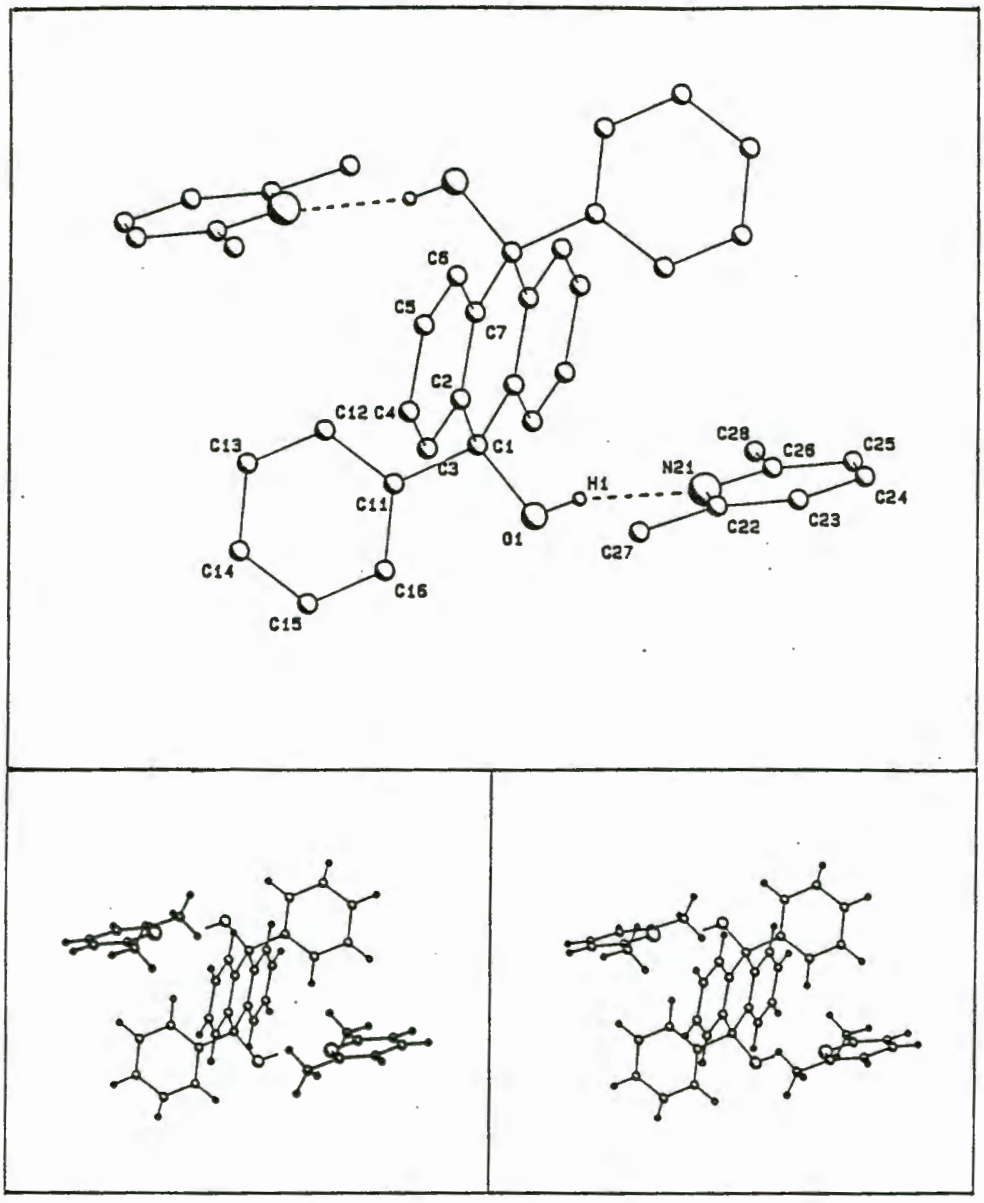

Figure 6.6.1 **26LU** - A perspective view a) indicating the numbering scheme used and b) in a stereoview. Dotted lines indicate hydrogen bonds between host and guest molecules.

26LU, the complex of the host with 2,6-dimethylpyridine (2,6-lutidine) is the only complex of the present series which crystallises in the space group $P\bar{1}$ and has only one formula unit per unit cell. The asymmetric unit, correspondingly, contains only a single guest molecule and half a host molecule. Figure 6.6.1, a perspective view of the structure, indicates the numbering scheme used and reflects, by means of dotted lines, the linkage between host and guest molecules in the form of hydrogen bonds.

In the crystal structure of the host [100], which is similar to that of **26LU** in that one formula unit occupies a triclinic cell of the space group $P\bar{1}$, weak π-interactions between parallel phenyl rings were postulated as the binding forces of the lattice. Such π-interactions must be excluded in **26LU**, however, as no stacking of aromatic rings is observed, despite molecular packing being achieved by translation only. This once again leaves van der Waals interactions as the only consolidating force of the structure apart from the hydrogen bonds binding the guest to the host.

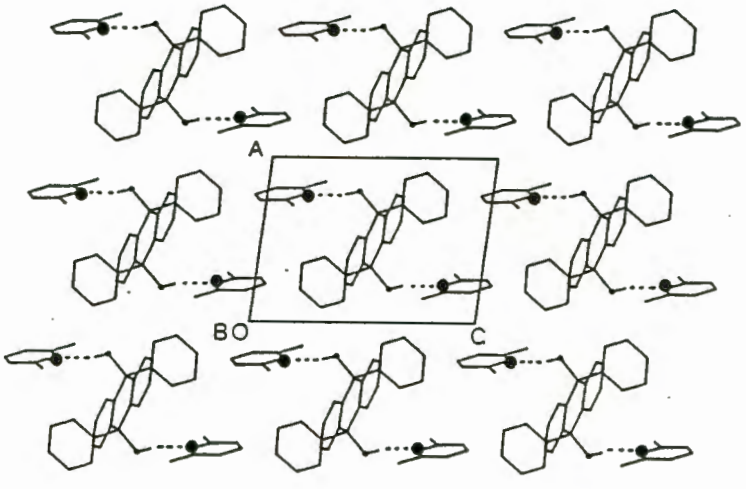

Figure 6.6.2. **26LU** - A packing diagram viewed down [010]. Hydrogen bonds are represented by dotted lines while ● and o indicate nitrogen and oxygen atoms respectively.

From figure 6.6.2, a packing diagram of **26LU** viewed down [010], it becomes clear that the guest molecules all lie in the ab-plane of the unit cell.

Initially it may be assumed that the guest molecules lie inside channels as has been observed for all similar crystal structures. Analysis of the packing mode with the help of OPEC, however, indicates that the structure can best be described as consisting of alternate layers of host and guest molecules. The situation at ½b, where maximum separation between the host molecules is observed, is depicted in figure 6.6.3. The opposite extreme occurs in the $(x,0,z)$ plane, where the host layers are separated by only 2,4 Å.

The realisation that the host molecules form a layered lattice, makes the question of whether this complex could, in the event of the guest being removed, result in a β_0-phase, superfluous. This conclusion was indeed verified (see Chapter 7) when

desorption of the guest caused the host molecules to re-adopt the packing characteristic of the α-phase.

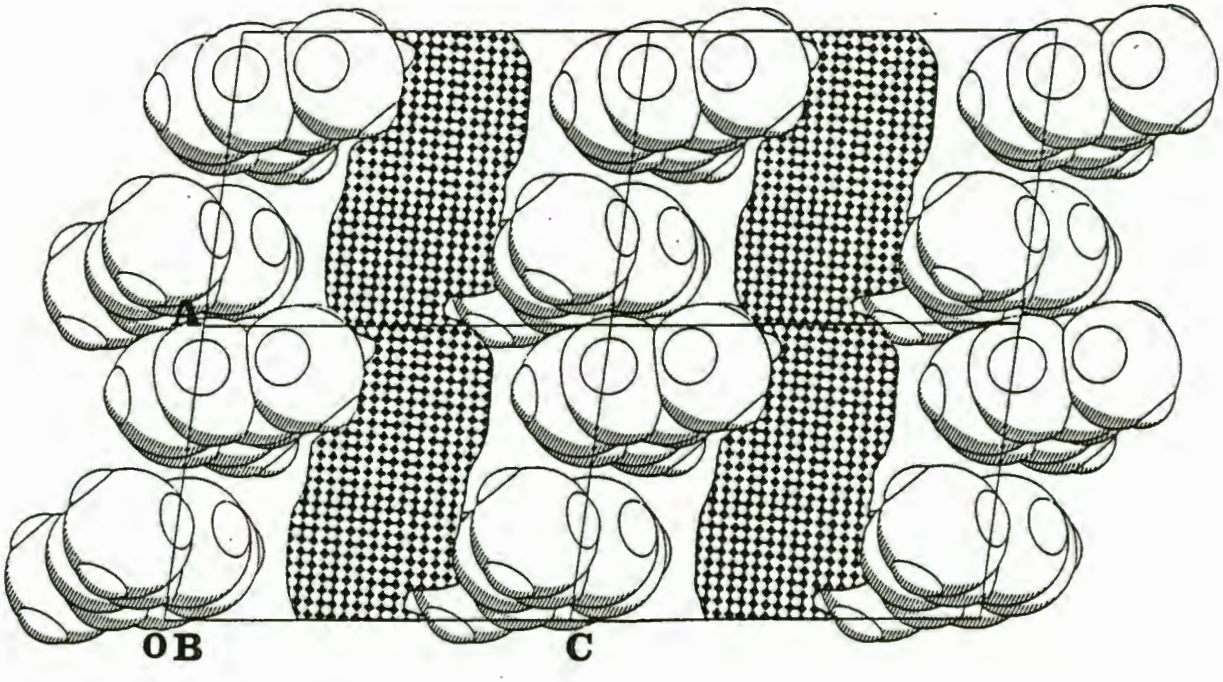

Figure 6.6.3. **26LU** - A cross-section through the host lattice at ½b (hatched area) indicating alternating layers of host and guest molecules.

CHAPTER 7.

THERMAL STABILITY STUDIES

7. THERMAL STABILITY STUDIES

7.1. INTRODUCTION

7.1.1. General

Four alternative techniques were employed to investigate the thermal and structural stability of the six complexes presented. They were chosen with a view to obtaining as complete a picture as possible of the thermal properties of the six crystalline adducts. The methods used include Thermal Gravimetric Analysis (TG), Differential Scanning Calorimetry (DSC), the determination of the energy of activation of the desorption process (by the method of Flynn and Wall) and guest desorption studies (to establish the stability of the host lattice) making use of X-ray Powder Diffraction (XRD).

In addition the potential energy of the system was calculated with the help of the program EENY [135] modified to account for the presence of hydrogen bonds.

7.1.2. Thermogravimetric Analysis (TG) and Differential Scanning Calorimetry (DSC)

Though Differential Scanning Calorimetry and Thermal gravimetric analysis are each powerful tools in their own right, their ability to complement each other has resulted in the two generally being used in conjunction with one other.

TG constitutes an irreplaceable tool to the structural chemist. The apparent simplicity of the principle involved belies the variety of its applications and the invaluable conclusions that may be drawn from its application. Thus it can be used to identify compounds composed of a homogeneous composite or aggregate of two or more distinct molecular species - inclusion compounds in the widest sense.

If the constituents of the inclusion compound are known, TG may be employed to determine the relative proportion of the molecular species present. It does this by accurately reflecting any loss (or gain) in the mass of the sample while it is being heated.

Whereas TG merely indicates physical processes involved in gain or loss in mass of a sample with change in temperature, DSC reveals the energy required or released by the

observed process. By integration of the resulting curve it can provide a measure of the enthalpy of the processes involved, whether they be endothermic or exothermic.

DSC has the added advantage in that it reveals processes that are not accompanied by a change in mass and consequently remain undetected by TG. The phenomenon of a rearrangement of the molecules making up a crystal and thus giving a phase change, constitutes an example of such a process.

DSC can furthermore be used to provide a measure of the strength of the binding forces that hold the molecules in place. This information may be inferred by comparing the temperature at which the smaller, volatile constituent, or guest, is released (T_r) with its boiling point under standard conditions (T_b). The quantity $T_r - T_b$ (or alternatively T_r/T_b) should, in a qualitative sense, indicate the strength of the intermolecular forces binding the guest to the host.

The problem inherent to this approach is that the process of the guest desorption is usually a complex one. Where channels provide a possible route of escape for the guest molecules the process of removing the guest from the crystal would require less energy than it would in crystals in which the guests are entrapped in cage-like cavities. In the latter case any ($T_r - T_b$) values would reflect the resistance to disruption of the host lattice in addition to the strength of intermolecular forces.

The final aim of these investigations must be to describe the crystal in energy terms. At present this is not yet possible, especially in view of the fact that the energy involved in weak interactions and hydrogen bonds is difficult to quantify. Thus the need to develop suitable models arises. Any values obtained by means of the method outlined above, should consequently be seen in the light of this discussion and should be taken to represent first approximations only.

7.1.3. Determination of Activation Energy

In 1966 J. H. Flynn and L. A. Wall published "a quick, direct method for the determination of activation energy from thermogravimetric data" [138]. It was designed to overcome the problem of having to apply curve-fitting techniques to individual desorption curves, a process generally found to be cumbersome and relying on an order parameter which usually is difficult to ascertain. The method developed by Flynn and Wall has been applied to various systems including inorganic complexes [139]. It requires - when applied to inclusion compounds - the desorption of the guest from the complex to be recorded at various rates of heating.

From the formula for the thermogravimetric rate of conversion:

$$dC/dT = (A/\beta)f(C)e^{-E/RT}$$

where: C is the degree of conversion,
β is the constant heating rate,
A is the pre-exponential factor of the Arrhenius equation,
E is the Energy of Activation,
R is the Universal Gas Constant and,
f(C) is a function of degree of conversion;

they derive a formula: $d(\log \beta)/d(1/T) \approx (0{,}457/R)E$

which holds for processes in which $E/RT \geq 20$, provided that
a) A, f(C), and E are independent of T and
b) A and E are independent of C.

Thus plotting the logarithm of the heating rate (log ß) versus the inverse of the absolute temperature for various fixed degrees of conversion, and assuming the conditions above hold, a set of parallel lines is obtained. The slope of these lines, when multiplied by the constant $c = -5{,}50.10^{-2}\ J.K^{-1}.mol^{-1}$ ($= R/0{,}457$), yield approximate values of E, $E_{approx.}$ Using these E_{approx} values to calculate E/RT constants permits the determination of refined values for the constant, c. These in turn allow refined values for E, the activation energy, to be calculated.

During the course of these experiments it was realised that the starting temperature as well as the shape of the individual curves are highly sensitive to the sample size used and to the method of the sample preparation. The preparation usually involves crushing the sample in order to obtain smaller, more uniformly sized crystallites. However, it is questionable whether the degree of crushing is reproducible from one run to the next. Sieving the crystals is not possible, however, because the inclusion compounds are highly labile and readily lose the guest component.

Thus despite care being taken in minimising errors, the $\log \beta$ vs. 1/T plots for most complexes reveal fairly poor degrees of correlation making a decision about the applicability of the method difficult and implying a large margin of error in the final results.

For this reason, the applicability of the method was assumed where the results permitted such an assumption. The values given for the activation energy of the desorption process are accepted to be approximations of possible true values.

7.1.4. Desorption Studies

Inclusion complexes can, in broad terms, be described as consisting of an open host lattice which gives rise to a system of voids filled by guest molecules. This is generally referred to as the β-phase.

In theory therefore, loss of the guest from the lattice can lead to two possible outcomes, depending on the rigidity of the host lattice. These different decomposition paths are illustrated in figure 7.1.4.

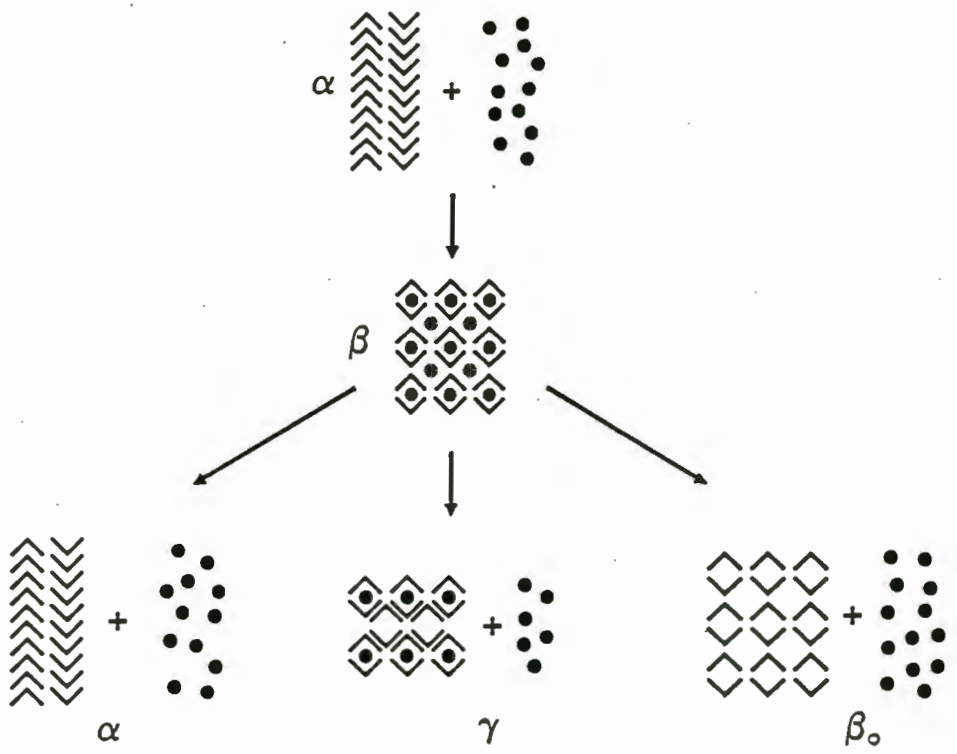

Figure 7.1.4. A schematic representation of possible decomposition paths for inclusion compounds.

Either the lattice is rigid and retains its structure despite the loss of the guest, giving rise to a so-called β_0-phase, (which is isomorphous with the β-phase) or alternatively, the host lattice is not rigid and collapses following the removal of the supporting guest molecules. This can result in a molecular arrangement equivalent to that adopted by the host in its unsolvated state (the α-phase) or the lattice collapses to a form (crystalline or amorphous), different to both the α- and the β-phases.

Where such an intermediate is crystalline and stable or partially stable the resulting structure is generally referred to as the γ-phase.

The stability of this host lattice can thus be investigated by means of desorption studies. These involve analysing the solvated, partially desolvated (where possible) and entirely desolvated form of a complex by means of powder X-ray diffraction (XRD) and comparing the patterns of the d-spacings thus obtained to that of the α-phase. Corresponding diffraction patterns are taken to indicate equivalent structures.

To record the β-phase pattern of a compound the crystalline complex was ground, packed into an appropriate sample holder and exposed to X-rays. The intensity of diffracted radiation was monitored and recorded over an angle-2θ range of 10 to 30°.

To obtain diffraction patterns of partially and entirely desorbed complexes the ground samples were heated to a suitable temperature in a vacuum oven over varying lengths of time. The percentage guest loss was monitored intermittently by means of TG until the required desorption has been achieved after which the procedure outlined for the β-phase was repeated.

7.1.5 Potential Energy Calcultion

The potential energy program EENY[0] was used to calculate the overall potential energy of a crystallographic system. Recently it was modified to incorporate the angle dependent hydrogen bonding energy into the overall potential energy calculations (HEENY)[140].

The function used was derived from a modification[141] of the equation introduced by Gelin and Kaplan[142] in 1979 and looks as follows:

$$V_{total} = V_{hb} + (1-\lambda)V_{normal}$$
$$= [\,A/(R^{12}) - C/(R^{10})]\lambda + (1-\lambda)V_{normal}$$

where: V_{total}, V_{hb} and V_{normal} are the total, the hydrogen bonded and the full non-bonded potentials respectively

$\lambda = \cos^2(\theta)$ where θ is the angle at the hydrogen atom defined by the acceptor and the donor atoms, with $90° \leq \theta \leq 180°$

R is the distance between the hydrogen bonded hydrogen atom and the acceptor atom

$A = -5R_0^{12}V_{min}$

$C = -6R_0^{10}V_{min}$

V_{min} and R_0 are the well depth and the equilibrium distance at 180°

For all six structures of this study the potential for each distinct guest was determined in relation to the host lattice. While the host lattice was taken as rigid the guest molecules were allowed to vary rotationally as well as translationally in order to determine the energetically most favoured position.

7.2. TG AND DSC

7.2.1. NITRANN

As can be seen in referring to figure 7.2.1 a) the mass loss registered for NITRANN for a sample size of 3,45 mg and a heating rate of 10°C.min^{-1} is 18,5 % of the initial total mass of the sample (Process A). The theoretical percentage by mass of guest for an inclusion compound of acetonitrile with a Host:Guest ratio of 1:2 is 18,4 %. Consequently the Host:Guest ratio can be accepted to be 1:2.

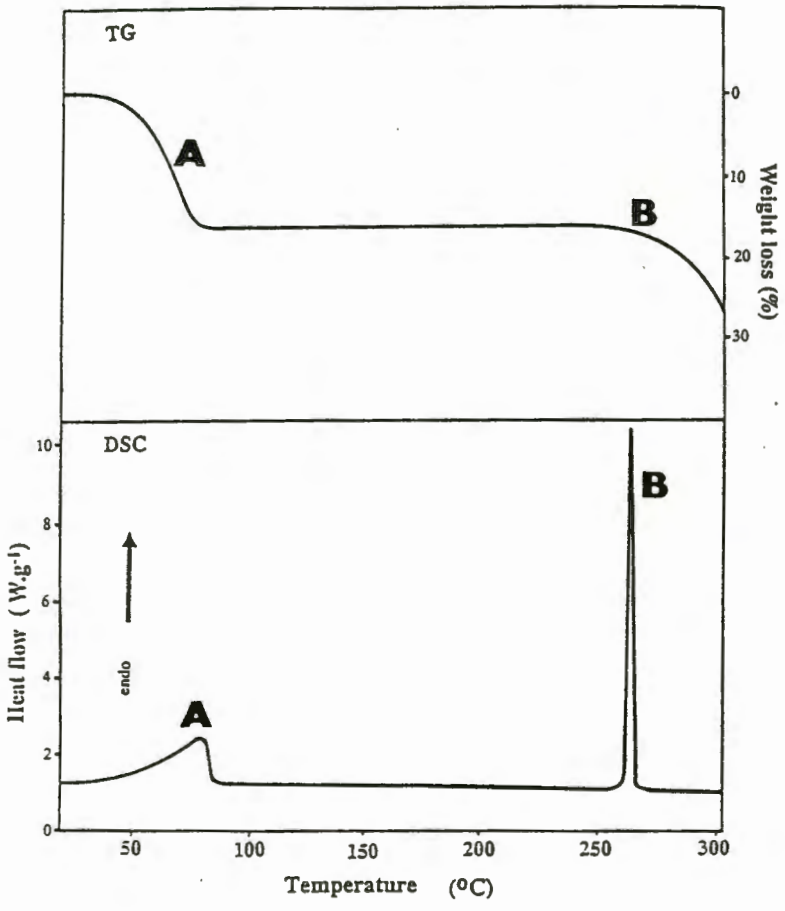

Figure 7.2.1 NITRANN - TG and DSC curves. Both were obtained using a heating rate of 10°C.min^{-1}.

Furthermore figure 7.2.1 indicates that the guest is lost in a one-step process which is endothermic with an enthalpy of 60,6 kJ.mol^{-1}. The guest desorption is observed to start at room temperature and to be complete at 90°C for the scanning rate of 10°.min^{-1} . The lability of the complex is obvious from the fact that guest desorption commences as soon as the sample is removed from the mother liquor. Nonetheless,

because only a few seconds are required to initialise the scan, this method proves to be the most accurate in determining the Host:Guest ratio. The host (1) melts as expected at just above 262°C (process B).

7.2.2. PROP

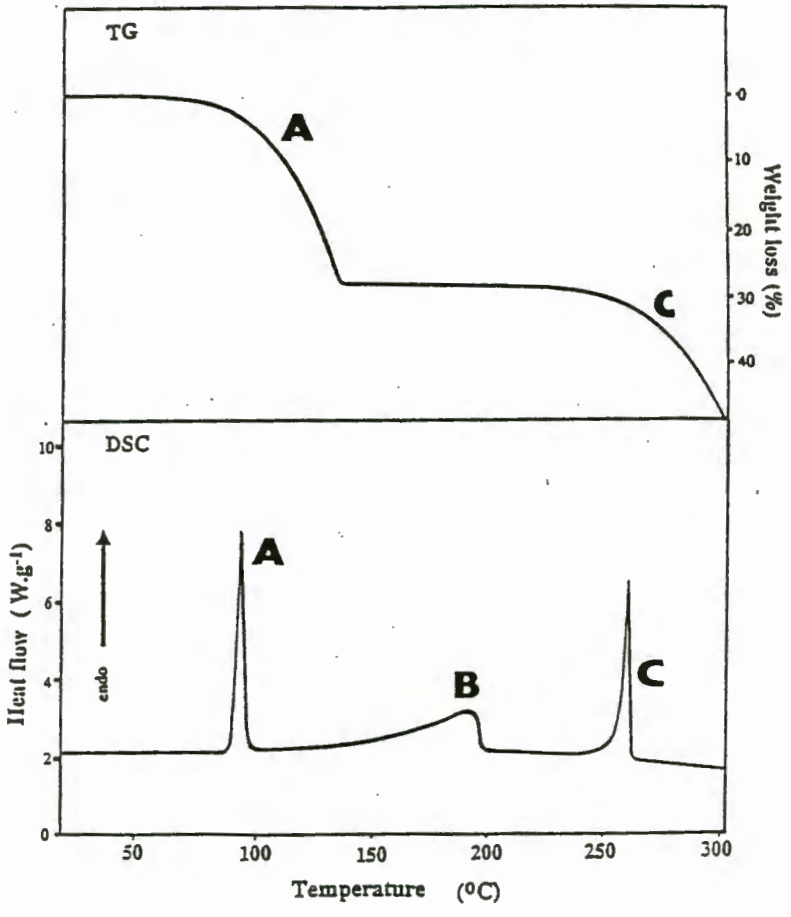

Figure 7.2.2 **PROP** - a) TG and b) DSC curves obtained using a heating rate of 10°C.min^{-1} .

The TG curve for **PROP** (figure 7.2.2 a) indicates that all the 3-hydroxypropionitrile molecules are lost in one step (process A). The percentage of the total mass lost amounts to 27,8 %. This compares well with a theoretically expected value of 28,1 % for a complex with a host to guest ratio of 1:2.

By contrast the DSC curve reveals two peaks apart from C (which indicates the melting of the host). Of these, the first (A) no doubt corresponds to the loss of the guest with an associated enthalpy of 40,4 kJ.mol^{-1}. The second peak unaccounted for by the TG curve, and consequently not associated with a change in mass, must result from a

rearrangement of the host lattice. Again the process is endothermic with enthalpy of ΔH = 50,0 kJ.mol^{-1}.

An attempt to establish the nature of the processes more clearly was undertaken as part of the desorption studies and will be discussed in Section 7.3.2.

7.2.3. PYD

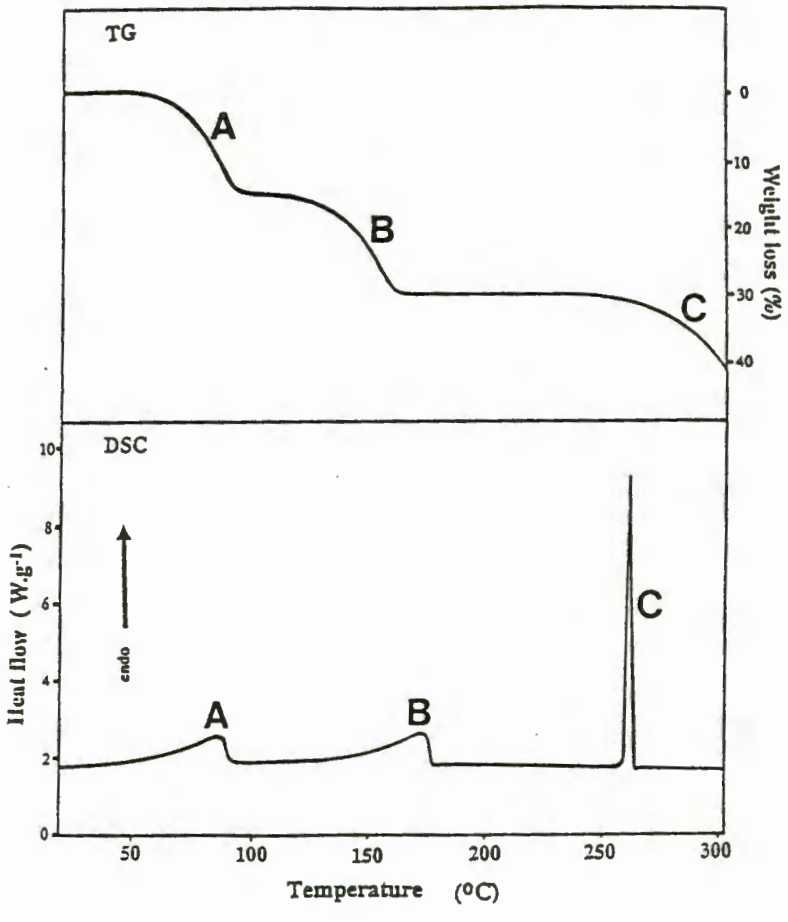

Figure 7.2.3 **PYD** - a) TG and b) DSC curves using a heating rate of 10°C.min^{-1} .

As can be verified by reference to figure 7.2.3 the complex **PYD** loses its guest molecules as part of two distinct processes (A and B). The mass lost during each of these two steps corresponds to 15,0 and 15,4 % of the sample mass respectively. This therefore establishes without ambiguity that **1** includes pyridine in a complex with a host:guest ratio of 1:2. The total mass loss expected for such a complex would in theory be 30,3 % as opposed to the observed 30,4 %. Furthermore these two desorptions occur entirely independently of each other. In other words, the loss of the first half of

the included guest molecules (A) ends before the desorption of the second (B) commences.

Initially one may come to the conclusion that since the structure of **PYD** includes two crystallographically distinct guest molecules (cf. Section 6.2.4), each of the guest desorptions can be attributed to the loss of either one of these groups of molecules.

In fact, as demonstrated in section 6.2.4, there are two crystallographically identical channels each consisting of two fused half-channels which permeate the crystal in the direction [011]. Each group of crystallographically distinct guest molecules occupies its half-channel but, because there is no boundary between the two 'half-channels', it is unlikely that molecules from one half would not move from their half to the other. It can therefore not be ruled out that guest molecules from both groups are lost during the first guest-loss process, which implies that this process corresponds solely to a statistical loss of two of the four solvent molecules per unit cell. A redistribution of the remaining guest molecules would then give rise to the observed intermediate arrangement. This secondary structure, in turn, loses all remaining guest molecules during the second desorption process, giving rise to the desolvated form.

The enthalpies for the two steps are 38,6 (A) and 53,6 $kJ.mol^{-1}$ (B) respectively, indicating that resistance to loss of the second guest molecule is greater than to the first.

7.2.4. 3PIC

In referring to figure 7.2.4, it will become clear that the 3-methylpyridine included by the host in the complex **3PIC** is also lost in two separate processes. During the first decay step (A), which occurs between 85°C and 120°C, approximately 16,9 % of the compound mass is lost. The DSC for this process is more complicated. The complex endothermic peak probably indicates a desorption process partially overlapped by a concomitant rearrangement of the crystal lattice. The combined enthalpy surprisingly amounts to only 16,8 $kJ.mol^{-1}$.

In the second step (B) occurring from 120 to just below 150°C, an additional 18,7 % of the total mass of the complex is lost. Thus the total loss of mass amounts to 35,6 %. Since a host to guest ratio of 1:2 would result in a theoretical percentage mass loss of 33,8 % this result conclusively indicates that the host to guest ratio is indeed 1:2. Each of the observed steps therefore indicates a statistical loss of half the guest molecules. The enthalpy determined from the corresponding, second endothermic peak is 63,2 $kJ.mol^{-1}$.

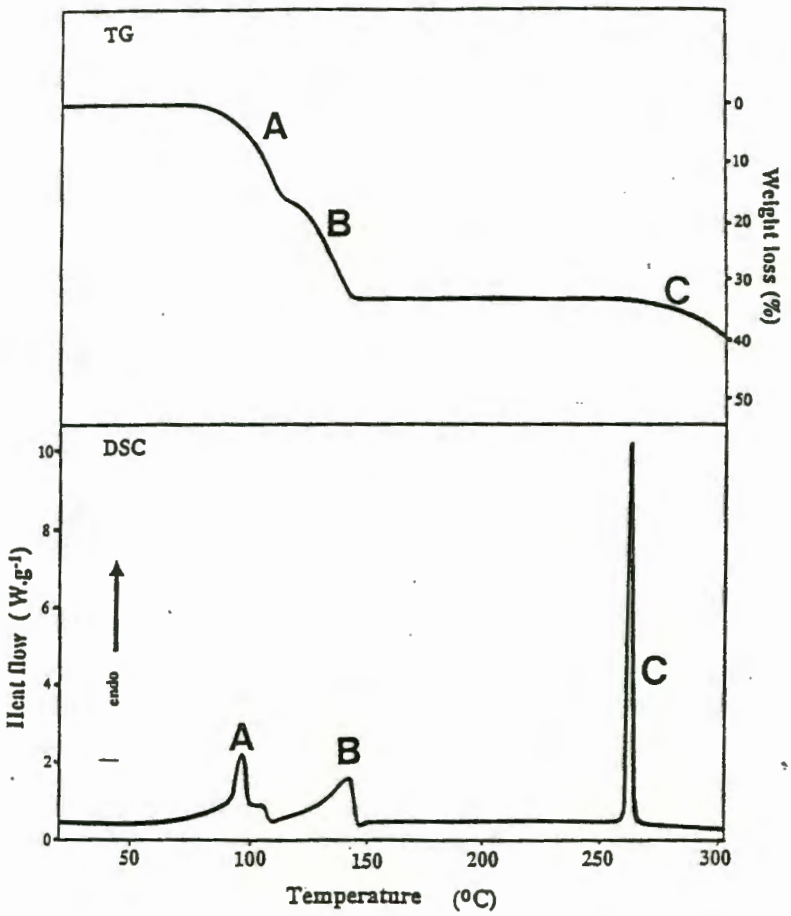

Figure 7.2.4 3PIC - a) TG and b) DSC curves. The heating rate used was 10°C.min^{-1} in either case.

The reason for the imperfect proportions of guest lost in the two desorption processes (16,9 % for the first and 18,7 % for the second) is a partial overlap of the two processes. In Section 7.3.4 it will become apparent that a much better separation is achieved at lower heating rates. Using a heating rate of 1°C.min^{-1} a nearly perfectly equal division of guest loss between the two steps is observed.

By contrast, a glance at figure 7.2.4 indicates that in the case of DSC, where the sample is heated inside a closed pan, two clearly separate peaks are observed. Thus, despite the fact that the pan has small slits, to prevent an excessive build-up of pressure, it nevertheless results in measurements being made under an atmosphere containing large amounts of desorbed guest. This appears to prevent the second process commencing before the first is complete, even at a heating rate as high as 10°C.min^{-1}.

With a view to the structure of this complex, which was discussed in detail in Section 6.2.4, it may be inferred that each of the desorption processes is attributed to the loss of crystallographically distinct guest molecules. Unfortunately the available

thermoanalytical data do not permit either set of guest molecules to be assigned to a specific guest loss process. On considering the hydrogen bonding data obtained crystallographically, it appears likely that the guest molecules located at ¼c (bound by the longer and correspondingly weaker hydrogen bond, - O(1)···N(21) = 2,925 Å) are lost first. The second group of guest molecules is bound to the corresponding host by a O(1)B···N(21)B distance of 2,788 Å making this the stronger of the two hydrogen bonds.

7.2.5. 24LU

Both TG and DSC for the inclusion compound **24LU** (figure 7.2.5) indicate that all the included solvent 2,4-dimethylpyridine is desorbed in a single step process (A). Furthermore the percentage mass loss incurred by the desorption amounts to 23,0 % which clearly implies that the host:guest ratio is 1:1 as the guest would be expected to contribute 22,7 % of the mass to a complex of this constitution.

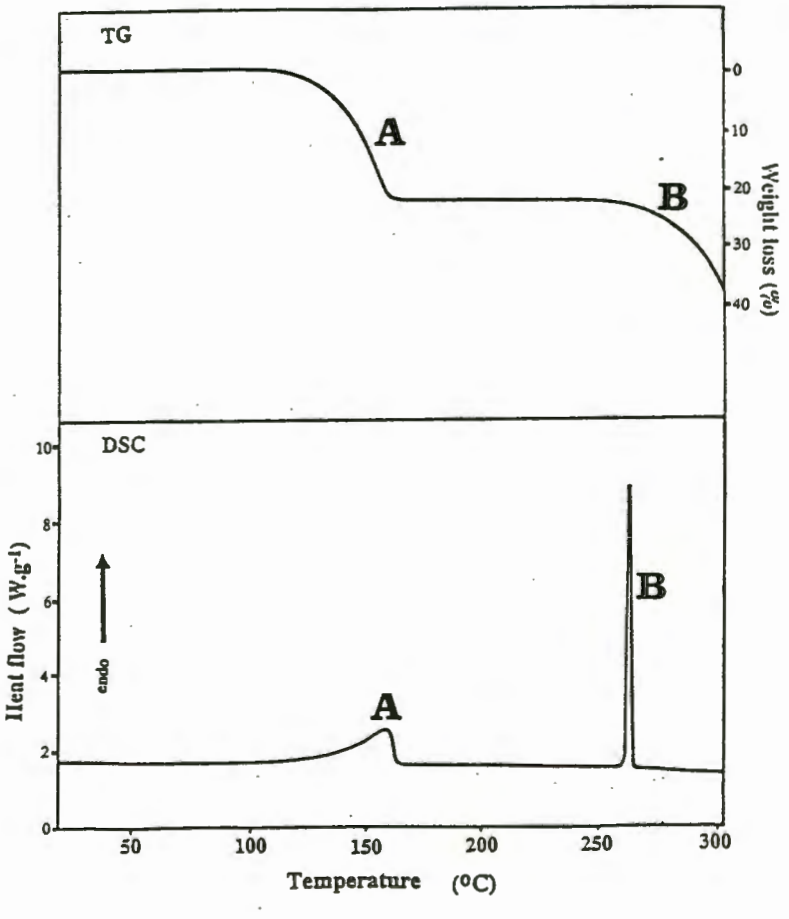

Figure 7.2.5 **24LU** - a) TG and b) DSC curves corresponding to a heating rate of 10°C.min^{-1} for both.

The enthalpy for the single-step desorption endotherm was found to be 68,4 kJ.mol^{-1}. Interestingly, the process of guest loss is complete by 145°C at a heating rate of 10°C.min^{-1}. Thus the guest is lost at temperatures appreciably lower than its boiling point, 159°C, under atmospheric pressure. This is particularly surprising as this is the only complex of the present series in which the guest is enclosed in cavities created by the host molecules. In other words, not only do the hydrogen bonds holding the guest have to be broken to allow the guest molecules to escape, but the host lattice has to be disrupted as well.

A possible explanation for this is that the forces between the 2,4-dimethylpyridine molecules in its liquid phase are stronger than those they are exposed to in the crystal. The fact that no forces exist between guest molecules in the crystal means that they can be described as existing in a pseudo-gaseous phase.

7.2.6. 26LU

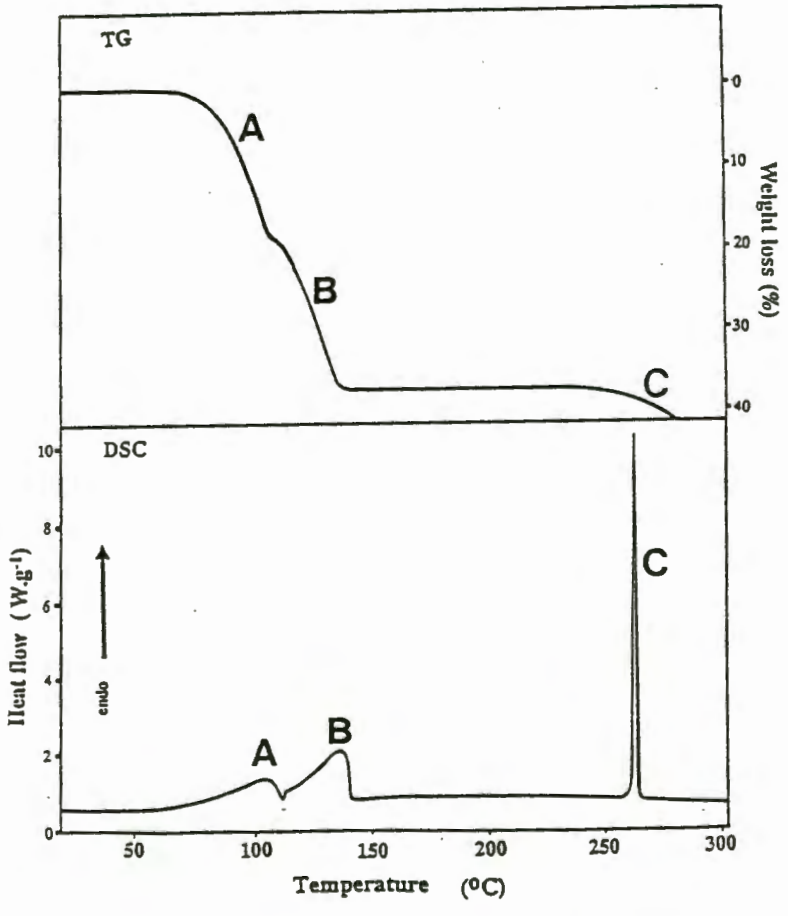

Figure 7.2.6 26LU - a) TG and b) DSC curves for the complex obtained using a heating rate of 10°C.min^{-1} .

In the case of the complex **26LU** thermal analysis indicates that the host to guest ratio is 1:2, as was expected from density measurements. Of the complex mass, it was found that 36,6 % could be attributed to the 2,6-dimethylpyridine molecules (figure 7.2.6 a). This accords well with a theoretical guest proportion of 37,0 %.

The information obtained by means of DSC (figure 7.2.6 b) concurs with that determined by TG: Two partially overlapping endothermic peaks support the interpretation that the guest is lost in a two-step process. During the first of these (A), a mass loss of approximately 21,1 % of the total complex mass is observed. This is slightly more than would be expected were one half of the included guest to be released before the second desorption process gets under way. The enthalpy for this process with an onset temperature of 74°C was determined to be 41,8 kJ.mol^{-1}

The second desorption (B), attributable to the loss of the second half of the guest present, has an associated enthalpy of 55,2 kJ.mol^{-1}. Because of the overlap of the two processes the values obtained for the two enthalpies of desorption can only be accepted to represent approximate estimates of the true values. Their combined value should therefore rather be relied upon as a value for the entire desorption process.

As with **24LU** the desorption of the guest is complete by 140°C which is below the boiling point of 143°C for 2,6-dimethylpyridine. In this case the discrepancy is not as large however, indicating that the guest in **26LU** is more firmly held than was the case for **24LU**.

7.2.7. Discussion

In trying to correlate the onset temperature of the desorption process and the strength of the hydrogen bond binding the guest to the host, it was proposed that the quantity $T_r - T_b$ (or alternatively T_r/T_b) could provide a useful parameter.

In order to test this hypothesis, $T_r - T_b$ for all complexes involving O-H···N hydrogen bonds was plotted against the O···N distance. For the three complexes with two different hydrogen bonds only the onset temperature of the first peak and the data for the weaker of the hydrogen bonds was used. (This was necessary because no hydrogen bonding data are available for the γ-phase.) Furthermore, the complex **PROP** was not included in this plot as each of its guest molecules is held by two hydrogen bonds, making direct comparisons with the other complexes difficult.

Thus two groups of complexes remain, respectively characterised by host to guest ratios of 1:1 and 1:2. The resulting scatter plot of $T_r - T_b$ versus O···N is supplied in figure 7.2.7.

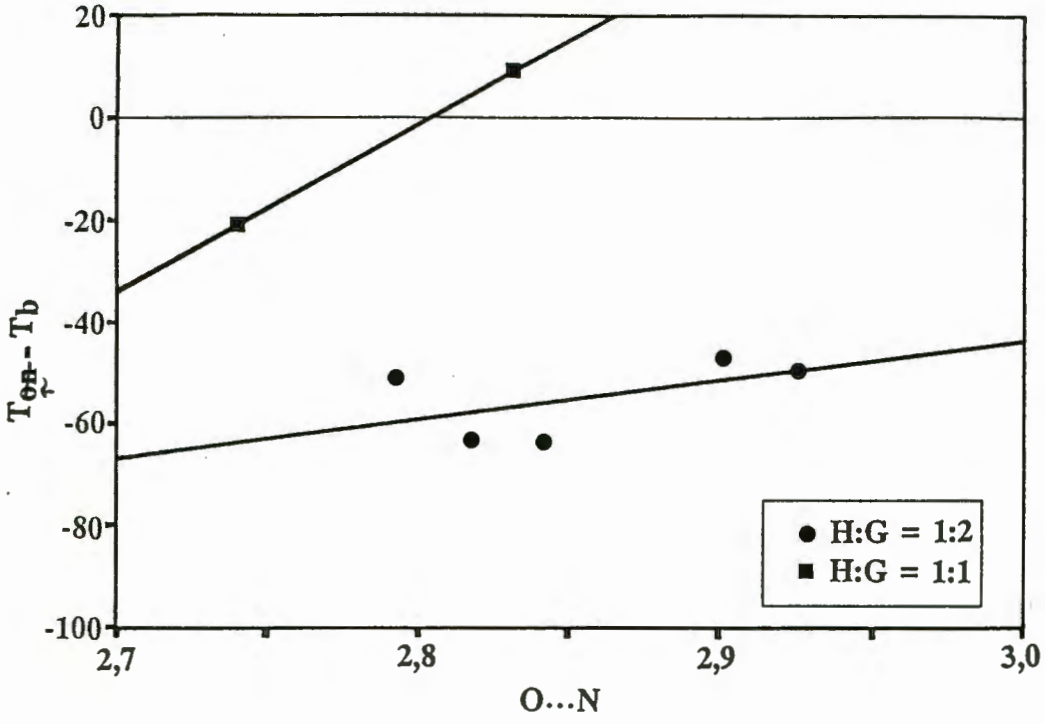

Figure 7.2.7. Scatter Plot of $T_r - T_b$ versus O···N for complexes of (1) with pyridine derivatives, displaying O-H···N hydrogen bonds.

As can be seen from figure 7.2.7, no correlation between the parameters employed is immediately apparent. Though this may partially be ascribed to the small number of data points available, it does indicate that the system is too simplistic to give any reliable information. One of the main difficulties with the present approach is that it attempts to include the boiling point for a solvent. This assumes that the guest molecules in the crystal have pseudo-liquid characteristics which is highly debatable.

Furthermore, the complexity of forces and interactions in any crystal makes it unlikely that a simple correspondence between two parameters that account for only a part of the whole will be found. Instead a holistic approach, though far more complicated, would appear to offer more prospects of success.

7.3. DETERMINATION OF ACTIVATION ENERGY

7.3.1. NITRANN

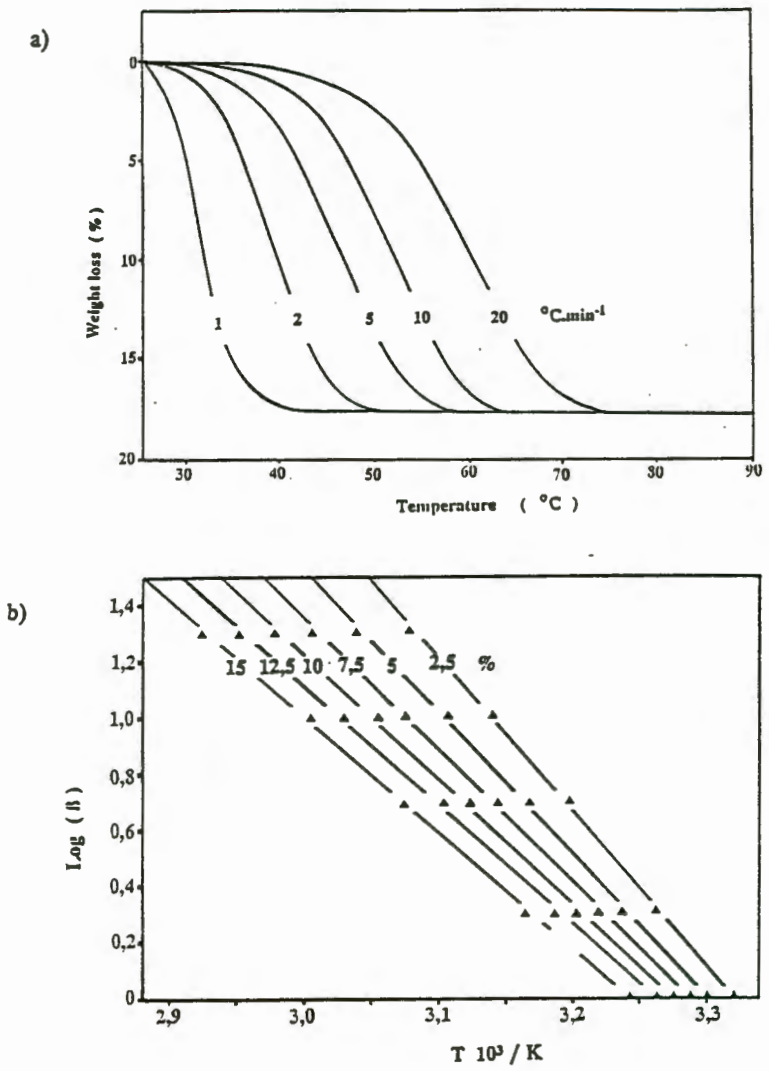

Figure 7.3.1 **NITRANN** - Activation energy determination for the guest desorption process. a) TG curves obtained employing various heating rates and b) the a plot of log β versus the inverse of absolute temperature for percentage conversions in the range of 2 to 15%.

The desorption curves for **NITRANN** for heating rates 1, 2, 5 and 10°C.min^{-1} are shown in figure 7.3.1 a) and the corresponding log ß versus 1/T plots in figure 7.3.1 b). The extreme lability of the complex **NITRANN** - resulting from the high vapour pressure of the guest acetonitrile at room temperature - calls for this experiment to be performed with the utmost care and speed.

The results displayed in figure 7.3.1 b) show that the process of desorption of acetonitrile is not uniform. The individual slopes corresponding to increasing degrees of desorption change continuously, giving rise to values for the activation energy in the range 83 to 115 $kJ.mol^{-1}$. This indicates that one or more of the assumptions made by Flynn and Wall [138] does not hold for **NITRANN**. Consequently the method cannot be relied upon to yield accurate results in this case.

In the present system the facile loss of guest may be held responsible for the failure of the method. However, it is equally if not more probable, that the activation energy of desorption is indeed dependent on temperature as indicated by figure 7.3.1.

Such a result is not entirely unexpected in view of the fact that it has been shown that the activation energy of desorption in the case of zeolites was found to be dependent on the coverage ie. the degree to which the host lattice is covered by guest solvent [143].

7.3.2. PROP

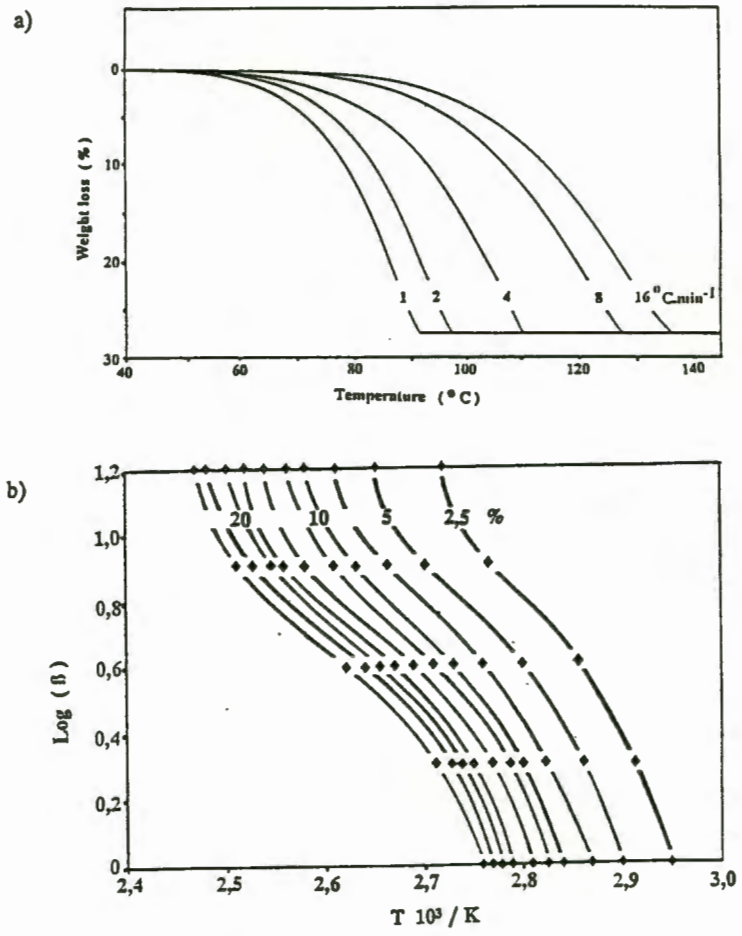

Figure 7.3.2 **PROP** - The determination of the activation energy of desorption. a) TG curves recorded using various heating rates as indicated and b) the corresponding plot of the logarithm of the heating rate versus the inverse of the absolute temperature for a range of percentage conversions.

The log β versus 1/T plots for **PROP** were found not to be linear. This was taken to indicate that the process of guest desorption is non-uniform. Whether this may be traced to the two different hydrogen bonds in the complex, or to the interference of the rearrangement process of the lattice reverting to the α-phase (see Section 7.2.2) with the desorption, is uncertain. The desorption curves and log β versus 1/T plots for **PROP** may be found in figure 7.3.2.

7.3.3. PYD

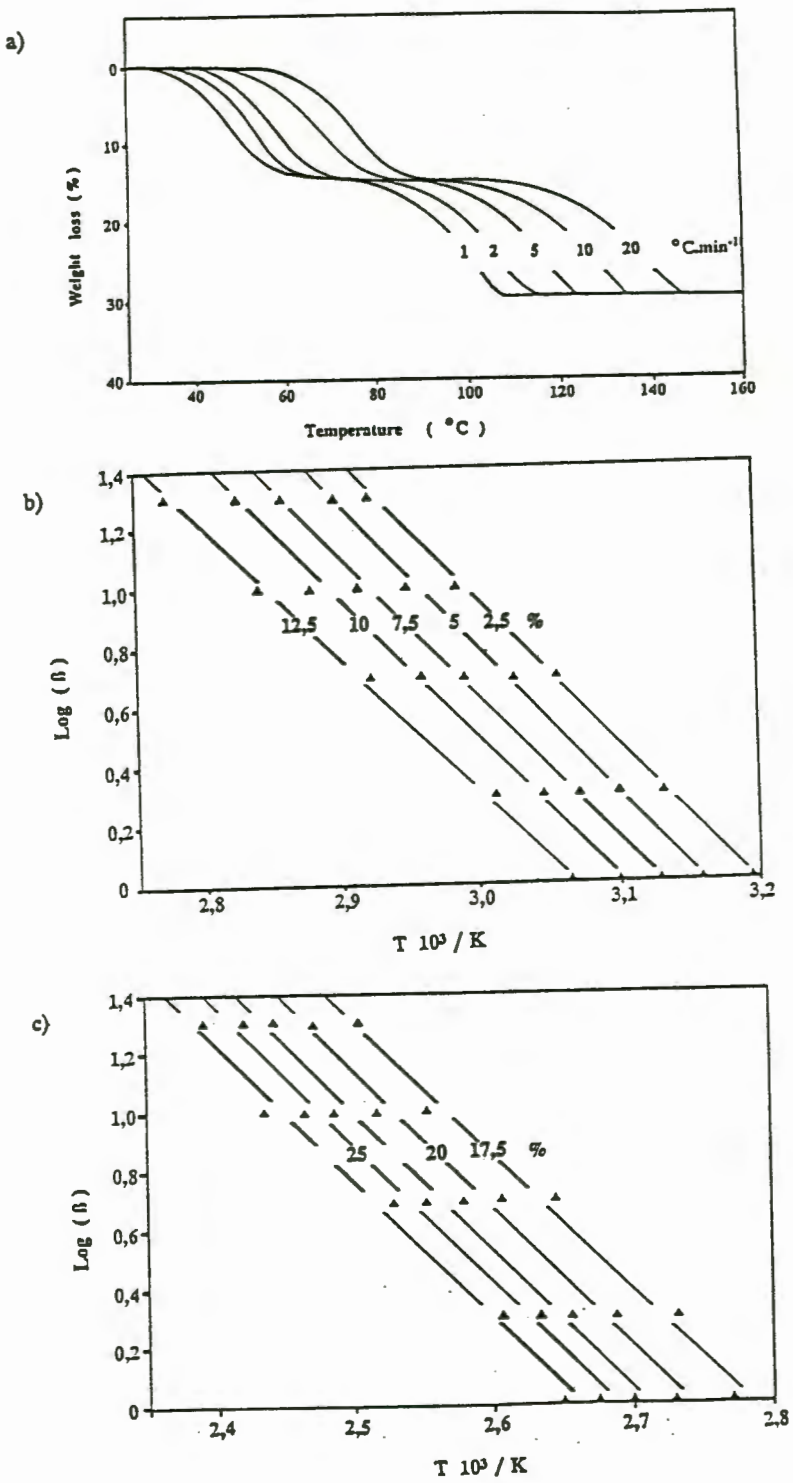

Figure 7.3.3 PYD - Desorption curves (a) and the plots of log β versus (1/T), where T is the absolute temperature, required to determine the activation energy of the guest desorption process (b and c).

The desorption of pyridine from the host-guest complex **PYD** was recorded at rates of 1, 2, 5, 10 and 20°C.min^{-1}. The superimposed scans are reproduced in figure 7.3.3 a).

The plots of log β versus 1/T for the two desorption processes required in the determination of the activation energies are shown in figure 7.3.3 b) and c). The activation energy determined by means of these plots average to 87 kJ.mol^{-1} for the first guest loss and 82 kJ.mol^{-1} for the second.

7.3.4. 3PIC

The superimposed desorption curves for the complex **3PIC** are shown in figure 7.3.4 a). The incomplete separation of the two desorption processes though of little consequence at low heating rates, leads to difficulties being experienced at higher heating rates, where the second desorption process begins to overlap the first to ever larger degrees (this was already visible in the TG curve described in Section 7.2.4, which was run at 10°C.min^{-1}). A heating rate of 1°C.min^{-1} results in a nearly perfect desorption curve being obtained in that the total guest mass is equally divided between the two processes.

The log β versus 1/T plots for the two steps are to be found in figure 7.3.4 b) and c). Because of the sensitivity of the method to factors such as sample size and sample preparation, fairly poor correlation between the data points is observed. But it is clear from the fact that all points for one particular heating rate are deflected to the same degree, that the poor correlation is a consequence of experimental errors, rather than the method not being applicable to this system.

The activation energy values obtained for the two processes respectively amount to 80 and 71 kJ.mol^{-1}.

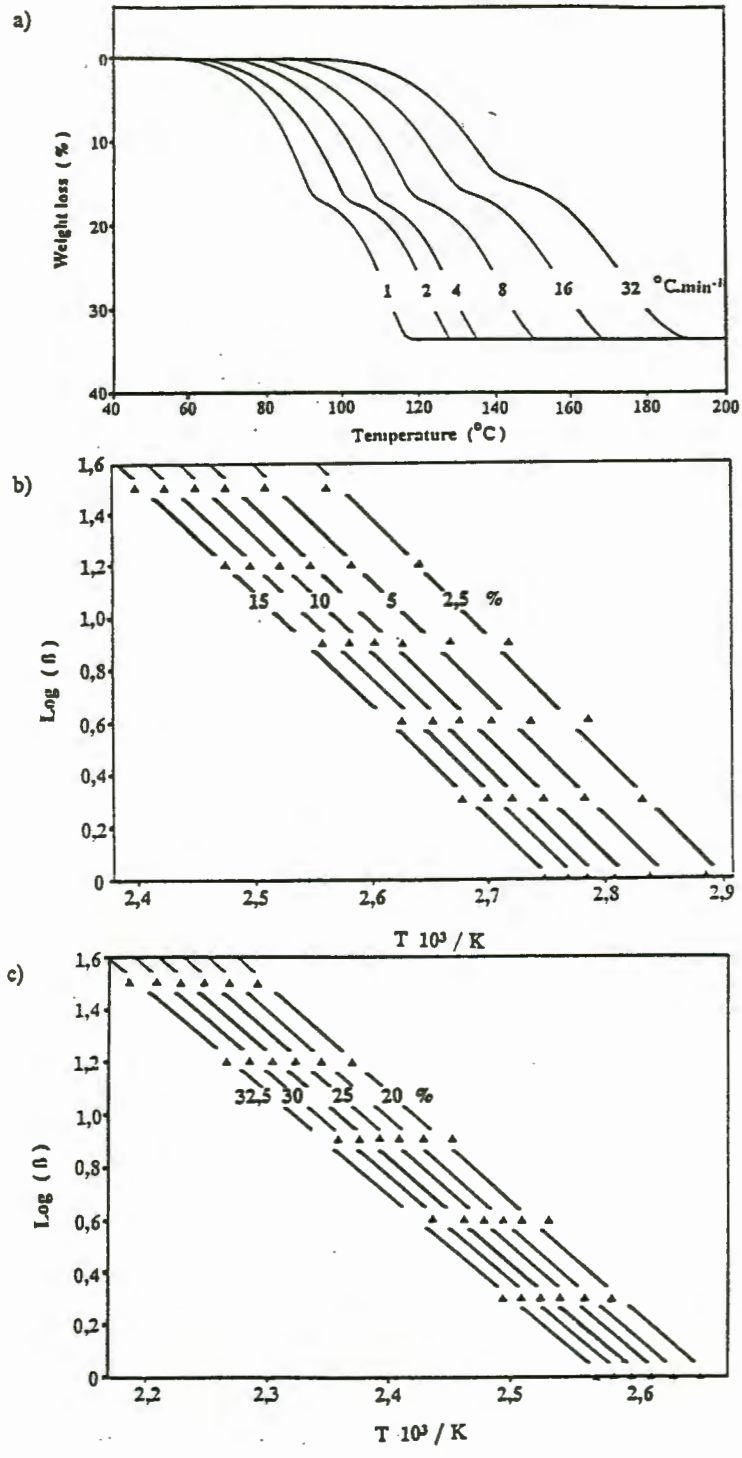

Figure 7.3.4 3PIC - The determination of the activation energy using the method of Flynn and Wall [138]. a) The desorption curves obtained for various heating rates and the corresponding plots of log β versus the inverse of absolute temperature for the two step guest desorption process b) and c).

7.3.5. 24LU

Surprisingly, the difficulties experienced in determining the activation energies for the activation processes for the previously discussed complexes did not arise to the same degree in the complex **24LU.**

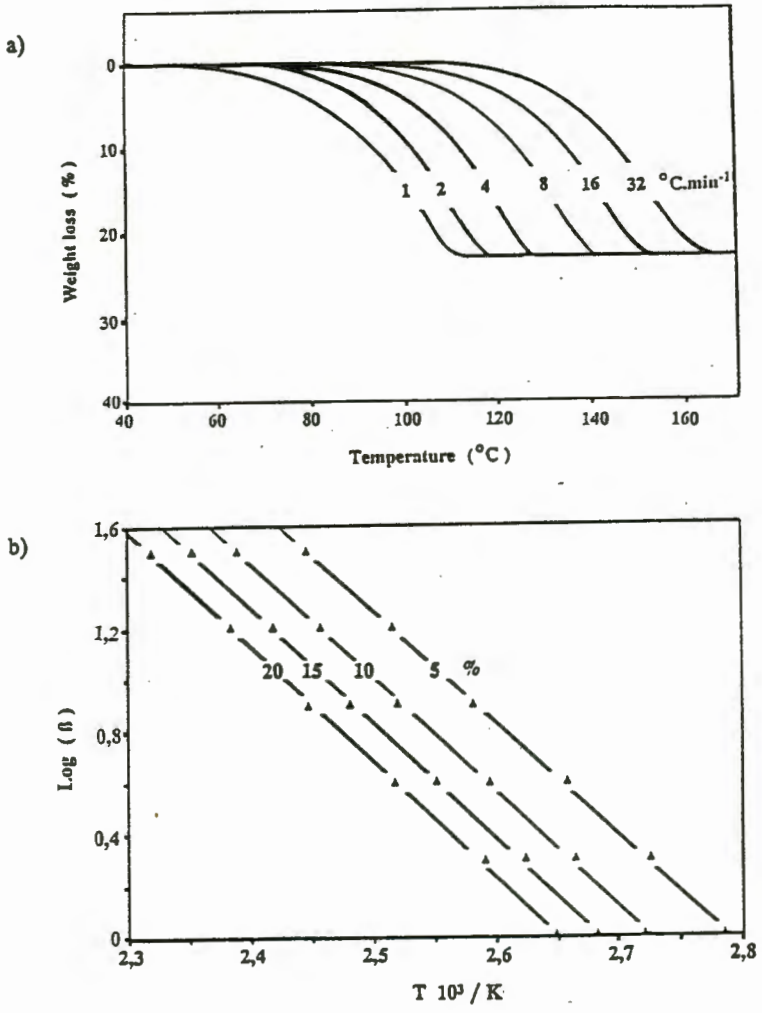

Figure 7.3.5 **24LU** - a) the superimposed desorption curves and b) the corresponding plots of log β versus absolute temperature required to determine the activation energy of the desorption process.

The plots for the loss of 2,4-dimethylpyridine obtained for the heating rates 1, 2, 4, 8, 16 and 32°C.min^{-1} are superimposed in figure 7.3.5 a) while the log β versus 1/T plots for 5, 10, 15 and 20% desorption appear in figure 7.3.5 b). Good correlation between the points was obtained and the value obtained for the activation energy is 81 kJ.mol^{-1}.

7.3.6. 26LU

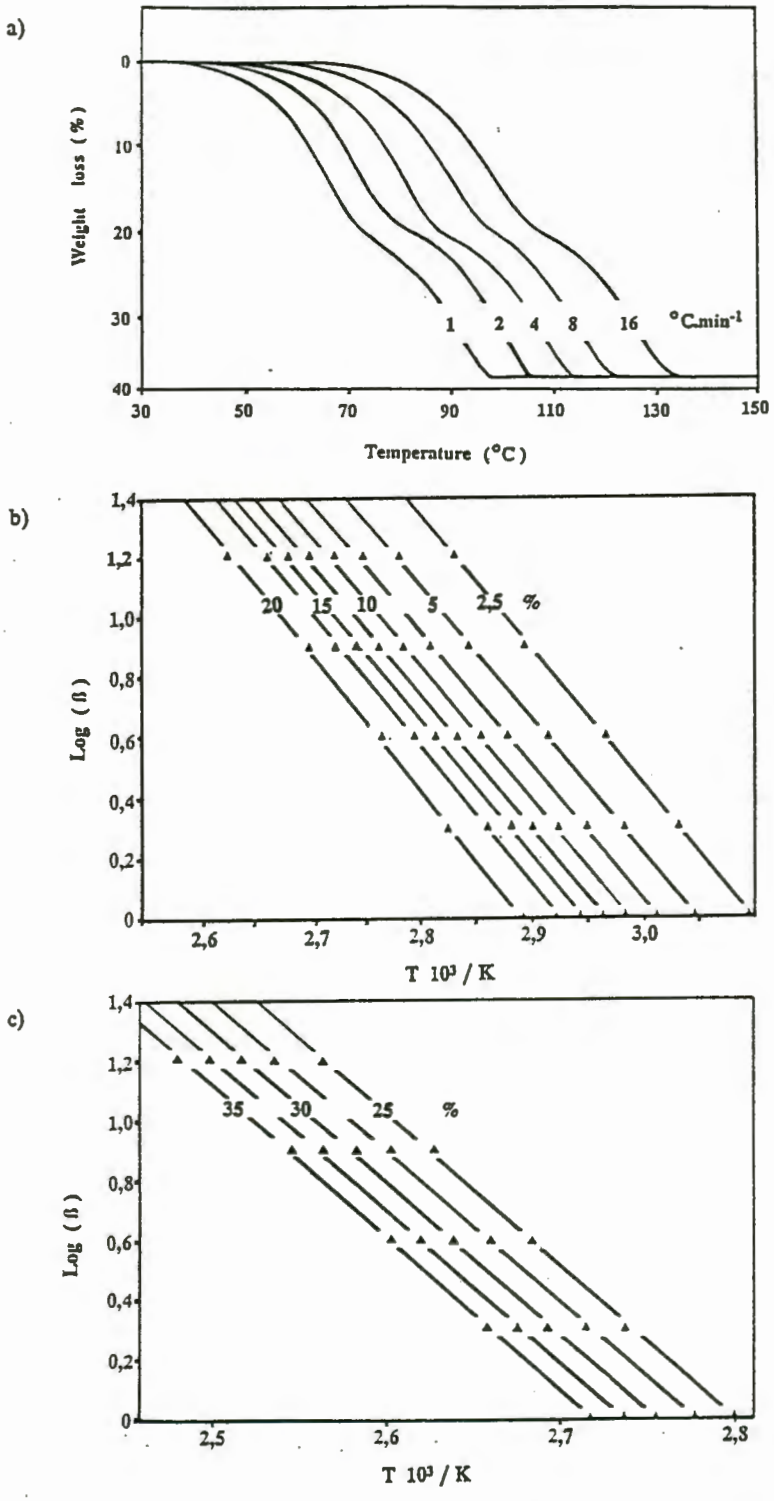

Figure 7.3.6 **26LU** - a) Superimposed TG desorption curves, and plots of log b versus the inverse of absolute temperature for various degrees of conversion (b and c), required for the determination of the activation energy of desorption for the double desorption process.

In the crystalline adduct **26LU** the desorption process once again takes place in the form of two partially overlapping steps. As had been observed for the complex **3PIC** problems arise from varying degrees of overlap of the two guest desorption processes. This is reflected by the relative positions of the points of inflection being shifted (figure 7.3.6 a). Though the shift is not as pronounced as it was for **3PIC**, the trend is not systematic, probably due to variability in the crystallite size distribution occuring between the various runs.

The plots of the logarithm of the heating rates versus the inverse of the absolute temperature corresponding to 2⅓, 5, 7⅓, 10, 12⅓, 15 and 17⅓ % desorption are shown in figure 7.3.6 b) while those for 25, 27⅓, 30, 32⅓ and 35 % conversion follow in figure 7.3.6 c).

Despite the unexplained shifts in points of inflection described above the points in parts b) and c) of figure 7.3.6 correlate well. The values for the activation energy of desorption for the processes calculated from these plots are 81 and 93 $kJ.mol^{-1}$ respectively.

7.3.7. Discussion

As indicated in the introduction, the method introduced by Flynn and Wall overcomes some of the difficulties and ambiguities of other methods employed in determining activation energies. However, it suffers from a number of problems, which make the interpretation of results difficult.

Primarily these problems are experimental in nature. The sensitivity of individual desorption curves to factors such as sample size and sample preparation are the most important. However, the calculations involved in producing the $\log \beta$ versus $1/T$ plots cause small experimental errors to become magnified.

Only an in-depth study into the causes of experimental errors in thermal gravimetric analysis could reduce or eliminate these uncertainties. In turn, this would result in more accurate values of activation energies for the guest desorption process being obtained, allowing the researcher to report the values with more confidence.

7.4. DESORPTION STUDIES

7.4.1. NITRANN

The X-ray diffraction patterns for **NITRANN** appear in figure 7.4.1. Comparison of the diffraction patterns for the solvated and desolvated forms of **NITRANN** (figures 7.4.1 a) and b)) clearly indicates that there are substantial differences between the two. Thus, it must be concluded that the desorption of the guest from **NITRANN** leads to a considerable disruption of the original structure.

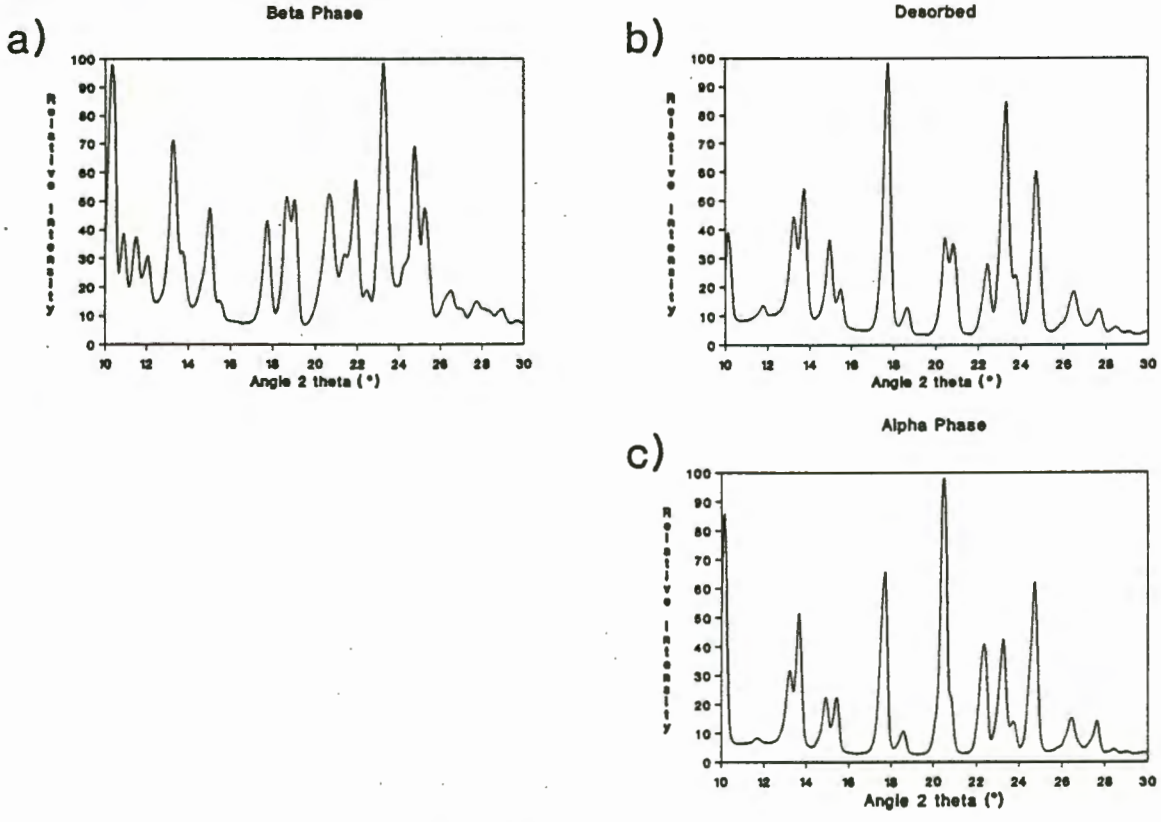

Figure 7.4.1. **NITRANN** - Diffraction patterns: a) of the β-phase, b) of the desorbed sample and c) of the α-phase.

On the other hand, comparing b) with the diffraction pattern of the α-phase (c) compels one to conclude that the patterns are in fact equivalent. In other words, on guest desorption, **NITRANN** is found to revert to the α-phase. Thus it must be concluded that the host lattice of the β-phase is not sufficiently rigid to survive the loss of the supporting guest molecules and it consequently collapses.

Close scrutiny of parts b) and c) of figure 7.4.1 reveals slight differences in intensity of individual peaks in the two patterns. As these differences are caused by varying degrees

of alignment of microcrystallites because of preferred orientation effects they are judged not to be significant. Instead the equivalence of two samples is judged primarily by the position of individual peaks, as these are unique for each crystal.

It was concluded therefore that the two patterns b) and c) prove the samples to be isomorphous.

7.4.2. PROP

The desorption of 3-hydroxypropionitrile from the complex **PROP** was found to be a one-step process (TG and DSC).. However, the DSC scan for **PROP** indicated a second endotherm not associated with a change in the mass of the sample. This implies that following the loss of its guest **PROP** forms an intermediate phase before the host molecule lattice collapses to the α-phase. To test whether this intermediate is a β_0- or a γ-phase, a sample of **PROP** was desolvated under mild conditions to prevent the deterioration of the intermediate phase.

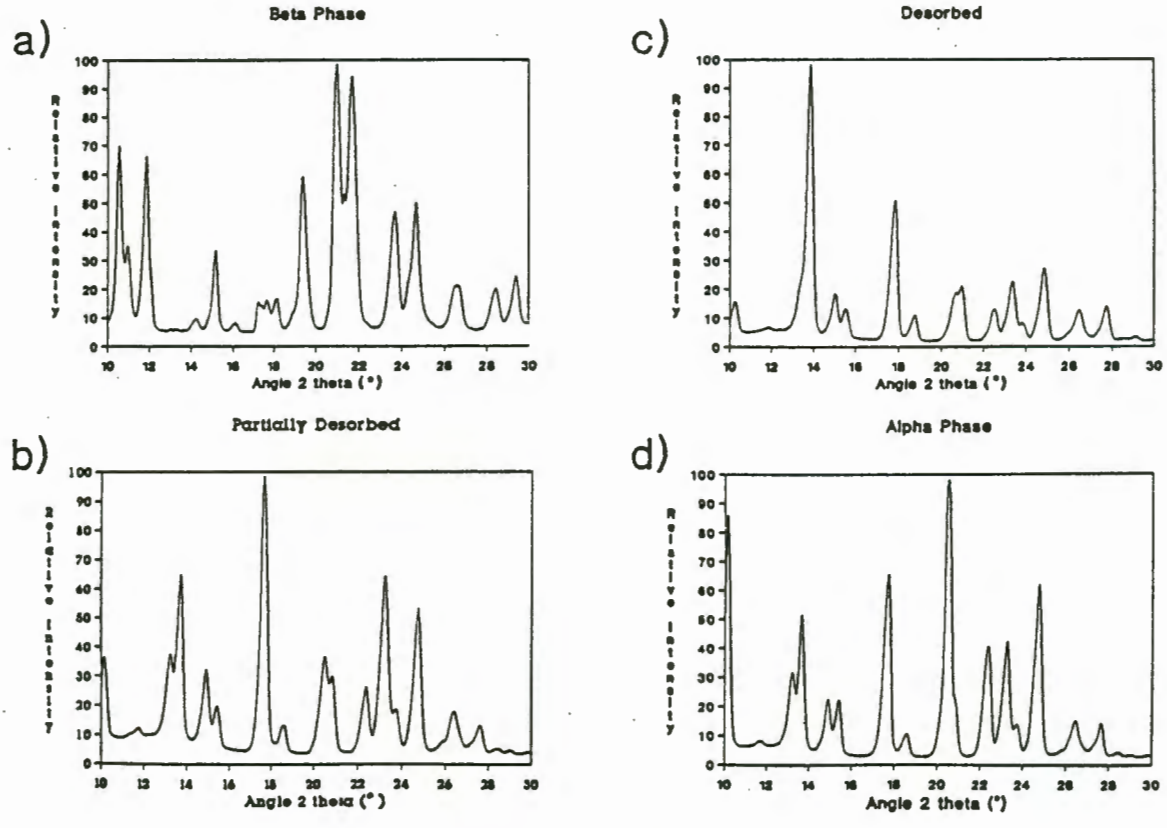

Figure 7.4.2 **PROP** - X-ray diffraction patterns: a) for the β-phase, b) for the sample desorbed under mild conditions, c) for the desorbed sample and d) for the α-phase.

However, the desorption of the guest was accompanied by a unexplained shift in the position of the second, rearrangement peak (B in figure 7.2.2). By the time the peak ascribed to the guest desorption had disappeared peak B had effectively coalesced with the endotherm representing the melting of the host. The resulting diffraction pattern (figure 7.4.2 b) was found to correspond closely with that of the α-phase, indicating that it had not been possible to isolate the highly unstable intermediate phase. The X-ray diffraction pattern obtained from a sample that was desorbed under more intense heat follows as part c) of figure 7.4.2. To enable these patterns to be compared to that of the host α-phase this is included as figure 7.4.2 d).

Thus it was impossible to identify the intermediate structure as either a β_0- or a γ-phase.

7.4.3. PYD

Figure 7.4.3 includes the X-ray diffraction patterns for the solvated, partially desolvated and desolvated forms of **PYD** and, for comparison, the α-phase of the host.

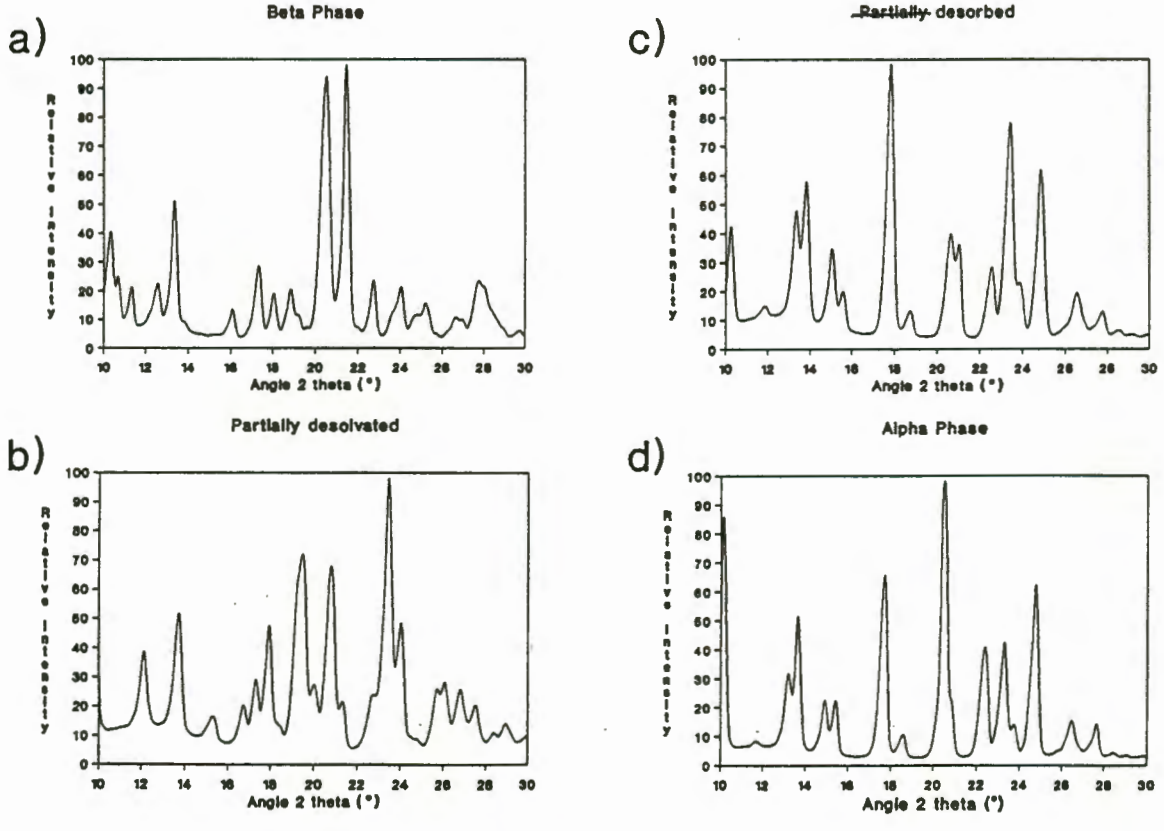

Figure 7.4.3 **PYD** - X-ray diffraction patterns: a) for the β-phase, b) for the partially desorbed sample, c) for the desolvated sample and d) for the α-phase.

As previously observed for **NITRANN**, the X-ray diffraction pattern of the desolvated form matches that of the host α-form, leading to the conclusion that desorption of the pyridine from the complex causes the host molecules to rearrange to adopt the α-phase.

In theory, the partial loss of the guest from an inclusion compound could result in two intermediate stages. Either the host framework remains intact while voids are left in the positions previously occupied by guest molecules (a half filled β_0-phase) or the host lattice of the complex rearranges, leading to the formation of a γ-phase.

Both alternatives would, in theory, be stable or metastable but, while the first would be isomorphous with the β-phase, the second would be crystallographically different to both the α- and the β-phases. Comparing part b) of figure 7.4.3 to part a) and d) shows that the second of the above options applies. Thus the formation of a γ-phase results from the loss of half the guest molecules.

7.4.4. 3PIC

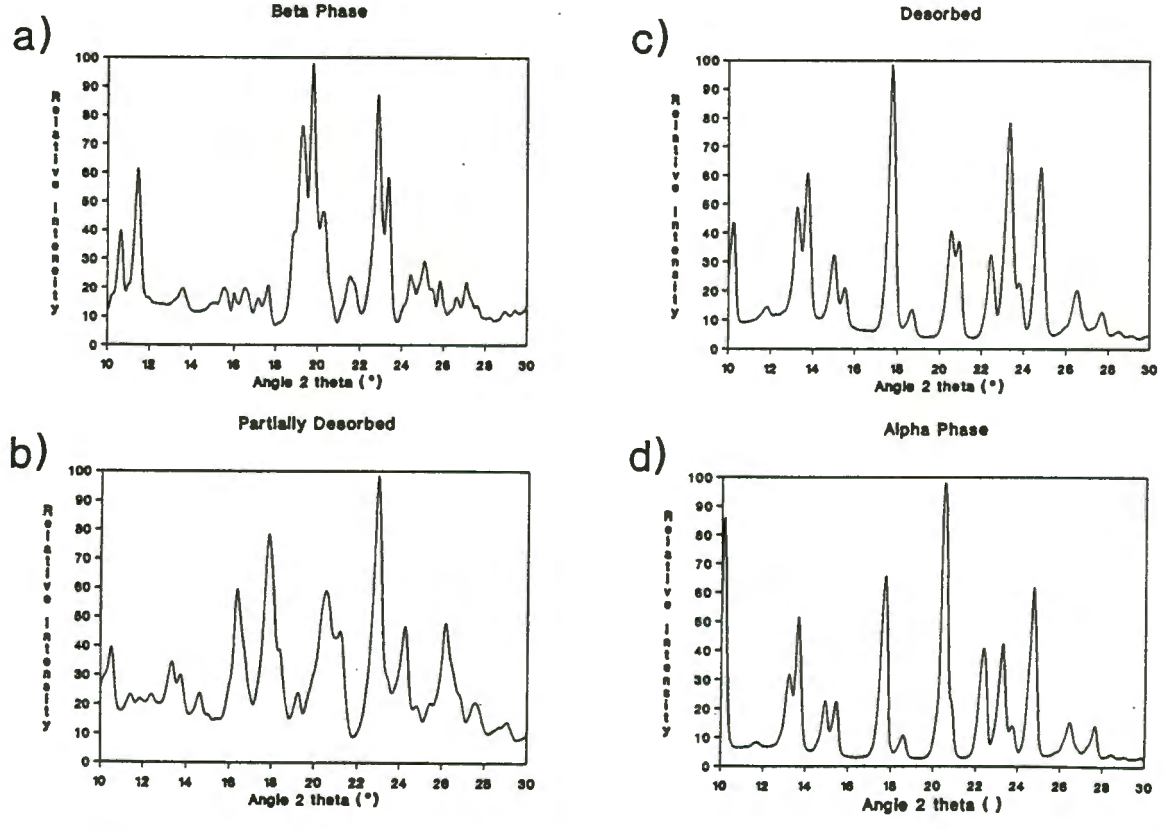

Figure 7.4.4 3PIC - X-ray diffraction patterns: a) for the beta phase, b) for the partially desolvated sample, c) for the desolvated sample and d) for the α-phase.

As may be concluded from figure 7.4.4, in the case of 3PIC essentially equivalent results as those observed for PYD (7.4.3) were obtained: On losing half the total amount of guest the complex rearranges to give a γ-phase structure. Then, after losing the remainder of the guest, the γ-phase reverts to the host α-phase as had been the case for NITRANN and PROP.

7.4.5. 24LU

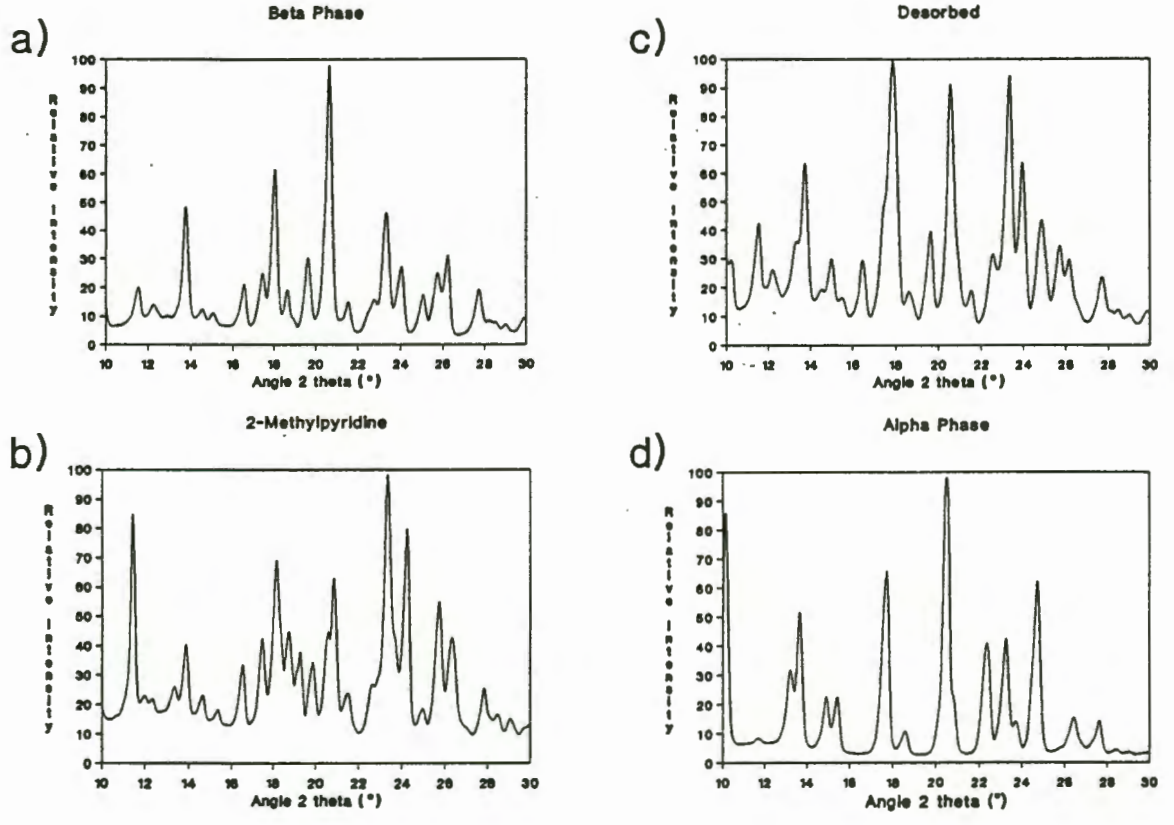

Figure 7.4.5 24LU - X-ray diffraction patterns: a) for the β-phase, b) for the complex of (1) with 2-methylpyridine, c) for the desorbed sample of 24LU and d) for the host α-phase.

Figure 7.4.5 displays the X-ray diffraction patterns for 24LU. Part b) depicts the pattern obtained from a sample of the complex the host forms with 2-methylpyridine. (The crystals were grown under identical conditions to those used to obtain those of 24LU and the samples were prepared by identical methods.) As was mentioned in chapter 6, the structures corresponding to the solvents 2-methylpyridine and 2,4-dimethylpyridine were found to be very nearly isomorphous. This should be clearly visible from their X-ray powder diffraction patterns as isomorphous structures have equivalent *d* spacings.

Comparing a) and b) vindicates the hypothesis that the two structures are isomorphous. Though individual peaks have greatly differing intensities they are found to occur at the same 2θ angle values.

In figure 7.4.5 c) the powder diffraction pattern obtained from a sample of **24LU**, which had been heated in a vacuum oven at 80°C for approximately three hours, is shown. Comparison of c) with the α- and β-phases indicates that c) strongly resembles d), the powder pattern of the α-phase. However, the appearance of some β-phase features overlapping the α-phase pattern indicates that possibly not all the guest had been removed from the lattice. As a result the host framework of the β-phase is partially retained.

This stability of the β-phase could be due to the guest being isolated in cavities in the host lattice, rather than lying in channels which provide a route of escape. Consequently complete guest desorption would require a severe disruption of the host lattice, which had not occurred in this sample.

7.4.6. 26LU

The X-ray diffraction patterns for **26LU** depicted in figure 7.4.6 (p155) indicate that **26LU** does not follow the same general pattern observed for the other structures discussed above. After partial desorption of the guest under mild conditions (warming at 80°C under vacuum for 2 hours), an intermediate is formed whose X-ray diffraction patterns (figure 7.4.6 b) strongly resembles that of the β-phase (figure 7.4.6 a). This intermediate could therefore best be described as a partially filled β-phase.

After complete desorption of the guest, the structure reverts to the alpha phase (figure 7.4.6 c). To ensure complete desorption of the guest, the sample of this compound was maintained at a temperature of 120°C in a vacuum oven overnight.

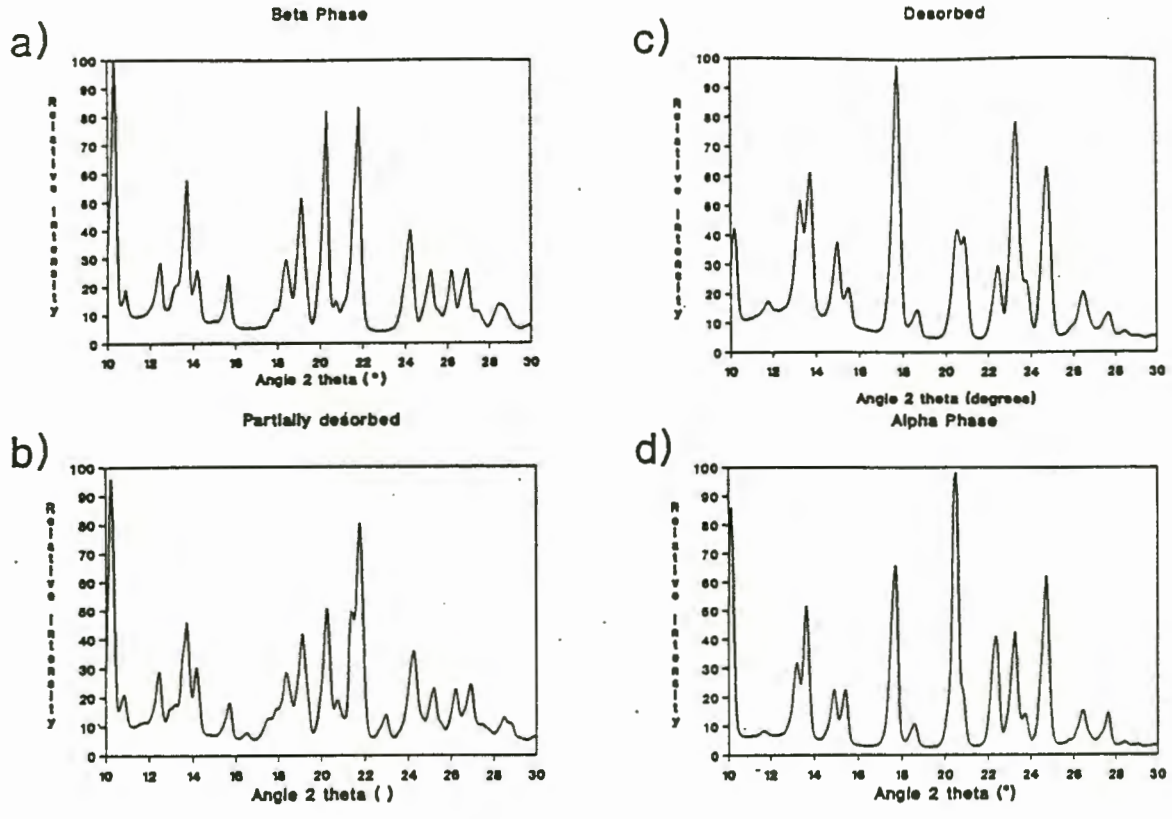

Figure 7.4.6 26LU - X-ray diffraction patterns: a) the complex β-phase, b) the partially desorbed sample, c) the desorbed sample of the complex and d) the host alpha phase.

7.5. POTENTIAL ENERGY CALCULATIONS

The objective of carrying out thermal analysis on these compounds was to reconcile thermodynamics with structure. Thus it should, in principle, be possible to find a relation between the measured enthalpies of the guest release reactions and the host-guest interactions which occur in the crystal structure.

The interactions are of two kinds: van der Waals forces and hydrogen bonds. The potential energy environment of the guest molecules in the lattice made up of host molecules was evaluated using the method of atom-atom potentials. The program HEENY uses empirical atom pair potential curves to evaluate non-bonded van der Waals interactions. The coefficients of the atom-atom potential are of the form

$$V(r) = a \exp((-br)/r^d - c/r^6)$$

where r is the distance between any pair of atoms and the coefficients a, b, c, d are those given by Giglio [144], and recently reviewed by Pertsin and Kitaigorodsky [145].

The hydrogen bond potential, V_{hb} was calculated using the equation given on page 129.

For each compound the guest molecule was completely surrounded by host molecules. The positions of the latter were held constant while the guest molecule was allowed to find its minimum energy environment by incremental translations and rotations. The minimum potential energies thus calculated are given in table 7.5.

It must be pointed out that calculations of energies for different guest molecules cannot be directly compared, because the very nature of the atom-atom potential depends on the summation of atomic interactions of the guest with atoms of its surrounding environment. Thus only guests with the same number of atoms ie. isomers can strictly be compared. Consequently our discussion will concentrate on the results obtained for the **24LU** and **26LU** structures, although the other energy results are listed for interest.

Table 7.5 presents the essential results derived from the structure, the thermal analysis and the energy calculations.

The ΔH column lists the enthalpy changes of each guest release reaction. When this is a two stage process, the ΔH for each process is reported. All the compounds except **24LU** have a host:guest ratio of 1:2. Thus the total ΔH listed is for the release of both guest molecules. In the case of **24LU** the result was doubled in order to make comparison meaningful.

Table 7.5. Potential Energy for Guest molecules in Relation to the Host Lattice.

Compound name	Reaction	T_{on}-T_b K	O···N Å	ΔH kJ.mol^{-1}	ΔH_{Tot} kJ.mol^{-1}	V_{Total} kJ.mol^{-1}
NITRANN	H·2G→ H+2G	-46	2,88	57,2		-48,1
PROP	H·2G→ H+2G	-137	2,88	40,4		-66,7
PYD (A)	H·2G→ H·G+G	-51	2,84	42,0		-65,4
PYD (B)	H·G → H+G		2,79	52,1	94,1	-59,1
3PIC (A)	H·2G→ H·G+G	-49	2,93	16,8		-84,7
3PIC (B)	H·G → H+G		2,79	52,5	69,3	-77,7
24LU	H·G → H+G	-21	2,74	68,5 x2 =	137,0	-110,7
26LU	H·2G→ H·G+G	-47	2,90	31,5		-107,4
	H·G → H+G			49,6	81,1	

With regard to the isomeric guest structures, **24LU** and **26LU** we note that the **24LU** structure has the lower energy, the greater value of ΔH and the lower T_{on}-T_b. Thus it is the more stable by all three criteria.

Comparing all the structures, we note that T_{on}-T_b for structures **NITRANN, PYD, 3PIC** and **26LU** are all very close, but we can infer the following stability patterns:

		most stable						least stable
ΔH	:	**24LU**	> **PYD**	> **26LU**	> **3PIC**	> **NITRANN**	> **PROP**	
T_{on}-T_b	:	**24LU**	> **PYD**	≈ **3PIC**	≈ **26LU**	≈ **NITRANN**	> **PROP**	

Thus we have partially correlated the thermal stability parameters of all the compounds, and in the case of the two isomers **24LU** and **26LU** there is an excellent correlation between the structural parameters which give rise to the crystal energies and the thermal parameters: T_{on}-T_b and the enthalpies of the guest release reactions.

7.6. CONCLUSION

As may be seen from the discussions above, all structures have a similarly unstable host framework. For the complexes that decay in a two step desorption process, an intermediate γ-phase is generally observed; the only exception being **26LU**, where a half-filled β_0-phase is formed. After complete desorption of the guest, the host lattice collapses to give the α-phase, presumably the form of the host with the lowest potential energy.

This result is not unexpected since none of the structures with the exception of **24LU** (cf. Chapter 6) reveals any hydrogen bonding between host molecules. Hydrogen bonds, where they do occur, generally only bind host to guest molecules. As a result, the host lattice collapses as soon as the support of the intermediate guest molecules is removed. Even in **24LU**, where inter-host hydrogen bonds do occur, these do not survive the disruption of the lattice caused by the escape of the 2,4-dimethylpyridine molecules.

CHAPTER 8.

COMPETITION EXPERIMENT

8. COMPETITION EXPERIMENT

8.1. INTRODUCTION

One of the most important characteristics of a host compound in making it economically interesting is its selectivity towards one molecular shape in preference to others. As mentioned in the introduction (Chapter 1) the host compound (1) was originally chosen because it appeared that it would selectively include alcohols, particularly ethanol. It was hoped at the time that it would prove possible to devise a cost-effective method of isolating these solvents from aqueous solutions through selective inclusion by the host.

In order to test the ability of (1) to discriminate between molecules other than water and alcohols, a competition experiment was designed making use of the isomeric solvents 2,4- and 2,6-dimethylpyridine. The two solvents were chosen because both are known to be included by (1) - as demonstrated in the preceding chapters - and because they are closely related structurally.

(Throughout this chapter the symbols x_{24M} and x_{24S} have been used to denote the mole fraction of 2,4-dimethylpyridine in the solvent mixtures (liquid) and as included by (1) (solid) respectively.)

8.2. THE EXPERIMENT

The aim of this competition experiment was to test the selectivity of the host (1) towards either 2,4- or 2,6-dimethylpyridine.

To achieve this, mixtures of the two solvents were prepared with x_{24M} ranging from 0,1 to 0,9 in intervals of 0,1. (for $x_{24M} = 0$ and $x_{24M} = 1{,}0$, $x_{24S} = x_{24M}$.)

The host was permitted to crystallise from dilute solutions of (1) in these mixtures by slow evaporation of solvents. A large excess of solvent mixture was required to ensure that the relative proportions of the solvents were as far as possible unaffected by the process of inclusion.

When sufficient amounts of crystals had formed these were dissolved in suitable solvents - initially acetone was used but later hexane was found to be more suitable. Solutions of 0,01 M concentration were prepared assuming a host to guest ratio of 1:1

(Exact concentrations were not required as only relative proportions of dimethylpyridines were of interest). A concentration of 0,01 M was found to be useful as it enabled complete crystal dissolution while still being well within the detectable limits for Gas Chromatography.

To prepare the solutions, the crystals were removed from their mother liquor, dried between two sheets of filter paper without crushing, weighed and transferred to sample tubes containing the solvent. Once in the solvent, the crystals were crushed using a glass rod and heated to bring about rapid dissolution of the crystals, after which the solutions were cooled in ice and securely sealed to prevent any dimethylpyridine being lost.

The solutions had to be prepared shortly before the measurement commenced so as to prevent evaporation of either dimethylpyridine and also to prevent the host from recrystallising and including either one of the dimethylpyridines or the solvent in the case of acetone ((1) does not included n-hexane).

The relative proportions of 2,4- and 2,6-dimethylpyridines were then determined with the help of gas chromatography.

8.3. RESULTS

No particular difficulties were encountered either during the preparation of solutions or with the growth of crystal. However finding a suitable gas chromatographic setup proved to be more problematic than had initially been assumed.

8.3.1. Squalane on Chromosorb - Packed Column

Initially, in accordance with a handbook of gas chromatography [115] a packed column of 10% Squalane on Chromosorb (40/60 mesh) was prepared. The gas chromatograph used was a Philips Pye Unicam PU4500. (Further details concerning the instrumental setup may be obtained from Section 3.4.4.) Acetone was used as the solvent both for the system calibration and for the experiment, as it was found that, due to its low retention time, it did not overlap with either of the dimethylpyridine peaks.

After trying various temperature programs, a setup including an isothermal column temperature of 120°C, a carrier gas flow rate 30 $ml.min^{-1}$ (N_2), and injector and detector temperatures of 200°C was found to yield the optimal separation. Unfortunately the retention time for 2,6-dimethylpyridine was found to be excessively

long causing the corresponding peaks to suffer from pronounced broadening. In addition, the flame ionization detector, FID, registered a disproportionately low readout for 2,6-dimethylpyridine. As an example the print out for the calibration solution with x_{24M} = 0,5 is shown in figure 8.1.

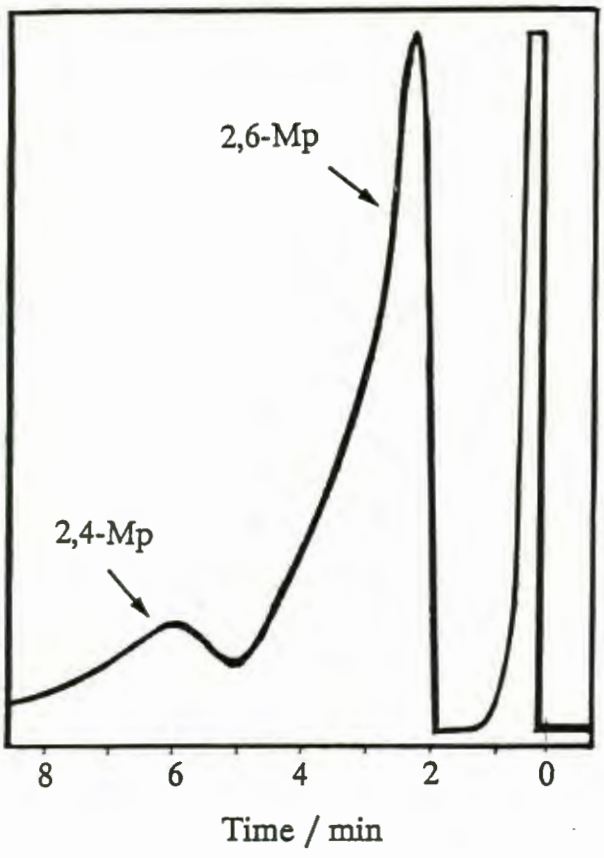

Figure 8.1. A representative print-out (x_{24M} = 0,5) obtained using a packed column of 10% Squalane on Chromosorb.

These problems combined to result in excessively skewed data being obtained, especially at low concentrations of 2,6-dimethylpyridine, and it was decided to abandon this instrumental setup.

8.3.2. OV225 Capillary Column

As part of our second attempt, a Carlo Erba Strumentazione Vega Series 2 model 6000 Chromatograph in conjunction with an Intelligent Control Unit ICU 600 equipped with a Spectra-Physics SP4290 Integrator was used. Out of a range of available capillary columns a column coated with OV225 was chosen as the most suitable.

The program found to yield maximum separation of peaks included an isothermal column temperature of 80°C, a carrier gas flow rate of 1,5 ml.min^{-1} and a detector temperature of 250°C. However, because of the stationary phase of the column a non-polar solvent was required. Since n-hexane was found to be the only non-polar solvent capable of dissolving the host in suitably high concentration it was used as solvent throughout the experiment.

Because of the relatively poor solubility of the host in n-hexane, solutions with dimethylpyridine concentrations of 0,01 M were found to be the highest achievable. This unfortunately, resulted in excessively large solvent peaks being registered which partially obscured the 2,6-dimethylpyridine peak, the first dimethylpyridine eluted by this column. A representative example of the output obtained is included in figure 8.2

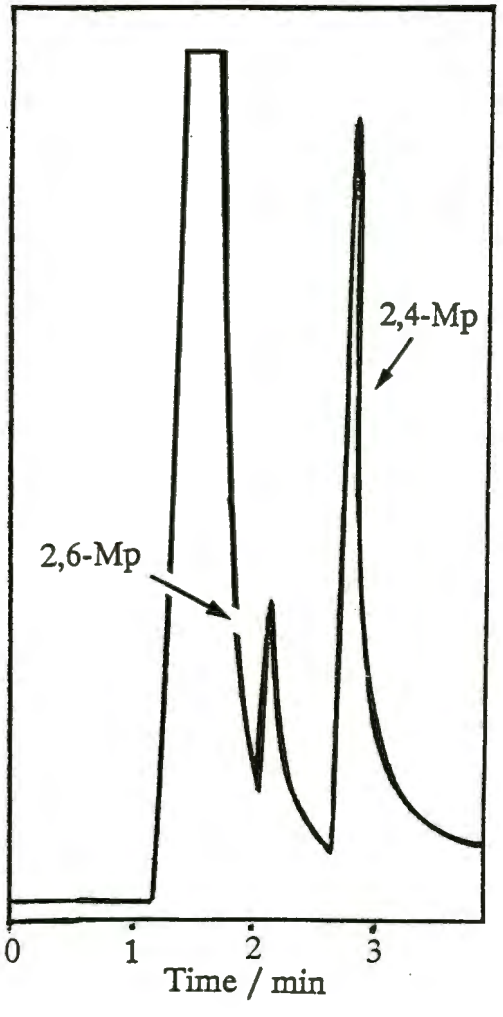

Figure 8.2 A representative print-out (x_{24M} = 0,5) obtained using an OV225 capillary column.

Though it can be argued that these results implied an improvement over those previously obtained, the overlap of the n-hexane and 2,6-dimethylpyridine peaks meant that these were not sufficiently accurate. The calibration curve plotted from the data obtained is depicted in figure 8.3 while the overall results for the experiment as determined by the present setup are included in figure 8.6 to allow them to be compared to the final results.

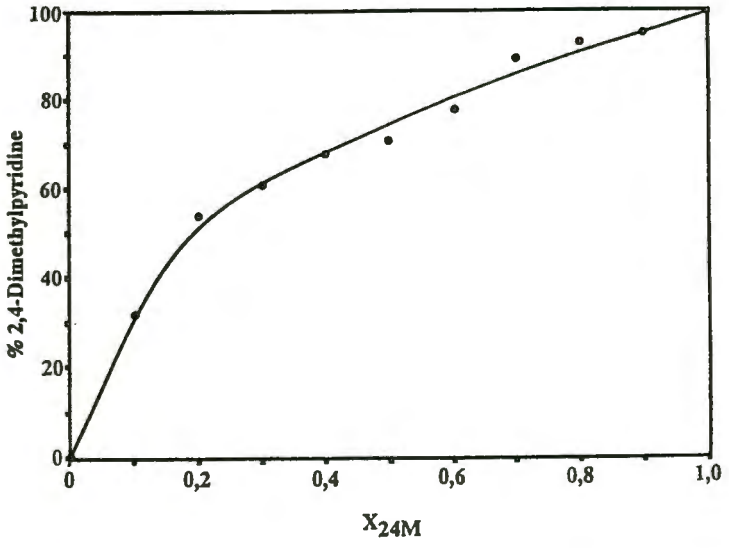

Figure 8.3 The calibration curve obtained using an OV225 capillary column.

8.3.3. OV225 Packed Column

Finally a Carlo Erba Strumentazione Fractovap 4200 series FTV/4200-41 Chromatograph equipped with a Spectra-Physics SP4290 Integrator was chosen together with a packed column with OV225 as the stationary phase.

Here a program similar to the one used in 8.3.2 was found to be most suitable in giving optimal peak separation. Again an isothermal column temperature of 80°C was chosen together with a carrier gas flow-rate of 45 $ml.min^{-1}$, as well as detector and injector temperatures of 250°C.

The results obtained by means of this system proved to be far superior to those previously achieved. No overlapping of peaks, no excessive broadening and nearly perfect detector responses were achieved, cf. figure 8.4.

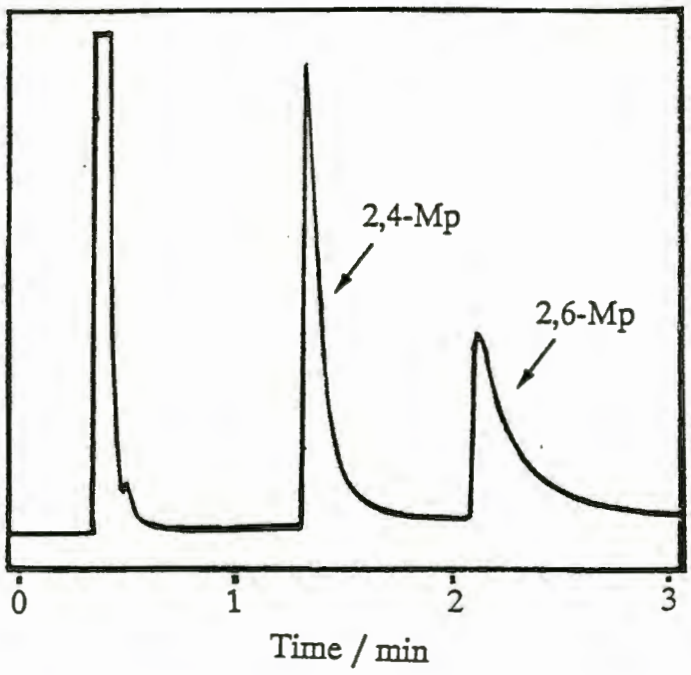

Figure 8.4 A representative print-out (x_{24M} = 0,5) obtained using the OV225 packed column.

The peak areas, as determined by the Spectra-Physics Integrator, were used for the calibration curve (depicted in figure 8.5) and for the sample readings. The final graph correlating x_{24S} and x_{24M} can be seen in figure 8.6.

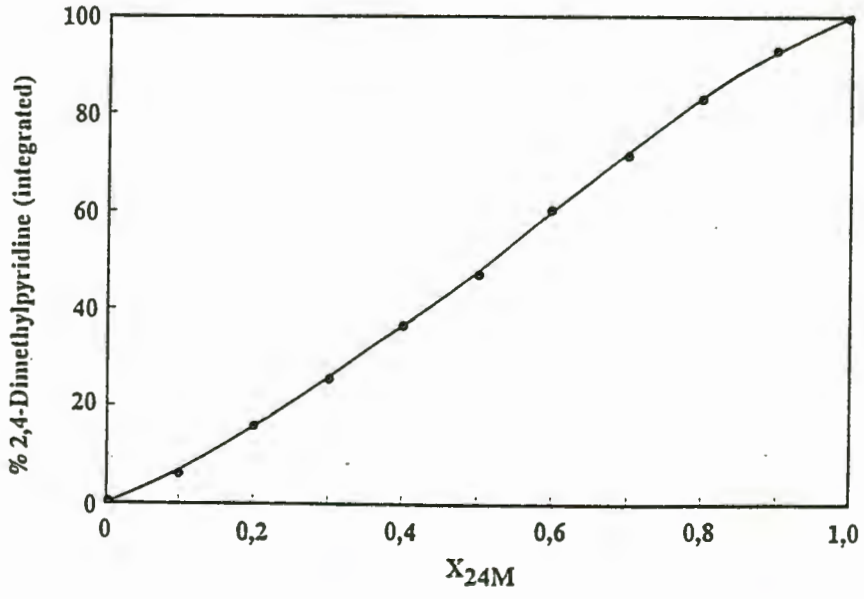

Figure 8.5 The calibration curve obtained using the OV225 packed column.

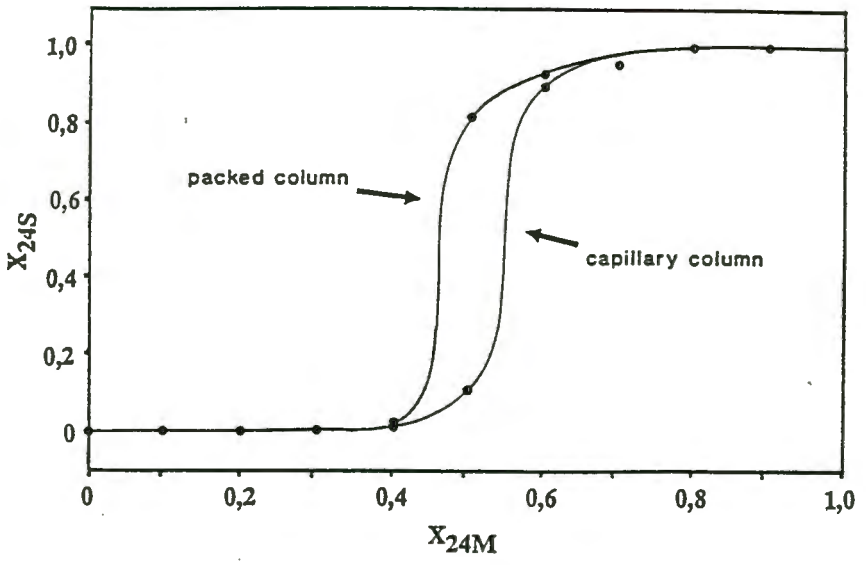

Figure 8.6 A plot of x_{24M} versus x_{24S} for the results of Sections 8.3.2 and 3. The former is indicated by dotted lines, while solid lines were used for the second.

8.4. CONCLUSION

The results for this experiment as summarised by figure 8.6 indicate that the host (1) is unable to discriminate between the two dimethylpyridines when an equimolar mixture of the two is used. On either side of x_{24M} = 0,5 however, even a slight excess of either one of the solvents causes essentially only that isomer to be included.

Instead the curve is indicative of catalytic behaviour in crystal formation. Thus an excess of one of the two solvents causes an initial inclusion of that solvent. The formation of the crystal, however, triggers the formation of further crystals of the same type to the virtual exclusion of the second pyridine derivative.

Consequently, a separation of the two solvents by this method is achievable, provided the two dimethylpyridines are present in unequal proportions. If the two are present in equal proportion, or if by removal of one, the proportions equilibrate the technique loses it applicability.

CHAPTER 9.

CONCLUSION

9. CONCLUSION

The host compound *trans*-9,10-dihydroxy-9,10-diphenyl-9,10-dihydroanthracene was found to include a range of pyridine derivatives as well as two nitrile compounds.

Of this group of crystalline adducts, a set of six was chosen for further analysis, structural and thermodynamic. In all cases the guest molecules were observed to act as a structural support of the host lattice. Removal of the guest resulted in the collapse of the host lattice, which rearranged to its energetically most favourable form, the α-phase.

Host to guest ratios of 1:2 were found to characterise five of the complexes, while the sixth revealed a host to guest ratio of 1:1. All crystals were observed to belong either to the triclinic space group $P\bar{1}$ or to the monoclinic space group $P2_1/c$. The structure **PYD** was solved in the unusual setting $C\bar{1}$ for computational reasons.

In four of the five complexes with host to guest ratios of 1:2 the hydrogen bonding scheme proved to follow the same pattern, reported for most previous structures, in that the host molecule, via its hydroxyl substituents, is hydrogen bonded to two symmetry related guest molecules; no other hydrogen bonding occurs in the complexes. The structure of the inclusion compound of the host and 3-hydroxypropionitrile by contrast, displays a more complicated hydrogen bonding scheme: both the guest's nitrile and hydroxyl groups participate in hydrogen bonding. As each guest molecule thereby links two different host molecules this results in infinite layers of host and guest molecules lying in planes parallel to the (011) plane.

The structure of the inclusion compound of the host with 2,4-dimethylpyridine was demonstrated to be virtually isomorphous with that of the 2-methylpyridine complex. Its hydrogen bonding scheme is characterised by infinite bands of hydrogen bonded host molecules with guest molecules bonded laterally to every alternate host molecule.

A competition experiment indicated that the host molecule (**1**) does not preferentially include either of the isomers 2,4- and 2,6-dimethylpyridine from an equimolar mixture of the two. However, even a minimal excess of one of the solvents results in that isomer being included, to the virtual exclusion of the other.

The enthalpy of the guest desorption processes were found to span the range from 16,8 to 68,4 $kJ.mol^{-1}$, while the activation energy of the desorption processes were calculated to lie between 71 and 93 $kJ.mol^{-1}$ (that is, excluding **NITRANN** for which the

activation energy of desorption was found to be dependent on temperature resulting in a range of values from 83 to 115 $kJ.mol^{-1}$).

Attempts at determining a possible connection between the O··N distance of the O-H··N hydrogen bonds to the difference between the desorption onset temperature, T_r, and the boiling point, T_b failed. More work would be required to quantify the overall potential energy of the crystal, and to correlate this, in total or parts, to experimentally observed, structural parameters.

To this end, similar series of closely related complexes, as the one used in the present work, would seem to offer the best route to success.

REFERENCES

REFERENCES

1. H. Davy, *Philos. Trans. R. Soc. London.*, 1811, **101**, 1.
2. M. Faraday, *Quart. J. Sci.*, 1823, **15**, 71.
3. J. E. D. Davies, W. Kemula, H. M. Powell and N. O. Smith, *J. Incl. Phenom.*, 1983, **1**, 3.
4. C. Schafhäutl, *J. Prakt. Chem.*, 1841, **21**, 129.
5. F. Wohler, *Ann. Chem. Liebigs,* 1849, **69**, 297.
6. A. Villiers, *C. R. Hebd. Sceances Acad. Sci.*, 1891, **112**, 536.
7. K. A. Hofmann and F. Küspert, *Z. Anorg. Allg. Chem.*, 1897, **15**, 204.
8. F. Mylius, *Chem. Ber.*, 1886, **19**, 999.
9. K. A. Hofmann, Lehrbuch der Anorganischen Chemie, 1828.
   (The extract is taken from Reference 3)
10. D. E. Palin and H. M. Powell, *Nature*, 1945, **156**, 334.
11. D. E. Palin and H. M. Powell, *Journal of the Chemical Society*, 1947, 208.
12. A. Clemm, *Annalen*, 1859, **110**, 352.
13. W. A. Caspari, *Journal of the Chemical Society*, 1926, 2944.
14. W. H. Zachariasen, *Zeitschrift für Kristallographie*, 1934, **88**, 150.
15. H. M. Powell, *Journal of the Chemical Society*, 1948, 61.
16. H. M. Powell, *Research*, 1948, **1**, 353.
17. a) H. M. Powell, *Journal of the Chemical Society*, 1948, 571.
    b) H. M. Powell, *Journal of the Chemical Society*, 1948, 815.
    c) H. M. Powell, *Nature*, 1949, **163**, 566.

18. J. L. Atwood, J. E. D. Davies, D. D. MacNickol (eds), *Inclusion Compounds* (Vol.s 1-4), 1984, Academic Press.

19. J. E. D. Davies, *Journal of Molecular Structure*, 1981, **75**, 1.

20. D. D. MacNickol, J. J. McKendrick, D. R. Wilson, *Chem. Soc. Rev.*, 1978, **7**, 65.

21. C. Löwig, *Ann. Chem. Phys. Sci.*, 1829, **42**, 113.

22. a) M. von Stackelberg and H. R. Müller, *Naturwiss.*, 1951, **38**, 456.

    b) M. von Stackelberg and H. R. Müller, *Naturwiss.*, 1952, **39**, 20.

    c) M. von Stackelberg and H. R. Müller, *J. Chem. Phys.*, 1951, **19**, 1319.

23. W. F. Claussen, *J. Chem. Phys.*, 1951, **19**, 259, 662, 1425.

24. L. Pauling and R. E. Marsh, *Proc. Natl. Acad. Sci.* U.S.A., 1952, **38**, 112.

25. A. S. Quist and H.S Frank, *J. Phys. Chem.*, 1961, **65**, 560.

26. A. D. Potts and D. W. Davidson, *J. Phys. Chem.*, 1965, **69**, 996.

27. M. G. Vuilland and N. Satragno, *Compt. Rend. Acad. Sci. C*, 1960, **250**, 3841.

28. O. Maass and E. H. Boomer, *J. Am. Chem. Soc.*, 1922, **44**, 1709.

29. M. von Stackelberg and H. R. Müller, *Z. Electrochem.*, 1954, **58**, 25, 40, 99, 126.

30. R. M. Barrer, Chapter 6 in 'Inclusion Compounds', 1984, **1**, reference 18.

31. D. W. Breck, 'Zeolite Molecular Sieves', 1974, John Wiley & Sons, New York.

32. T. Way, *J. Roy. Soc.*, 1850, **11**, 313.

33. T. Iwamoto, Chapter 2 in 'Inclusion Compounds', 1984, **1**, reference 18.

34. J. Lipkowski, Chapter 3 in 'Inclusion Compounds', 1984, **1**, reference 18.

35. H. M. Powell and J. H. Rayner, *Nature*, 1949, **163**, 566.

36. J. H. Rayner and H. M. Powell, *J. Chem. Soc.*, 1952, 319.

37. W. D. Schaeffer, W. S. Dorsey, D. A. Skinner and C. G. Cristian, *J. Am. Chem. Soc.*, 1957, **79**, 5870.

38. E. Weber, In the Preface to 'Topics in Current Chemistry', 1988, **149**, Springer Verlag, Berlin.

39. C. J. Pedersen, Nobel lecture, *Angew. Chem. Int. Ed. Engl.*, 1988, **27**, 1021.

40. C. J. Pedersen, *J. Am. Chem. Soc.*, 1967, **89**, 2495, 7071.

41. C. J. Pedersen, *Aldrichimica Acta.*, 1971, **4**, 1.

42. D. J. Cram, Nobel lecture, *Angew. Chem. Int. Ed. Engl.*, 1988, **27**, 1009.

43. D. J. Cram, T. Kaneda, R. C. Helgeson and G. M. Lein, *J. Am. Chem. Soc.*, 1979, **101**, 6752.

44. J.-M. Lehn, Nobel lecture, *Angew. Chem. Int. Ed. Engl.*, 1988, **27**, 90.

45. B. Dietrich, J.-M. Lehn, J.-P. Sauvge, *Tetrahedron Lett.*, 1969, 2885, 2889.

46. a) B. Dietrich, J.-M. Lehn, J.-P. Sauvge, J. Blanzat, *Tetrahedron*, 1973, **29**, 1629.

    b) B. Dietrich, J.-M. Lehn, J.-P. Sauvge, J. Blanzat, *Tetrahedron*, 1973, **29**, 1647.

47. E. Weber, in Phase Transfer Catalysts, 1988, Merck-Schuchardt.

48. a) E. W. Spanagel and W. A. Carothers, *J. Am. Chem. Soc.*, 1935, **57**, 935.

    b) E. Fourneau and P. M. Baranger, Bull. Soc. Chim., 1931, **49**, 1161

49. a) L. Ruzicka, J. Buijs, and M. Stoll, *Helv. Chim. Acta*, 1932, **15**, 1220.

    b) R. Kelly, D. M. MacDonald and K. Weisner, *Nature* , 1950, **166**, 225.

50. C. J. Brown and A. C. Farthing, *Nature*, 1949, **164**, 915.

51. D. J. Cram, H. J. Steinberg, *J. Am. Chem. Soc.*, 1951, **73**, 5691.

52. D. J. Cram, *Acc. Chem. Res.*, 1971, **4**, 204.

53. S. P. Miller and H. W. Whitlock, *J. Am. Chem. Soc.*, 1984, **106**, 1492.

54. I. Tabushi, K. Yamamura, H. Nonoguchi, K. Hirotsu and T. Higuchi, *J. Am. Chem. Soc.*, 1984, **106**, 2621.

55. K. Saigo, R.-J. Lin, M. Kubo, A. Youda and M.Hasegawa, *J. Am. Chem. Soc.*, 1986, **108**, 1996.

56. I. Goldberg, Chapter 1 in 'Topics in Current Chemitry', 1988, **149**, ed. E. Weber, Springer Verlag, Berlin.

57. D. D. MacNicol, J. J. McKendrick and D. R. Wilson, *Chem. Soc. Rev.*, 1978, **1**, 65.

58. E. Weber and M. Czugler, Chapter 1 in 'Topics in Current Chemitry', 1987, **140**, ed. E. Weber, Springer Verlag, Berlin.

59. E. Weber, Chapter 2 in 'Topics in Current Chemitry', 1988, **149**, ed. E. Weber, Springer Verlag, Berlin.

60. E. Weber , *J. Mol. Graph.*, 1989, **7**, 12.

61. E. Weber , in 'Inclusion Compounds', 1989, **4**, eds. J. L. Atwood, J. E. D. Davies, D. D. McNicol, Academic Press, London.

62. E. Weber, *Chem. Ber.*, 1990, **123**, 811.

63. H. Hart, L.-T. Lin, D. L. Ward, *J. Am. Chem. Soc.*, 1984, **106**, 4043.

64. a) H. R. Alcock, in Chapter 8 of 'Inclusion Compounds', 1984, **1**, eds. J. L. Atwood, J. E. D. Davies, D. D. McNicol, Academic Press, London.

b) H. R. Alcock, *Acc. Chem. Res.*, 1978, **11**, 81.

65. "Fourth International Symposium on Inclusion Phenomena and Third International Symposium on Cyclodextrins", 20-25 July 1986, Lancaster.

66. E. Weber, I. Csöregh, B. Stensland, M. Czugler, *J. Am. Chem. Soc.*, 1984, **106**, 3297.

67. F. Toda, *Chem. Lett.* (Japan), 1983, 1521.

68. F. Toda, K. Tanaka and T. C. W. Mak, *Bull. Chem. Soc. Jpn.*, 1985, **58**, 2221.

69. K. Tanaka and F. Toda, *J. Incl. Phenom.*, 1984, **2**, 99.

70. L. R. Nassimbeni, M. L. Niven, D. A. Stuart and K. J. Zemke, *J. Crystallogr. Spectrosc. Res.*, 1986, **16**, No.4, 557.

71. D. R. Bond, S. A. Bourne, L. R. Nassimbeni and F. Toda, *J. Crystallogr. Spectrosc. Res.*, 1989, **19**, No.5, 809.

72. S. A. Bourne, L. R. Nassimbeni and E. Weber, *J. Org. Chem.*, 1991, in preparation.

73. F. Toda, *Chem. Lett.*, 1986, 109.

74. M. R. Caira, L. R. Nassimbeni, M. L. Niven, W.-D. Schubert, E. Weber and N. Dörperinghaus, *J. Chem. Soc. Perkin Trans. 2*, 1990, 2129.

75. F. Toda, in 'Topics in Current Chemistry', 1987, **140**, ed. E. Weber, Springer Verlag, Berlin.

76. A. J. Birch, A. L. Hinde and L. Radom, J. Am. Chem. Soc., 1981, **103**, 284.

77. K. B. Lipkowitz, P. W. Rabideau, D. J. Raber, L. E. Hardee, P. v.R. Schleyer, A. J. Kos, and R. A. Kahn, *J. Org. Chem.*,1982, 47, 1002

78. P. W. Rabideau, *Acc. Chem. Res.*, 1978, **11**, 141

79. E. L. Eliel, N. L. Allinger, S. J. Angyal and G. A. Morrison, "Conformational Analysis", Interscience, New York, N. Y., 1965, p 125.

80. H. Gerding and F. A. Haak, *Recl. Trav. Chim. Pays-Bas*, 1949, **68**, 293.

81. H. D. Stidham, *Spechtrosc. Acta.*, 1965, 21

82. G. Dallinga and L. H. Toneman, *J. Molec. Struct.*, 1967, **1**, 117.

83. G. Ahlgren, B. Akermark and J. E. Backvall, *Tetrahedron* Letters, 1975, 3501.

84. H. Oberhammer and S. H. Bauer, *J. Am. Chem. Soc.*, 1969, **91**, 10.

85. F. Herbstein, *J. Chem. Soc.*, 1959, 2292.

86. L. J. Durham, J. Studebaker, and M. J. Perkins, *Chem Commun.*, 1965, 456.

87. J. L. Marshall and T. K. Folsom, *J. Org. Chem.*, 1972, **37**, 1863.

88. J. W. Paschal and P. W. Rabideau, *J. Am. Chem. Soc.*, 1974, **96**, 272.

89. J. L. Marshall, A. M. Ihrig and P. N. Jenkins, *J. Org. Chem.*, 1972, **37**, 1863.

90. J. L. Marshall, L. G. Faehl, A. M. Ihrig and M. Barfield, *J. Am. Chem. Soc.*, 1976, **98**, 3406.

91. W. G. Ferrier and Iball, *Chem. Ind.*, 1954, 1296.

92. F. H. Herbstein, M. Kapon and G. M. Reisner, *Acta. Cryst.*, 1986, **B42**, 181.

93. A. Sygula and T. A. Holak, *Tetrahedron Letters*, 1983, **24**, 2893.

94. N. Ahmad, R. J. Goddard, I. K. Hatton, J. A. K. Howard, N. J. Lewis and J. MacMillan, *J. Chem. Soc. Perkin Trans. I*, 1985, 1859

95. F. Leroy, C. Courseille, M. Daney and H. Bouas-Laurent, *Acta. Cryst.*, 1976, **B32**, 2792.

96. a) T. Brennan, E. F. Putkey and M.Sundaralingham, *Chem. Commun.*, 1971, 1490

    b) R. H. Stanford, *Acta. Cryst.*, 1973, **B29**, 2849.

97. J. Iball and D. W. Young, *Acta. Cryst.*, 1958, **11**, 476.

98. F. H. Herbstein, *Acta. Cryst.*, 1961, **14**, 77.

99. N. Ahmad, C. Cloke, I. K. Hatton, N. J. Lewis and J. MacMillan, *J. Chem. Soc. Perkin Trans. I*, 1985, 1849.

100. F. Toda, K. Tanaka, S. Nagamatsu, and T. Mak, *Israel Journal of Chemistry*, 1985, **25**, 346.

101. F. Toda, K. Tanaka and T. C. W. Mak, *Tetrahedron Letters*, 1984, **25**, 1359.

102. F. Toda, K. Tanaka, and T. C. W. Mak, *J. Incl. Phenom.*, 1985, **3**, 225.

103. Haller and Guyot, *C. R. Hebd. Sceances Acad. Sci.*, 1904, **138**, 327.

104. C. K. Ingold and P. G. Marshall, *J. Chem. Soc.*, 1926, 3080.

105. F. Toda, K. Tanaka, G. Ulbarri Daumas and M. C. Sanchez, *Chem. Lett.*, 1983, 1521.

106. K. Tanaka, F. Toda and T. C. W. Mak, *J. of Incl. Phen.*, 1984, **2**, 99.

107.F. Toda, *Topics in Current Chemistry*, 1987, **140**, 43.

108.G. Gawalek (ed.), 'Einschlußverbindungen, Additionsverbindungen, Clathrate', 1969, Deutscher Verlag der Wissenschaft, VEB, Berlin.

109.M. Dobler, Ionophores and their Structures, 1981, John Wiley & Sons, New York.

110.D. M. Walba, R. M. Richards and R. C. Haltiwanger, *J. Am. Chem. Soc.*, 1982, **104**, 3219.

111.C. J. Suckling, *J. Chem. Soc. Chem. Comm.*, 1982, 661.

112.F. Vögtle, H. Sieger and W. M. Müller, *Topics in Current Chemistry*, 1981, **98**, 107.

113.E. Weber and H.-P. Josel, *J. Incl. Phen.*, 1983, **1**, 79.

114.D. R. Bond, R. L. Nassimbeni and F. Toda, *J. Incl. Phenom. Mol. Recognition Chem.*, 1989, **7**, 623

115.Handbook of Chromatography, Gas Chromatography Tables, Table GC 131 Pyridines, p164.

116.International Tables for Crystallography, (1967), vol. III, Table 5.3.6B, p 302, The Kynoch Press, Birmingham, England.

117.G. M. Sheldrick, SHELXS-86, in *Crystallographic Computing 3*, eds. G. M. Sheldrick, C. Kruger and R. Goddard, Oxford University Press, 1985, p. 175.

118.G. M. Sheldrick, SHELX-76, in *Computing in Crystallography*, eds. H. Schenk, R. Olthof-Hazekamp, H. von Koningsveld and G. C. Bassi, Delft University Press, 1978, p. 34.

119.D. T. Cromer and J. B. Mann, *Acta Cryst.*, Section A, 1968, **24**, 321.

120.R. F. Stewart, E. R. Davidson and W. T. Simpson, *J. of Chem. Phys.*, 1970, **42**, 3175.

121.D. T. Cromer and D. Lieberman, *J. of Chem Phys*, 1970, **53**, 1891.

122.M. Nardelli, *Comput. Chem.*, 1983, **7**(3), 95.

123.W. D. S. Motherwell, PLUTO, Structure Plotting Program, personal communication, 1974.

124.D. R. Bond, M. R. Caira, G. A. Harvey, R. L. Nassimbeni and F. Toda, *Acta Cryst.*, 1990, **B46**, 771.

125.G. H. Stout and L. H. Jensen, " 'X-ray Structure Determination - A Practical Guide', Second Edition, 1989, John Wiley & Sons, New York.

126.J. P. Glusker and K. N. Trueblood, 'Crystal Structure Analysis - A Primer', 1972, Oxford University Press, London.

127.M. J. Buerger, 'Crystal Structure Analysis, 1967, John Wiley and Sons, Inc., New York.

128.I. Olovsson and P.-G. Jönsson, Chapter 8: 'X-Ray and Neutron Diffraction Studies' of The hydrogen Bond - Recent Developments in Theory and Experiments, Eds. P. Schuster, North-Holland Publishing Co., (1976)

129.Cambridge Structural Database & Cambridge Structural Database System, January 1991, Version 4.4, Cambridge Crystallographic Data Centre, University Chemical Laboratory, Cambridge.

130.Karle, Dragonette and Brenner, *Acta Cryst.*, 1965, **19**, 713.

131.International Tables for Crystallography, (1974), vol. IV, Table 2.1B, p 55, The Kynoch Press, Birmingham, England.

132.International Tables for Crystallography (1983), Vol. A, Sections 5.1, 2 and 3, pp 70-73, Kluwer Academic publishers.

133.D. R. Bond, R. L. Nassimbeni and F. Toda, J. Crystallogr. Spectrosc. Res., 1989, **19**, 847

134.W. L. Duax and D. A. Norton (Eds.), "Atlas of Steroid Structure", 1975, Vol. 1, Plenum Press, London.

135.W. D. S. Motherwell, EENY (Potential Energy Program), June 1974, Cambridge, unpublished.

136.A. Gavezotti, *J. Am. Chem. Soc*, 1983, **105**, 5220.

137.A. Gavezotti and M. Simonetta, *Chem. Rev.*, 1982, **82**, 1.

138.J. H. Flynn and L. A. Wall, *Polymer Letters*, 1966, **4**, 323.

139.M. A. Herman, H. Hoffmans and H. O. Desseyn, *Thermochimica Acta*, 1985, **85**, 63.

140.C. F. Marais, HEENY, 1990, unpublished.

141.A. Vedani and J. D. Dunitz, *J. Am. Chem. Soc.*, 1985, **107**, 7653.

142.B. R. Gelin and M. Karplus, *Biochemistry*, 1979, **18**, 1256.

143.C. Li-feng and L. V. C. Rees, *Zeolites*, 1988, **8**, 310.

144.E. Giglio, *Nature*, 1969, **222**, 339.

145.A. J. Pertsin and A. I. Kitaigorodsky, The atom-atom potential method, Chapter 3, Chemical Physics 43, Springer Verlag, 1987.

APPENDICES

APPENDIX 1

Figures of merit calculated for the reflection data set, using equivalent reflections (SHELXS-86 direct methods test):

$$R_{(\sigma)} = \Sigma\sigma(F^2) / \Sigma F^2$$

$$R_{(int)} = \Sigma|F^2-(F^2)_{mean}| / \Sigma F^2$$

Figures of merit calculated for all refined phase permutations (SHELXS-86 direct methods test):

$$R_\alpha = \Sigma w[\alpha-\alpha_{est})]^2 / \Sigma w[\alpha_{est})]^2$$

where $w = 1/[\alpha_{est} + 5]$

$$CFOM = R_\alpha + [0 \text{ or } (NQUAL - wn), \text{whichever is larger}]^2$$

where

$$NQUAL = \frac{\Sigma[\Sigma(E_{-1}*E_{-2})*\Sigma(E_{-3}*E_{-4}*E_{-5})]}{\Sigma[|\Sigma(E_{-1}*E_{-2})|*|\Sigma(E_{-3}*E_{-4}*E_{-5})|]}$$

Figures of merit calculated after each cycle of full-matrix least-squares refinement (SHELX-76):

$$R = (\Sigma||F_o|-|F_c||) / (\Sigma|F_o|)$$

$$R_W = (\Sigma||F_o|-|F_c||\cdot w^{1/2} / (\Sigma|F_o|\cdot w^{1/2})$$

APPENDIX 2

Calculation of asymetry parameters for torsion angles related by :
a) mirror plane, ΔC_s

$$\Delta C_s = \left(\sum_{i=1}^{m} (\psi_1 + \psi_1')^2 \ /m \right)^{1/2}$$

b) two-fold axis, ΔC_2

$$\Delta C_2 = \left(\sum_{i=1}^{m} (\psi_1 - \psi_1')^2 \ /m \right)^{1/2}$$

where m = number of torsion angle pairs to be compared
ψ_1, ψ_1' = torsion angle pair related either by a mirror plane or a two-fold axis

Runstreams used for the Cambridge Structural Database:

a) To locate all neutral nitrogen atoms in aromatic systems consisting only of the elements C, H, N, O and including at least one hydroxyl group.

```
T1*ELEM P
T2*ELEM AS
T3*ELEM SB
T4*ELEM S
T5*ELEM SE
T6*ELEM TE
T7*ELEM 4M
T8*ELEM 3A
T9*ELEM 4A
T11*ELEM 8A
T12*CONN
AT1 N 2 0 T2
AT2 C 2 1 T3
AT3 C 2 1 T3
AT4 O 1 1 T2
BO 1 2 5
BO 2 3 5
END
SAVE 3
QUEST T12 - T1 - T2 - T3 - T4 - T5 - T6 - T7 - T8 - T9 - T10 - T11
```

b) To locate all neutral nitrile nitrogen atoms in systems consisting only of the elements C, H, N, O and including at least one hydroxyl group.

```
T1*ELEM P
T2*ELEM AS
T3*ELEM SB
T4*ELEM S
T5*ELEM SE
T6*ELEM TE
T7*ELEM 4M
T8*ELEM 3A
T9*ELEM 4A
T11*ELEM 8A
T12*CONN
AT1 N 1 0 T2
AT2 C 2 0 T3
AT3 C 2
AT4 O 1 1
BO 1 2 3
BO 2 3 1
END
SAVE 3
QUEST T12 - T1 - T2 - T3 - T4 - T5 - T6 - T7 - T8 - T9 - T10 - T11
```

c) To locate all possible hydrogen bonds in the structures identified by the previous runstreams.

```
CALC INTER FROM O 1.6 TO N 1.6 EXT
FRAG OH...N
AT1 O 2
AT2 H 1
AT3 N 2
BO 1 2 0.70 1.15
BO 1 3 2.40 3.00
END
DEF O..N 1 3
DEF O-H 1 2
DEF H..N 2 3
DEF HANG 1 2 3
END
```